

# Radiation and Reaction at One Loop

---

**Asaad Elkhidir<sup>1</sup> Donal O'Connell<sup>1,2</sup> Matteo Sergola<sup>1,2</sup> Ingrid A. Vazquez-Holm<sup>2,3,4</sup>**

<sup>1</sup>*Higgs Centre, School of Physics and Astronomy, University of Edinburgh, EH9 3FD, Scotland*

<sup>2</sup>*Kavli Institute for Theoretical Physics, University of California, Santa Barbara, CA 93106-4030, USA*

<sup>3</sup>*Department of Physics and Astronomy, Uppsala University, Box 516, 75120 Uppsala, Sweden*

<sup>4</sup>*Nordita, Stockholm University and KTH Royal Institute of Technology, Hannes Alfvéns väg 12, 10691 Stockholm, Sweden*

*E-mail:* [A.E.H.Elkhidir@sms.ed.ac.uk](mailto:A.E.H.Elkhidir@sms.ed.ac.uk), [donal@ed.ac.uk](mailto:donal@ed.ac.uk),  
[matteo.sergola@ed.ac.uk](mailto:matteo.sergola@ed.ac.uk), [ingrid.holm@physics.uu.se](mailto:ingrid.holm@physics.uu.se)

**ABSTRACT:** We study classical radiation fields at next-to-leading order using the methods of scattering amplitudes. The fields of interest to us are sourced when two massive, point-like objects scatter inelastically, and can be computed from one-loop amplitudes. We show that the real and imaginary parts of the amplitudes both play important but physically distinct roles in the radiation field. The amplitude's imaginary part directly computes the portion of radiation emitted under the influence of a body's self-field, i.e., through radiation reaction. This aspect of radiation reaction is directly linked to one-loop Compton amplitudes in electrodynamics, Yang-Mills theory and gravity. We also discuss the fascinating interplay between renormalisation, radiation reaction and classical field theory from this perspective.

---

## Contents

<b>1</b>	<b>Introduction</b>	<b>2</b>
<b>2</b>	<b>Field strengths from amplitudes</b>	<b>4</b>
2.1	States and observables	4
2.2	Real and imaginary parts	7
<b>3</b>	<b>Technical simplifications</b>	<b>10</b>
3.1	Hierarchy of momenta	10
3.2	Classical LO waveshape and heavy-particle crossing	11
3.3	Vanishing cuts	13
3.4	Vanishing integrals	15
3.5	Real parts from single cuts and principal values	15
<b>4</b>	<b>Radiation</b>	<b>18</b>
4.1	QED	19
4.2	QCD	25
<b>5</b>	<b>Reaction</b>	<b>30</b>
5.1	QED radiation reaction...	30
5.2	...QCD radiation reaction...	33
5.3	...GR radiation reaction	35
<b>6</b>	<b>Renormalisation</b>	<b>37</b>
6.1	Infrared divergences	38
6.2	Real divergence	41
6.3	Imaginary part	42
6.4	QCD and gravity	42
6.5	Renormalisation	42
<b>7</b>	<b>Classical confirmation</b>	<b>47</b>
<b>8</b>	<b>Conclusions</b>	<b>51</b>
<b>A</b>	<b>A derivation of the ALD force with cuts</b>	<b>54</b>

---

# 1 Introduction

Gravitational waveforms sourced by compact binary coalescence events are now the basic physical observable in precision studies of General Relativity (GR). These waveforms are closely related to the Riemann curvature: in the transverse traceless gauge, the waveform’s second derivative is a curvature component. Future gravitational wave observatories will work at higher signal-to-noise ratios, and therefore will be sensitive to more subtle aspects of the waveform. This presents an exciting challenge for the theoretical physics community: to develop tools allowing for efficient determination of gravitational waveforms at new levels of precision [1–4].

Precision computations in GR are a challenge because of the non-linearity of its perturbative structure. One hope for simplifying this non-linearity comes from the study of scattering amplitudes in quantum field theory. Scattering amplitudes have a remarkable property known as the “double copy”, which allows us to obtain scattering amplitudes in gravitational theories given amplitudes in much simpler Yang-Mills theories [5–8]. Furthermore, elegant and powerful tools have been developed to compute scattering amplitudes with remarkable ease. In this article, we will make heavy use of generalised unitarity [9, 10]. This method allows us to construct loop-level scattering amplitudes from tree amplitudes. We can further combine the double copy and generalised unitarity, effectively building the dynamical information necessary for gravitational waveforms from tree amplitudes in Yang-Mills theory. The union of generalised unitarity and the double copy has already proven very fruitful in the study of General Relativity, and provides a fresh perspective on the relativistic two-body problem [11–55].

To date, much of the work on amplitudes and classical gravity has focused on the understanding the interaction potential between gravitating masses. In contrast, our interest is directly on the radiation emitted during a dynamical process. We make use of a method for constructing radiation fields from amplitudes which has been developed in recent years [37, 39, 56–61]. The basic idea is to use a quantum-mechanical language to describe the event; the physical observable to be computed becomes the expectation value of the Riemann curvature. In the classical limit, this expectation will equal the classical curvature, up to quantum corrections which can be systematically dropped. The formalism is general and can be applied to field strengths in a variety of theories: electromagnetism, Yang-Mills (YM) theory, and gravity.

As their name suggests, the methods of scattering amplitudes are most directly applicable to events where two objects scatter, generating radiation, rather than to the more physically relevant bound binaries. Nevertheless methods exist to connect scattering and bound case physics. In some cases, we can simply analytically continue observables from the scattering to the bound cases [62–65]. More generally, it is possible to build effective field theories (EFTs) describing general binary dynamics

[47, 48, 56, 66–101], see [102, 103] for reviews. These EFTs can be matched to scattering data and then applied to the bound case, effectively forming a bridge between the two.

Effective field theory is a powerful tool, and has been used very successfully in classical gravitational wave physics for many years now [92]. Most closely connected to this article are the “post-Minkowskian” effective theories [104–110] and worldline quantum field theories [25, 60, 111–119]. These methods were applied to describe conservative binary dynamics at  $\mathcal{O}(G)$  and  $\mathcal{O}(G^2)$  [66], at  $\mathcal{O}(G^3)$  [120, 121] and at  $\mathcal{O}(G^4)$  in references [38, 122]. Recently, the “HEFT” approach of [47, 48] has been introduced to the array of EFT based methods. Inspired by the success of heavy-quark effective theory [123–127], the HEFT approach implements the classical limit as a large mass limit. The resulting decoupling between the heavy and light degrees of freedom exposes certain simplifications associated with the classical limit and combines nicely with the double copy [20, 47–49, 74, 128].

In this article, we build on previous work which studied scattering encounters between classical, point-like objects at leading order (LO) [37, 56, 58, 59, 129]. We describe the structure of field strength observables at next-to-leading order (NLO) in terms of scattering amplitudes. As we will see, the structure is remarkably simple. The waveform, as determined by amplitudes, naturally has two pieces. These are associated with the real and imaginary parts of a one-loop five-point amplitude. We will see that the imaginary part has the classical interpretation of the portion of radiation emitted by an object accelerating under its own self-field. That is, the imaginary part arises as a consequence of radiation reaction at one loop order. This radiation from radiation-reaction is determined by Compton amplitudes in electrodynamics, YM theory, and in gravity. Our treatment makes it clear that this aspect of radiation reaction double-copies in a straightforward manner at NLO.

We begin in section 2 with a discussion the general structure of field-strength observables at NLO before describing some technical simplifications we can take advantage of at this order in section 3. After those preliminaries, we dive into the main computations of the paper. First, in section 4, we determine the radiation at one loop which is associated with the real part of the scattering amplitude. This part of the radiation field is classically associated with essentially conservative forces (eg the Lorentz force in electromagnetism). We focus on examples in electrodynamics and Yang-Mills theory. In section 5, we turn to the imaginary part of the amplitude which determines a well-defined, physically distinct portion of the waveform. This part is associated with the radiation emitted from the particle under the influence of its self-field. As radiation reaction is intimately associated with renormalisation, we present a thorough discussion of the renormalisation of the one-loop five-point amplitude in QED which determines the radiation field in section 6. In this section, we justify the omission of certain cuts which one might naively think could contribute to the classical radiation field. We show that these cuts are fully quan-

tum after renormalisation in the on-shell scheme. Along the way we discuss infrared divergences. Finally, we turn to a detailed classical verification of our results in the context of electrodynamics before concluding. In appendix A, we summarise a classical perspective on the Abraham-Lorentz-Dirac self-field inspired by an old article of Coleman. This perspective is intended to clarify how the quantum-mechanical approach coincides with the classical approach to radiation reaction.

### Note added

While finalising this paper we learned about parallel research presented in references [130] and [131] which contain some overlap with our work. Further related work by one of the present authors and collaborators will appear in the forthcoming article [132]. We thank the authors for cooperating with us in the submission of our work, and for sharing advance copies of their drafts with us.

## 2 Field strengths from amplitudes

Our goal is to compute the radiation field generated by a scattering event involving two point-like classical objects using the methods of scattering amplitudes. The basic observable of interest is the field strength (in electrodynamics and YM theory) or the Riemann curvature (in gravity), both of which are very similar in structure; we will refer to both generically as “field strengths”. In this section, we explain how to determine these field strengths from scattering amplitudes at next-to-leading order (NLO) accuracy. We begin with a short review of the connection between amplitudes and observables, focusing on the case of the field strength, which will also be an opportunity to introduce some notation.

### 2.1 States and observables

Field strengths, as observables in themselves, were first discussed from the perspective of amplitudes in references [37, 133] and were recently reviewed in [134, 135]. Amplitudes are quantum-mechanical objects, so we must start by specifying an initial quantum state which happens to be in the domain of validity of the classical approximation. If we also arrange initial conditions so that we may rely on the classical approximation throughout the scattering event, the equivalence principle guarantees that the quantum treatment will agree with a classical treatment up to small quantum corrections which we systematically drop. This is the basic philosophy of the KMOC approach [59] to extracting classical physics from scattering amplitudes. We will follow the notation of KMOC closely below.

We choose our initial state to be

$$|\psi\rangle = \int d\Phi(p_1, p_2) \phi_b(p_1, p_2) |p_1, p_2\rangle , \quad (2.1)$$

where, following [59], we write

$$d\Phi(p) \equiv \frac{d^D p}{(2\pi)^D} (2\pi) \delta(p^2 - m^2) \Theta(p^0) \equiv \hat{d}^D p \hat{\delta}(p^2 - m^2) \Theta(p^0) \quad (2.2)$$

for the on-shell phase-space measure of a single particle with mass  $m$ . Hatted derivatives and delta-functions are defined to absorb factors of  $2\pi$ . Meanwhile the ket  $|p_1, p_2\rangle$  involves two different particles — quanta of entirely different quantum fields — with masses  $m_1$  and  $m_2$  and momenta  $p_1$  and  $p_2$ .

Since a plane-wave state of a massive particle has no classical interpretation, we have placed our particles in a wavepacket  $\phi_b(p_1, p_2)$ . This wavepacket should individually localise each particle with an uncertainty which is very small compared to any relevant classical scale in our process (for example, the impact parameter). As an example, we could choose

$$\phi_b(p_1, p_2) \equiv e^{ib_1 \cdot p_1} e^{ib_2 \cdot p_2} \phi_1(p_1) \phi_2(p_2), \quad (2.3)$$

where  $\phi_i(p_i)$  are sharply-peaked functions of the momenta. The two-particle wavefunction in equation (2.3) displaces particle  $i$  by a distance  $b_i$  relative to an origin; then the impact parameter is  $b_{12} = b_1 - b_2$ .

We will soon find it very convenient to extend our notation for phase-space measures by writing the measure for several particles as

$$d\Phi(p_1, p_2, \dots) = d\Phi(p_1) d\Phi(p_2) \dots \quad (2.4)$$

We also define the appropriate delta-function  $\delta_\Phi(p)$  with respect to this norm such that

$$\int d\Phi(p) \delta_\Phi(p - p') f(p) = f(p'), \quad (2.5)$$

for any smooth function  $f(p)$ .

Our basic task is to compute the future expectation value of a field strength operator. In Yang-Mills theory, the relevant operator is the field strength tensor

$$\mathbb{F}_{\mu\nu}^a = \partial_\mu \mathbb{A}_\nu^a - \partial_\nu \mathbb{A}_\mu^a + g f^{abc} \mathbb{A}_\mu^b \mathbb{A}_\nu^c. \quad (2.6)$$

There is one immediate simplification from working in the far-field limit. In the far field, the expectation value of the Yang-Mills potential  $\mathbb{A}(x)$  is inversely proportional to the large radius  $r$  between the observer and the scattering event. We will only be interested in this leading  $1/r$  behaviour. As a result we may replace the full non-Abelian field strength with its abelianised version:

$$\mathbb{F}_{\mu\nu}^a \simeq \partial_\mu \mathbb{A}_\nu^a - \partial_\nu \mathbb{A}_\mu^a. \quad (2.7)$$

In gravity, we are only interested in the expectation value of the linearised Riemann tensor for the same reason. It may be worth emphasising that there is still non-linear (non-Abelian) dynamics in the core of spacetime.

The state in the far future is  $S|\psi\rangle$  since the  $S$  matrix is the all-time evolution operator. Placing our detector at a position  $x$  near lightlike future infinity, the observable of interest to us in Yang-Mills theory is

$$F_{\mu\nu}^a(x) \equiv \langle\psi|S^\dagger \mathbb{F}_{\mu\nu}^a(x) S|\psi\rangle . \quad (2.8)$$

To connect with scattering amplitudes, we use the mode expansion for the quantum field  $\mathbb{A}_\mu^a$ :

$$\mathbb{A}_\mu^a(x) = \sum_\eta \int d\Phi(k) [\varepsilon_\mu^\eta(k) a_\eta^a(k) e^{-ik\cdot x} + \text{h.c.}] , \quad (2.9)$$

so that

$$F_{\mu\nu}^a(x) = 2 \operatorname{Re} \sum_\eta \int d\Phi(k) \left[ -ik_{[\mu} \varepsilon_{\nu]}^\eta(k) \langle\psi|S^\dagger a_\eta^a(k) S|\psi\rangle e^{-ik\cdot x} \right] . \quad (2.10)$$

Most of our focus in this article will be on the computation of  $\langle\psi|S^\dagger a_\eta^a(k) S|\psi\rangle$ . Once this quantity is known, an explicit expression for the field strength can be found by integration.

In gravity, defining the curvature expectation

$$R_{\mu\nu\rho\sigma}(x) \equiv \langle\psi|S^\dagger \mathbb{R}_{\mu\nu\rho\sigma}(x) S|\psi\rangle , \quad (2.11)$$

it similarly follows that

$$R_{\mu\nu\rho\sigma}(x) = \kappa \operatorname{Re} \sum_\eta \int d\Phi(k) \left[ k_{[\mu} \varepsilon_{\nu]}^\eta(k) k_{[\rho} \varepsilon_{\sigma]}^\eta(k) \langle\psi|S^\dagger a_\eta^a(k) S|\psi\rangle e^{-ik\cdot x} \right] . \quad (2.12)$$

We have introduced the constant  $\kappa$ , defined in terms of Newton's constant by  $\kappa = \sqrt{32\pi G}$ , and the annihilation operator  $a_\eta(k)$  of a graviton state with helicity  $\eta$  and momentum  $k$ . As in gauge theory, the key dynamical quantity to be determined is  $\langle\psi|S^\dagger a_\eta^a(k) S|\psi\rangle$ .

The field strength of equation (2.10) and the curvature (2.12) both involve an integration over the phase space of a massless particle. At large distances, this integral can be reduced to a one-dimensional Fourier transform using standard methods (see [134, 135] for a recent review). Writing the observation coordinate as  $x = (x^0, \mathbf{x})$  and introducing the retarded time  $u = x^0 - |\mathbf{x}|$ , the results are

$$F_{\mu\nu}^a(x) = \frac{-1}{4\pi|\mathbf{x}|} 2 \operatorname{Re} \int_0^\infty \hat{d}\omega e^{-i\omega u} \sum_\eta k_{[\mu} \varepsilon_{\nu]}^\eta(k) \langle\psi|S^\dagger a_\eta^a(k) S|\psi\rangle , \quad (2.13)$$

in Yang-Mills theory, and

$$R_{\mu\nu\rho\sigma}(x) = \frac{-\kappa}{4\pi|\mathbf{x}|} \operatorname{Re} \int_0^\infty \hat{d}\omega e^{-i\omega u} \sum_\eta ik_{[\mu} \varepsilon_{\nu]}^\eta(k) k_{[\rho} \varepsilon_{\sigma]}^\eta(k) \langle\psi|S^\dagger a_\eta^a(k) S|\psi\rangle , \quad (2.14)$$

in gravity. Note that in both integrals (2.13) and (2.14) the momentum of the messenger reads  $k^\mu = \omega(1, \hat{\mathbf{x}})$ .

In terms of amplitudes and quantum field theory, then, the object we need to compute is

$$\alpha_\eta(k) \equiv \langle \psi | S^\dagger a_\eta(k) S | \psi \rangle , \quad (2.15)$$

where  $a_\eta(k)$  is an annihilation operator for the relevant field. We will refer to this quantity as the “waveshape”, since it is the parameter describing the coherent state of radiation which has the same field strength as given in equation (2.10). The connection between amplitudes, coherent states and radiation was the topic of reference [42].

Having discussed the general connection between amplitudes and field strengths, let us now understand how to construct the waveshape from perturbative scattering amplitudes.

One obvious way to proceed is simply to extend the KMOC framework of [59] to the computation of matrix element by expanding  $S = 1 + iT$ . This approach immediately leads to the leading order expression

$$\alpha_\eta(k) = \int d\Phi(p'_1, p'_2, p_1, p_2) \phi_b^*(p'_1, p'_2) \phi_b(p_1, p_2) \hat{\delta}^D(p_{\text{tot}}) i\mathcal{A}_{5,0}(p_1, p_2 \rightarrow p'_1, p'_2, k_\eta) , \quad (2.16)$$

where we are adopting the notation that  $\mathcal{A}_{n,L}$  is an  $n$  point,  $L$  loop amplitude. The waveshape is slightly more involved at one loop (order  $g^5$ ), where we encounter two terms

$$\begin{aligned} \alpha_\eta(k) = & \int d\Phi(p'_1, p'_2, p_1, p_2) \phi_b^*(p'_1, p'_2) \phi_b(p_1, p_2) \hat{\delta}^D(p_{\text{tot}}) (i\mathcal{A}_{5,1}(p_1, p_2 \rightarrow p'_1, p'_2, k_\eta) \\ & + \int d\Phi(\tilde{p}_1, \tilde{p}_2) \hat{\delta}^D(\tilde{p}_{\text{tot}}) \mathcal{A}_{5,0}(p_1, p_2 \rightarrow \tilde{p}_1, \tilde{p}_2, k_\eta) \mathcal{A}_{4,0}^*(\tilde{p}_1, \tilde{p}_2 \rightarrow p'_1, p'_2)) , \end{aligned} \quad (2.17)$$

with the delta functions imposing the usual conservation of energy and momentum

$$p_{\text{tot}} = p_1 + p_2 - p'_1 - p'_2 - k = 0, \quad \tilde{p}_{\text{tot}} = \tilde{p}_1 + \tilde{p}_2 - p'_1 - p'_2 = 0, \quad (2.18)$$

for external states and across the cut.

It is easy to see that the structure of the one-loop waveshape (2.17) is indeed very similar to the impulse described in [59]: one sums ( $i$  times) the one-loop amplitude and the specific cut shown in equation (2.17). However, in this article, we find it to be very useful to rearrange the observable in a form which clarifies the physics while also simplifying aspects of the computation.

## 2.2 Real and imaginary parts

One clue that there is another way of constructing the observable is the fact that the two terms in (2.17), instruct us to sum  $i$  times the amplitude and the cut of the

amplitude. Since cuts arise from the imaginary parts of the amplitude it is clear that the combination  $i\mathcal{A}_1 + \text{Im } \mathcal{A}_1$  is *removing* an imaginary part of the amplitude. However it is important to realise that the cut in equation (2.17) is not the complete imaginary part of the amplitude: the whole imaginary part is the sum of several distinct cuts. In fact we will see that one particular cut survives in the classical limit, and is directly relevant to radiation reaction.

The usefulness of real and imaginary parts of amplitudes in the construction of KMOC-style classical observables was first emphasised in reference [36] which studied the impulse in classical scattering. The authors found that classically-singular terms<sup>1</sup> are absent in the real part of the amplitude, while singular terms did appear in the imaginary part. These classically-singular terms cancelled among the different contributions to the imaginary part. We will soon find an analogous phenomenon in the waveshape. Real and imaginary parts also play a crucial role in eikonal methods, see for instance references [16, 42, 136–138].

Real and imaginary parts of amplitudes are intimately connected to unitarity of the  $S$  matrix. To separate these parts of the amplitude, we first use  $S = 1 + iT$  and the unitarity relation

$$-i(T - T^\dagger) = T^\dagger T \quad (2.19)$$

to write the waveshape (2.15) as

$$\begin{aligned} \alpha_\eta(k) &= \frac{1}{2} \langle \psi | i a_\eta(k) (T + T^\dagger) - i a_\eta(k) T^\dagger T + 2T^\dagger a_\eta(k) T | \psi \rangle \\ &= \frac{1}{2} \langle \psi | i a_\eta(k) (T + T^\dagger) - [a_\eta(k), T^\dagger] T + T^\dagger [a_\eta(k), T] | \psi \rangle . \end{aligned} \quad (2.20)$$

The first of these terms involves the combination  $(T + T^\dagger)/2$ ; up to a momentum-conserving delta function, this is the “real” part of the amplitude. It can be evaluated by cutting one internal propagator, and replacing all others by principal value prescriptions as we discuss below in section 3.5.

The other terms involve cuts of the amplitude and are therefore linked to its imaginary part.

Because the cuts involve two  $T$  matrices (one conjugated), and we work at order  $g^5$ , it follows that we need one insertion of a  $g^2$  tree amplitude and a  $g^3$  tree amplitude. There is a short list of possible amplitudes: at order  $g^2$ , we encounter four-point amplitudes involving four scalars, Compton-type amplitudes with two scalars and two messengers, or four messenger amplitudes. At order  $g^5$  we simply dress the order  $g^2$  amplitudes with one additional messenger. Furthermore, the commutator  $[a_\eta(k), T]$  vanishes unless the corresponding amplitude contains at least one outgoing messenger.

---

<sup>1</sup>These terms involve inverse powers of  $\hbar$  and must cancel in observables. They are sometimes known as “superclassical” or “hyperclassical” terms.

Let us first consider the term

$$\begin{aligned}\alpha_\eta(k) &\supset \frac{1}{2} \langle \psi | T^\dagger [a_\eta(k), T] | \psi \rangle \\ &= \frac{1}{2} \int d\Phi(p'_1, p'_2, p_1, p_2) \phi_b^*(p'_1, p'_2) \phi_b(p_1, p_2) \langle p'_1, p'_2 | T^\dagger [a_\eta(k), T] | p_1, p_2 \rangle.\end{aligned}\quad (2.21)$$

The  $T$  matrix here acts on the incoming two-scalar state, and (because of the commutator) must involve at least one outgoing messenger. The only possibility in our list of order  $g^2$  and  $g^3$  amplitudes is the  $2 \rightarrow 3$  amplitude involving radiation of one messenger as the two scalars scatter. Similarly  $\langle p'_1, p'_2 | T^\dagger$  must evaluate to the four-point four-scalar amplitude as the only order  $g^2$  amplitude with two final-state scalars. Thus<sup>2</sup>,

$$\langle p'_1, p'_2 | T^\dagger [a_\eta(k), T] | p_1, p_2 \rangle = \text{Diagram} \quad (2.22)$$

Now we turn to the final structure in our new formulation (2.20) of the wave-shape, namely

$$\begin{aligned}\alpha_\eta(k) &\supset -\frac{1}{2} \langle \psi | [a_\eta(k), T^\dagger] T | \psi \rangle \\ &= -\frac{1}{2} \int d\Phi(p'_1, p'_2, p_1, p_2) \phi_b^*(p'_1, p'_2) \phi_b(p_1, p_2) \langle p'_1, p'_2 | [a_\eta(k), T^\dagger] T | p_1, p_2 \rangle.\end{aligned}\quad (2.23)$$

First, consider the action of  $T$  on the initial state  $|p_1, p_2\rangle$ . There are two possibilities on our list of  $g^2$  and  $g^3$  trees: the  $2 \rightarrow 2$  four scalar scattering amplitude, or the  $2 \rightarrow 3$  five-point amplitude involving four scalars and an outgoing messenger. Considering first the order  $g^2$  possibility, the remaining factor  $\langle p'_1, p'_2 | [a_\eta(k), T^\dagger]$  must be the order  $g^3$   $2 \rightarrow 3$  five-point amplitude. On the other hand, if the  $T$  matrix contributes as the  $2 \rightarrow 3$  five-point amplitude then we must extract an order  $g^2$  amplitude from  $[a_\eta(k), T^\dagger]$ . The only order  $g^2$  amplitude with one final messenger that we can insert

---

<sup>2</sup>Throughout this paper, we adopt the convention of drawing massive particle lines as solid lines. We will always indicate particle 1 with a red line and particle 2 with a blue one.

here is the Compton amplitude. That is,

$$\begin{aligned}
 \langle p'_1, p'_2 | [a_\eta(k), T^\dagger] T | p_1, p_2 \rangle = & \quad \text{Diagram 1: Two shaded circles (photons) with a red loop between them. Blue lines } p_1, p_2 \text{ enter from the left, and red lines } p'_1, p'_2 \text{ exit to the right. A wavy line } k \text{ connects the two circles.} \\
 + & \quad \text{Diagram 2: Similar to Diagram 1, but the red loop is on the right side of the circles.} \\
 + & \quad \text{Diagram 3: Similar to Diagram 1, but the red loop is on the left side of the circles.} \\
 \end{aligned} \tag{2.24}$$

The presence of Compton amplitudes in this cut is significant. In fact, we will see that in the classical limit it is *only* these cuts which survive. To substantiate our arguments, in appendix A we will present a purely classical derivation which relates cuts and dissipative forces.

### 3 Technical simplifications

The full quantum structure of the waveshape  $\alpha_\eta(k)$  can be constructed from amplitudes using this formalism. While there are many interesting aspects of the quantum-mechanical case, the focus on this article is on the classical waveshape. Obviously the classical case is simpler than the full quantum case, and we now wish to discuss the details and the simplifications we can take advantage of to simplify our work. More specifically, we are interested in the classical limit of small angle scattering, often known as the “post-Minkowski” expansion in the gravitational context. This is a relativistically covariant perturbative expansion of classical quantities — in our case, of the classical radiation field. There are a number of aspects of this expansion, which have been discussed in detail elsewhere, for example in references [39, 59, 66, 122, 139]. We therefore only highlight key aspects for our work here.

#### 3.1 Hierarchy of momenta

One simple-minded way to separate classical and quantum effects is to restore factors of  $\hbar$ : clearly all  $\hbar$ ’s must disappear in classical expressions, and quantum corrections will be suppressed by (dimensionless ratios involving)  $\hbar$ . In this paper, the most important factors of  $\hbar$  appear in the momenta of messengers: the photons, gluons or

gravitons which mediate the interaction. Writing a generic messenger momentum as  $q$  compared to a point-particle momentum  $p$ , we note that  $q$  scales as  $\hbar$ ,

$$q = \hbar \bar{q}, \quad (3.1)$$

while the particle momentum  $p$  scales as its mass:

$$p = mu. \quad (3.2)$$

Here we introduced a classical wavenumber  $\bar{q}$  with dimensions of length, and the classical proper velocity  $u$ . The ratio of these, or rather of specific components, is of order the (reduced) Compton wavelength of the particle  $\hbar/m$ . The classical approximation is valid only when the wavelengths of messengers, described by  $\bar{q}$ , are much larger than the Compton wavelengths of the particles. Thus we treat messenger momenta as being very small compared to particle momenta, schematically

$$p \gg q. \quad (3.3)$$

Note that this can be implemented by treating the point particles as being very heavy, a point of view which is emphasised for example in references [20, 47–49, 74, 128, 129]. Here we simply proceed by Laurent expanding integrands in terms of variables suppressed by messenger momenta relative to particle momenta.

Throughout this paper the expansion will be essentially trivialised. The most dangerous superclassical terms are present only in the imaginary part, and cancel directly at the level of cuts without requiring detailed computation. For the remainder,  $\hbar$  power counting in a convenient gauge shows that all diagrams are classical at leading order in the  $\hbar$  expansion.

### 3.2 Classical LO waveshape and heavy-particle crossing

The waveshape (2.16) can be written at leading order as

$$\begin{aligned} \alpha_\eta(k) = & \int d\Phi(p'_1, p'_2, p_1, p_2) \phi^*(p'_1, p'_2) \phi(p_1, p_2) e^{ib_1 \cdot (p_1 - p'_1)} e^{ib_2 \cdot (p_2 - p'_2)} \\ & \times i\mathcal{A}_{5,0}(p_1, p_2 \rightarrow p'_1, p'_2, k_\eta) \hat{\delta}^D(p'_1 + p'_2 + k - p_1 - p_2). \end{aligned} \quad (3.4)$$

Now let's simplify this expression in the classical limit. As we do so we will learn something about the tree amplitude.

We will take the classical limit in two slightly different manners. First, write the “outgoing” momenta<sup>3</sup> as

$$p'_i = p_i + q_i. \quad (3.5)$$

---

<sup>3</sup>As our observable is an expectation value, the apparent in and out states are both in states. Nevertheless it can be convenient at times to think of the primed momenta as outgoing.

The momenta  $q_i$  are messenger momenta, satisfying  $k = -q_1 - q_2$ . Now, the on-shell phase space measure of the outgoing particle  $i$  is

$$d\Phi(p_i + q_i) = \hat{d}^D q_i \Theta(p_i^0 + q_i^0) \hat{\delta}(p_i^2 + 2p_i \cdot q_i + q_i^2 - m_i^2). \quad (3.6)$$

We simplify this as follows. First, the energy  $p_i^0$  is always much greater than  $q_i^0$  in the classical region (since pair-production must be kinematically suppressed.) Therefore we replace the theta functions by unity. Next, we note that  $p_i$  is an on-shell initial momentum so that  $p_i^2 = m_i^2$ . We further simplify the delta function noting that  $q_i^2$  is suppressed by a Compton wavelength relative to  $p_i \cdot q_i$ . Thus, the waveshape becomes

$$\begin{aligned} \alpha_\eta(k) = & \int d\Phi(p_1, p_2) \hat{d}^D q_1 \hat{d}^D q_2 \hat{\delta}(2p_1 \cdot q_1) \hat{\delta}(2p_2 \cdot q_2) \phi^*(p_1 + q_1, p_2 + q_1) \phi(p_1, p_2) \\ & \times e^{-ib_1 \cdot q_1} e^{-ib_2 \cdot q_2} i\mathcal{A}_{5,0}(p_1, p_2 \rightarrow p_1 + q_1, p_2 + q_2, k_\eta) \hat{\delta}^D(k + q_1 + q_2). \end{aligned} \quad (3.7)$$

Next, we simplify the wavefunctions by noting

$$\phi(p_1 + q_1, p_2 + q_1) \simeq \phi(p_1, p_2). \quad (3.8)$$

The origin of this fact is that the messenger momenta are suppressed by the Compton wavelength relative to the particle momenta, and on this scale the wavefunctions are rather flat. Indeed if the momentum-space wavefunctions were to localise the momenta to within a few Compton wavelengths, then the position-space uncertainty would be very large [59]. As a result, the leading-order waveshape is

$$\begin{aligned} \alpha_\eta(k) = & \int d\Phi(p_1, p_2) \hat{d}^D q_1 \hat{d}^D q_2 \hat{\delta}(2p_1 \cdot q_1) \hat{\delta}(2p_2 \cdot q_2) |\phi(p_1, p_2)|^2 e^{-ib_1 \cdot q_1} e^{-ib_2 \cdot q_2} \\ & \times i\mathcal{A}_{5,0}^*(p_1, p_2 \rightarrow p_1 + q_1, p_2 + q_2, k_\eta) \hat{\delta}^D(k + q_1 + q_2). \end{aligned} \quad (3.9)$$

On the other hand, returning to equation (3.4) and instead setting

$$p_i = p'_i + q_i, \quad (3.10)$$

we find, using the same logic,

$$\begin{aligned} \alpha_\eta(k) = & \int d\Phi(p'_1, p'_2) \hat{d}^D q_1 \hat{d}^D q_2 \hat{\delta}(2p'_1 \cdot q_1) \hat{\delta}(2p'_2 \cdot q_2) |\phi(p'_1, p'_2)|^2 e^{-ib_1 \cdot q_1} e^{-ib_2 \cdot q_2} \\ & \times i\mathcal{A}_{5,0}(p'_1 - q_1, p'_2 - q_2 \rightarrow p'_1, p'_2, k_\eta) \hat{\delta}^D(k + q_1 + q_2). \end{aligned} \quad (3.11)$$

There is nothing stopping us from dropping the primes in this equation, since  $p'_i$  are simply variables of integration.

Comparing equations (3.9) and (3.11), the only difference is in the details of the momentum dependence in the tree amplitude. The wavefunction is unspecified; we have only used properties it must have in the classical limit. We conclude that

$$\mathcal{A}_{5,0}(p_1, p_2 \rightarrow p_1 + q_1, p_2 + q_2, k_\eta) = \mathcal{A}_{5,0}(p_1 - q_1, p_2 - q_2 \rightarrow p_1, p_2, k_\eta). \quad (3.12)$$

This expression can only hold for the classical ‘‘fragment’’ of the amplitude, in the sense of reference [42]: at tree level, the classical fragment is simply the dominant term in the classical Laurent expansion. An alternative perspective is that this crossing relation follows from the scale separation between the heavy-mass scale  $m_1$  and  $m_2$  in the momenta of the scalar particles, and the light scale of order  $q$  in the messengers. This decoupling is made manifest in heavy particle effective theories, which could also be used to compute these amplitudes.

The result, then, is a kind of crossing relation valid for heavy particle effective theories. It essentially allows us to cross the messenger momentum leaving the large particle momentum untouched. We will find this result is very useful below. It is straightforward to check this heavy-particle crossing relation in explicit examples: the QED amplitude is visible in equation 5.46 of reference [59] while the gravitational five point case is written in equation 4.21 of reference [129]. In both cases, heavy-particle crossing is achieved by eliminating the momentum  $k$  in favour of  $q_1 + q_2$ , and then replacing  $q_i \rightarrow -q_i$ . This has the effect of replacing  $p_i + q_i$  with the desired  $p_i - q_i$  without clashing with the relation between  $k$  and the  $q_i$  (this relation does not pick up a sign in the crossing).

Returning to the waveshape, we shall write

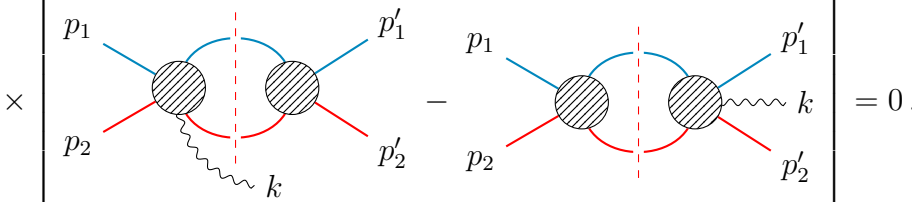
$$\alpha_\eta(k) = \left\langle\!\left\langle \int \hat{d}^D q_1 \hat{d}^D q_2 \hat{\delta}(2p_1 \cdot q_1) \hat{\delta}(2p_2 \cdot q_2) e^{-ib_1 \cdot q_1} e^{-ib_2 \cdot q_2} (\dots) \right\rangle\!\right\rangle \quad (3.13)$$

at LO and NLO. Here the dots signify a general integrand, made of amplitudes and cuts. The large angle brackets remind us that the result must be integrated against the wavefunctions. However, once the integrand has been fully simplified in the classical limit, in particular to cancel terms involving singular powers of  $\hbar$ , the integrand is smooth on the scale of the wavepacket. We can therefore formally take the wavepacket size to zero, so that the wavepacket integral simply localises the incoming momenta  $p_i$  on their classical values.

### 3.3 Vanishing cuts

Earlier, we advertised that certain cuts which contribute to the full quantum waveshape cancel in the classical waveshape. We are now in a position to show this in detail. The result of this subsection is that

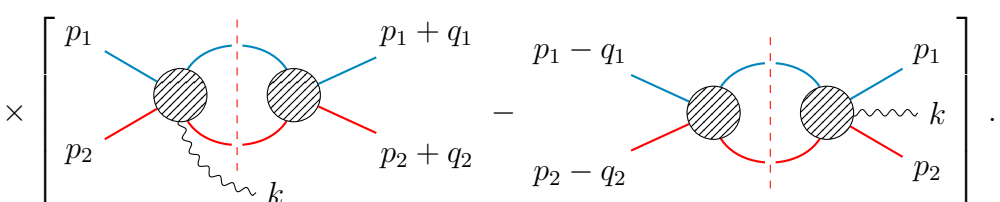
$$\int d\Phi(p'_1, p'_2, p_1, p_2) \phi^*(p'_1, p'_2) \phi(p_1, p_2) e^{ib_1 \cdot (p_1 - p'_1)} e^{ib_2 \cdot (p_2 - p'_2)} \hat{\delta}^D(p'_1 + p'_2 + k - p_1 - p_2) \times \left[ \begin{array}{c} p_1 \\ p_2 \end{array} \right] \times \left[ \begin{array}{c} p'_1 \\ p'_2 \end{array} \right] - \left[ \begin{array}{c} p_1 \\ p_2 \end{array} \right] \times \left[ \begin{array}{c} p'_1 \\ p'_2 \end{array} \right] = 0. \quad (3.14)$$



In other words, these two cuts make no contribution to the classical waveshape. This cancellation can be interpreted as the cancellation of classically-singular (“superclassical”) terms which occur in the five point one-loop amplitude. The result can be seen as a generalisation of the removal of iterated trees in an exponentiated form of the amplitude along the lines of the eikonal or radial action at four points. There is more discussion of this kind of exponentiation in reference [42].

To see how the cancellation works, we adjust the initial and final states under the integral signs to reach

$$\int d\Phi(p_1, p_2, p_1 + q_1, p_2 + q_2) |\phi(p_1, p_2)|^2 e^{-ib_1 \cdot q_1} e^{-ib_2 \cdot q_2} \hat{\delta}^D(k + q_1 + q_2)$$

$$\times \left[ \begin{array}{c} p_1 \\ p_2 \end{array} \begin{array}{c} p_1 + q_1 \\ p_2 + q_2 \end{array} - \begin{array}{c} p_1 - q_1 \\ p_2 - q_2 \end{array} \begin{array}{c} p_1 \\ p_2 \end{array} \right].$$

(3.15)

Writing out the cut, this becomes

$$\begin{aligned} & \left\langle \left\langle \int \hat{d}^D q_1 \hat{d}^D q_2 \hat{\delta}(2p_1 \cdot q_1) \hat{\delta}(2p_2 \cdot q_2) \hat{\delta}^D(k + q_1 + q_2) e^{-ib_1 \cdot q_1} e^{-ib_2 \cdot q_2} \right. \right. \\ & \quad \times \int \hat{d}^D \ell_1 \hat{d}^D \ell_2 \hat{\delta}(2p_1 \cdot \ell_1) \hat{\delta}(2p_2 \cdot \ell_2) \hat{\delta}^D(\ell_1 + \ell_2 + k) \\ & \quad \left. \left. \left[ \mathcal{A}_{5,0}(p_1, p_2 \rightarrow p_1 + \ell_1, p_2 + \ell_2, k) \mathcal{A}_{4,0}(p_1 + \ell_1, p_2 + \ell_2 \rightarrow p_1 + q_1, p_2 + q_2) \right. \right. \\ & \quad \left. \left. - \mathcal{A}_{4,0}(p_1 - q_1, p_2 - q_2 \rightarrow p_1 - \ell_1, p_2 - \ell_2) \mathcal{A}_{5,0}(p_1 - \ell_1, p_2 - \ell_2 \rightarrow p_1, p_2, k) \right] \right\rangle. \end{aligned}$$
(3.16)

Using heavy-particle crossing, the two five point trees are shown to be equal. As for the four point trees, one could use a result analogous to this crossing to show that they match. Alternatively, it is a simple point that these trees only depend on the  $t$  channel Mandelstam variable, which is the same in both terms, times the point-particle data. Thus, we conclude that the result vanishes.

Our argument for this cancellation is somewhat indirect, and our confidence was improved after performing some detailed tests. First, we computed the gauge invariant and well-defined parts of the waveshape in QED and QCD with an automated code based on references [29] and [140], making no use of this heavy-particle crossing. As we discuss below we also computed  $\alpha$  analytically taking advantage of the cancellation due to heavy particle crossing, and find agreement with both results. Furthermore, another check is achieved through the eikonal formalism. There, the removal of superclassical terms relies on a factorisation property first outlined in [42] and [141] which is essentially equivalent to classical crossing. This cancellation is also made manifest in the HEFT approach [47, 48].

### 3.4 Vanishing integrals

In our one-loop computations, we will encounter topologies including pentagons, boxes, triangles etc. Here we largely work at the level of the integrand. Nevertheless it is very useful to simplify our integrand by dropping terms which integrate to zero.

The situation with loop integrals in the classical limit at four-points at one and two loops is very well understood and is thoroughly discussed for example in references [19, 39]. There are some similarities between four and five points. For example, we note that

$$\int \hat{d}^D \ell \frac{(\ell - q_1)^2}{\ell^2 (\ell - q_1)^2 (p_1 \cdot \ell) (p_2 \cdot \ell)} = 0. \quad (3.17)$$

One viewpoint is that this occurs because the integral is scaleless in dimensional regulation. An alternative viewpoint is that the integral is irrelevant classically with any choice of regulator because it leads to a contact term connecting the two point-like particles. These contact terms are only non-vanishing outside the domain of validity of the classical theory when the two particles are spatially separated by less than their Compton wavelength.

As another example, consider the integral

$$\begin{aligned} \int \hat{d}^D \ell \frac{\ell^2}{\ell^2 (\ell - q_1)^2 (p_1 \cdot \ell) (p_2 \cdot \ell)} &= \int \hat{d}^D \ell \frac{1}{(\ell - q_1)^2 (p_1 \cdot \ell) (p_2 \cdot \ell)} \\ &= \int \hat{d}^D \ell \frac{1}{\ell^2 (p_1 \cdot \ell) (p_2 \cdot (\ell + q_1))}. \end{aligned} \quad (3.18)$$

In the second step, we simply set  $\ell' = \ell - q_1$ , and then dropped the prime. We also set  $p_1 \cdot q_1 = 0$ , assuming that the  $\hbar$ -suppressed correction term of order  $q_1^2$  could be neglected. This integral is *not* scaleless: indeed, there is a scale  $p_2 \cdot q_1 = -p_2 \cdot k$  in the integral. Nevertheless we may still drop this integral:

$$\int \hat{d}^D \ell \frac{\ell^2}{\ell^2 (\ell - q_1)^2 (p_1 \cdot \ell) (p_2 \cdot \ell)} \rightarrow 0. \quad (3.19)$$

Again, the reason is that it leads to a contact term in position space. Note that care must be taken in the context of eg pentagon diagrams with three massless internal propagators; pinching one of these need not necessarily lead to a vanishing contact term.

### 3.5 Real parts from single cuts and principal values

Let us now return to the waveform, and look in more detail at the term containing the real part of the amplitude:

$$\begin{aligned} \alpha_\eta(k)|_1 &\equiv \frac{1}{2} \langle \psi | i a_\eta(k) (T + T^\dagger) | \psi \rangle \\ &= \frac{1}{2} \int d\Phi(p'_1, p'_2, p_1, p_2) \phi_b^*(p'_1, p'_2) \phi_b(p_1, p_2) i \langle p'_1, p'_2, k_\eta | T + T^\dagger | p_1, p_2 \rangle. \end{aligned} \quad (3.20)$$

The matrix element appearing here can be expressed in terms of amplitudes as

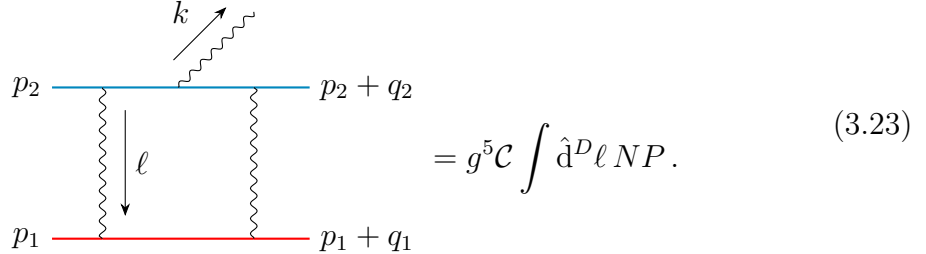
$$\langle p'_1, p'_2, k_\eta | T + T^\dagger | p_1, p_2 \rangle = (\mathcal{A}_{5,0} + \mathcal{A}'_{5,0}^*) \hat{\delta}^D(p_1 + p_2 - p'_1 - p'_2 - k), \quad (3.21)$$

where the five-point tree amplitudes are more explicitly

$$\begin{aligned} \mathcal{A}_{5,0} &\equiv \mathcal{A}(p_1, p_2 \rightarrow p'_1, p'_2, k_\eta), \\ \mathcal{A}'_{5,0} &\equiv \mathcal{A}(p'_1, p'_2, k_{-\eta} \rightarrow p_1, p_2). \end{aligned} \quad (3.22)$$

Notice that the initial and final states are swapped in  $\mathcal{A}'_{5,0}$  relative to  $\mathcal{A}_{5,0}$ . The close relationship between the conjugated amplitude  $\mathcal{A}'_{5,0}^*$  and the amplitude  $\mathcal{A}_{5,0}$  is discussed in many quantum field theory textbooks, though the focus is typically on the imaginary part  $i(\mathcal{A}_{5,0} - \mathcal{A}'_{5,0}^*)$  because of its relevance to unitarity (see, for example, [142–145] for helpful discussions in this particular context). Because the real part  $\mathcal{A}_{5,0} + \mathcal{A}'_{5,0}^*$  is relevant to us, it is worth giving an example to see how the combination works.

We consider a one-loop diagram contributing to the amplitude  $\mathcal{A}_{5,0}$  in Yang-Mills theory:



$$= g^5 \mathcal{C} \int \hat{d}^D \ell N P. \quad (3.23)$$

This diagram depends on a color factor  $\mathcal{C}$ , a kinematic numerator  $N$  and a propagator structure  $P$ . The Feynman rules lead to

$$\begin{aligned} P^{-1} &= (\ell^2 + i\epsilon)[(q_1 - \ell)^2 + i\epsilon][(p_1 + \ell)^2 - m_1^2 + i\epsilon][(p_2 - \ell)^2 - m_2^2 + i\epsilon] \\ &\quad \times [(p_2 - \ell - k)^2 - m_2^2 + i\epsilon], \\ N &= \varepsilon_\eta^* \cdot (2p_2 - 2\ell) (2p_1 + \ell) \cdot (2p_2 - \ell) (2p_1 + \ell + q_1) \cdot (2p_2 - \ell + q_1 + 2q_2). \end{aligned} \quad (3.24)$$

Note the appearance of the (possibly complex) polarisation vector  $\varepsilon_h^*$ . To describe the color factor, we suppose the initial color of particle  $i$  is specified by a color vector  $\chi_i$ , while another vector  $\chi'_i$  defines the final color. Let us further suppose that the outgoing gluon has adjoint color  $a$ . Then we have

$$\mathcal{C} = \bar{\chi}'_1 \cdot T_1^b \cdot T_1^c \cdot \chi_1 \bar{\chi}'_2 \cdot T_2^b \cdot T_2^a \cdot T_2^b \cdot \chi_2. \quad (3.25)$$

The contribution of this diagram to the amplitude is

$$\mathcal{A}_{5,0} \supset -ig^5 \mathcal{C} \int \hat{d}^D \ell N P, \quad (3.26)$$

since (in our conventions) the Feynman rules evaluate to  $i$  times the amplitude<sup>4</sup>.

As the initial and final states are interchanged in  $\mathcal{A}'_{5,0}$ , we instead encounter the diagram

$$= g^5 C' \int \hat{d}^D \ell N' P'. \quad (3.27)$$

The color factor, numerator and propagators are now

$$\begin{aligned} P'^{-1} &= (\ell^2 + i\epsilon)[(q_1 - \ell)^2 + i\epsilon][(p_1 + \ell)^2 - m_1^2 + i\epsilon][(p_2 - \ell)^2 - m_2^2 + i\epsilon] \\ &\quad \times [(p_2 - \ell - k)^2 - m_2^2 + i\epsilon], \quad (3.28) \\ N' &= \varepsilon_\eta \cdot (2p_2 - 2\ell)(2p_1 + \ell) \cdot (2p_2 - \ell)(2p_1 + \ell q_1) \cdot (2p_2 - \ell + q_1 + 2q_2), \\ C' &= \bar{\chi}_1 \cdot T_1^c \cdot T_1^b \cdot \chi'_1 \bar{\chi}_2 \cdot T_2^c \cdot T_2^a \cdot T_2^b \cdot \chi'_2. \end{aligned}$$

It is important that  $N'$  is the complex conjugate of  $N$ , and  $C'$  is the complex conjugate of  $C$  while the propagator structures are equal:  $P = P'$ . As a consequence, we can write

$$\mathcal{A}'_{5,0}^* \supset i g^5 C \int \hat{d}^D \ell N P^*. \quad (3.29)$$

This is a general fact: the one-loop Feynman diagrams contributing to  $\mathcal{A}'_{5,0}^*$  can be obtained from the diagrams for  $\mathcal{A}_{5,0}$  by (i) changing the overall sign, and (ii) replacing the  $i\epsilon$  prescription in propagators by  $-i\epsilon$ . For the two diagrams at hand, we have

$$\begin{aligned} \mathcal{A}_{5,0}(p_1, p_2 \rightarrow p'_1, p'_2, k_\eta) + \mathcal{A}'_{5,0}^*(p'_1, p'_2, k_{-\eta} \rightarrow p_1, p_2) &\supset g^5 C \int \hat{d}^D \ell N [-i(P - P^*)] \\ &= 2g^5 C \int \hat{d}^D \ell N \text{Im } P. \end{aligned} \quad (3.30)$$

The general conclusion is that

$$\begin{aligned} \alpha_\eta(k)|_1 &= \int d\Phi(p'_1, p'_2, p_1, p_2) \phi_b^*(p'_1, p'_2) \phi_b(p_1, p_2) \hat{d}^D(p_1 + p_2 - p'_1 - p'_2 - k) \\ &\quad \times i \text{Im}_{\text{prop}} \mathcal{A}_{5,0}(p_1, p_2 \rightarrow p'_1, p'_2, k_\eta). \end{aligned} \quad (3.31)$$

The instruction  $\text{Im}_{\text{prop}}$  tells us to take the imaginary part of the propagator structure of the amplitudes. Alternatively, we can think of this instruction as the imaginary part of the amplitude, treating colour factors and polarisation vectors as real quantities.

---

<sup>4</sup>This is consistent with  $S = 1 + iT$ , and the convention that, for example, the tree four-point amplitude in  $\lambda\phi^4/4!$  theory is  $\lambda$ .

It is very natural to obtain the imaginary part of the propagator structure using

$$\frac{1}{p^2 - m^2 + i\epsilon} = \text{PV} \left( \frac{1}{p^2 - m^2} \right) - \frac{i}{2} \hat{\delta}(p^2 - m^2), \quad (3.32)$$

where PV is the principal value<sup>5</sup>. The delta function here is equivalent to cutting a single particle. By counting powers of  $i$ , it is clear that the imaginary part of our propagator structure is obtained by cutting an odd number of propagators. (This contrasts with the usual unitarity cuts at one loop which involve cutting two propagators.)

Our diagrams contain five propagators, so in principle there are imaginary parts when we cut one, three or five propagators. However, three point amplitudes have no support in Minkowski space — so there is no need to consider cutting five propagators. It is also easy to see that cutting three propagators necessarily leads to one three-point amplitude. Thus our imaginary parts necessarily arise from single cuts; all other propagators are then to be evaluated with the principal-value pole prescription. It is worth emphasising that this pole prescription appears naturally from general considerations.

## 4 Radiation

In this chapter we discuss the complete real part of the QED and QCD waveshape in detail at the level of their integrand. As we will see, taking the real part of the one-loop amplitude corresponds to isolating “conservative” contributions in radiative fields. By that we mean all radiation which is caused by one particle accelerating in the Lorentz/geodesic fields of the second one. That is, the forces acting on the particle are conservative, and (classically) omit the self-field of the particle. We return to these intrinsically dissipative self-force corrections to the radiation field in the next chapter of this manuscript. It may be worth commenting that the factor of  $i$  between the real and imaginary parts of the waveshape is itself a signal of time-reversal violation.

We begin with electrodynamics. The waveshape in QED is remarkably simple yet it is physically interesting and closely connected to more complicated radiation fields. This is why we find it is a useful to discuss it in detail. Indeed the QED waveshape computes well-defined parts of the QCD waveshape, associated with specific ordered amplitudes. We will discuss how QED is embedded in QCD in more detail later.

In this section, we will omit certain cuts that in principle could contribute to the real part of the amplitude, but which are intuitively quantum-mechanical. Examples are the one-loop correction to the QED vertex. In the later section 6 we will return

---

<sup>5</sup>In the closed time-path (Schwinger-Keldysh) approach to computing expectation values in field theory, the  $T^\dagger$  matrix arises from the part of the contour which goes “backwards” in time.

to all of these cuts and demonstrate that they are removed by renormalisation in the real part of the waveform. They nevertheless contribute to the imaginary part: counterterms must of course be real.

## 4.1 QED

We are now at a good place to compute the QED waveshape. At NLO, this is fifth order in the coupling. But in electrodynamics we are free to give our two particles different charges  $Q_1$  and  $Q_2$ , and correspondingly the five coupling powers in the NLO waveshape can be decomposed into four different charge sectors:  $Q_1 Q_2^4$ ,  $Q_1^2 Q_2^3$ ,  $Q_1^3 Q_2^2$ , and  $Q_1^4 Q_2$ . (There can be no terms of order  $Q_1^5$  or  $Q_2^5$  since at least one photon must connect the two particles for radiation to occur.) In the language of scattering amplitudes, the one-loop five-point amplitude in QED can be decomposed into four different partial amplitudes corresponding to these four charge sectors. There are really only two independent partial amplitudes to compute, which we can take to be the  $Q_1^2 Q_2^3$  and  $Q_1 Q_2^4$  amplitudes. The  $Q_1^3 Q_2^2$  and  $Q_1^4 Q_2$  partial amplitudes can be recovered by interchanging particles 1 and 2.

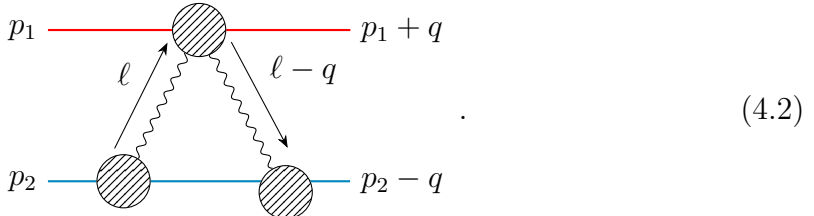
In this section, we start with the  $Q_1^2 Q_2^3$  partial amplitude. In order to show how this waveshape can be extracted most simply, it is convenient to digress briefly on a related computation: the impulse at next-to-leading order.

### NLO impulse

The impulse at NLO involves a one-loop four-point amplitude. This amplitude has real and imaginary parts, which play rather different roles in the observable. In particular, at one loop, the real part controls the scattering angle, while the imaginary part ensures that the on-shell condition is satisfied. Here it is most relevant to focus on the contribution of the real part of the amplitude to the observable, so we define

$$\Delta p_1^\mu|_{\text{real}} \equiv \int d^D q \hat{\delta}(2p_1 \cdot q) \hat{\delta}(2p_2 \cdot q) i q^\mu e^{-iq \cdot b} \text{Re } \mathcal{A}_{4,1}(p_1, p_2 \rightarrow p_1 + q, p_2 - q). \quad (4.1)$$

One-loop four-point amplitudes involve at most four propagators. In this case, two of those propagators involve photons while the other two are associated with the massive particles with momenta  $p_1$  or  $p_2$ . The real part of the amplitude arises by replacing a propagator with the corresponding delta function: this places one line on shell, effectively performing a single cut of the amplitude. First, we consider the result of placing the propagator for line 2 on shell. Diagrammatically, we must then consider



The contribution of this diagram to the amplitude is

$$\text{Re } \mathcal{A}_{4,1}|_{p_2} = \int \hat{d}^D \ell \frac{1}{\ell^2(\ell - q)^2} \frac{1}{2} \hat{\delta}(2p_2 \cdot \ell) N(\ell), \quad (4.3)$$

where  $N(\ell)$  is a numerator function we must fix.

We fix the numerator by cutting all the propagators in the diagram: we have explicitly cut the massive propagator, and any terms in  $N(\ell)$  which are proportional to  $\ell^2$  or  $(\ell - q)^2$  integrate to zero. In other words we can take each of the blobs in the diagram to be on-shell amplitudes, so that

$$N(\ell) = \sum_{\text{helicities}} \mathcal{A}_{3,0}(p_2, \ell) \mathcal{A}_{4,0}(p_1, \ell, \ell - q) \mathcal{A}_{3,0}(p_2 - \ell, \ell - q). \quad (4.4)$$

In  $D$  dimensions, the helicity sum is straightforward using formal polarisation vectors. Let us write the polarisation vector for a photon of momentum  $k$  and gauge  $q$  as  $\varepsilon(k; q)$ . If we choose the gauge to be  $q = p_1$ , then the Compton amplitude appearing in the cut is

$$\mathcal{A}_{4,0}(p_1, \ell, \ell - q) = 2Q_1^2 \varepsilon(\ell, p_1) \cdot \varepsilon^*(\ell - q, p_1). \quad (4.5)$$

The three-point amplitudes are trivially obtained from

$$\mathcal{A}_{3,0}(p_2, \ell) = 2Q_2 \varepsilon(\ell, p_1) \cdot p_2. \quad (4.6)$$

To perform the helicity sum, we only need the completeness relation which, in case of a massive gauge vector, is

$$\sum_{\text{helicities}} \varepsilon^\mu(k, q) \varepsilon^{\nu*}(k, q) = - \left( \eta^{\mu\nu} - \frac{k^\mu q^\nu + k^\nu q^\mu}{k \cdot q} + q^2 \frac{k^\mu k^\nu}{(k \cdot q)^2} \right). \quad (4.7)$$

This summation involves products of a polarisation vector and its conjugate. As usual in generalised unitarity, this structure naturally arises in the product of amplitudes appearing in the diagram (4.2) because a photon connecting two amplitudes must be outgoing with respect to one amplitude and incoming with respect to the other.

It then follows that the numerator is

$$N(\ell) = 8Q_1^2 Q_2^2 \left( m_2^2 + \frac{(p_1 \cdot p_2)^2}{(p_1 \cdot \ell)^2} \ell \cdot (\ell - q) \right). \quad (4.8)$$

As a result, the contribution to the observable is

$$\begin{aligned} \Delta p_1^\mu|_{\text{real}, p_2} &= \frac{iQ_1^2 Q_2^2}{2} \int d^D q \hat{\delta}(u_1 \cdot q) \hat{\delta}(u_2 \cdot q) q^\mu e^{-iq \cdot b} \\ &\quad \times \int \frac{\hat{d}^D \ell}{\ell^2(\ell - q)^2} \frac{\hat{\delta}(u_2 \cdot \ell)}{m_1} \left( 1 + \frac{(u_1 \cdot u_2)^2}{(u_1 \cdot \ell)^2} \ell \cdot (\ell - q) \right), \end{aligned} \quad (4.9)$$

where we used the proper velocities  $u_i = p_i/m_i$ .

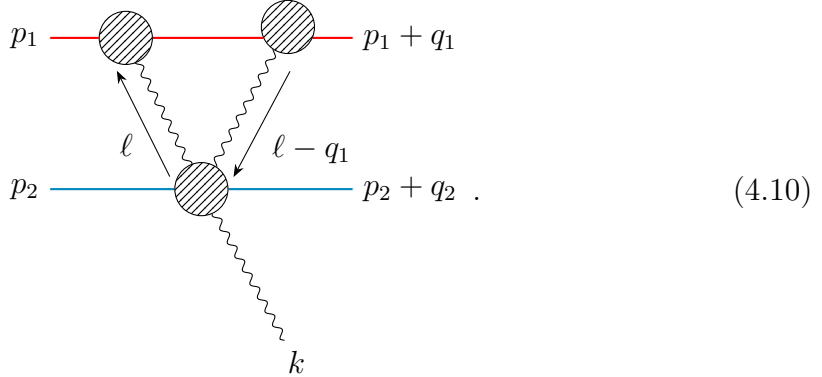
The contribution from cutting the massive propagator with incoming momentum  $p_1$  can be obtained from equation (4.9) by symmetrising on particles 1 and 2. By summing these two contributions we find agreement with the impulse given in equation 5.38 of reference [59]<sup>6</sup>.

In this way, we reproduce the one-loop impulse in a very straightforward manner. However we did so by cutting only the massive propagators, omitting possible cuts of the massless photon propagators. These cuts do not contribute to the classical impulse. Indeed, from a purely classical perspective the messengers are Fourier transforms of the Coulomb field, and therefore can transport no energy in the rest frame of the source. Thus, they cannot go on shell. From the perspective of amplitudes and cuts, one can show that when one the messenger lines are cut the resulting amplitude is suppressed by a power of  $\hbar$ . (This involves choosing a specific gauge for the polarisation objects of the messengers and a remaining cancellation among Feynman diagrams.) We shall omit this class of cuts in the following discussion for the same reason.

### Lorentz impulse: heavy mass

We now turn to the radiation at order  $Q_1^2 Q_2^3$ . Classically, this radiation results from the acceleration of particle 2 due to the Lorentz force in the field of particle 1. To determine the radiation field we recycle much of the computation of the impulse.

As in the case of the impulse above, we do not cut internal photon lines (the internal photons are both potential modes.) We focus first on the contribution arising by cutting line 1, leading to the diagram

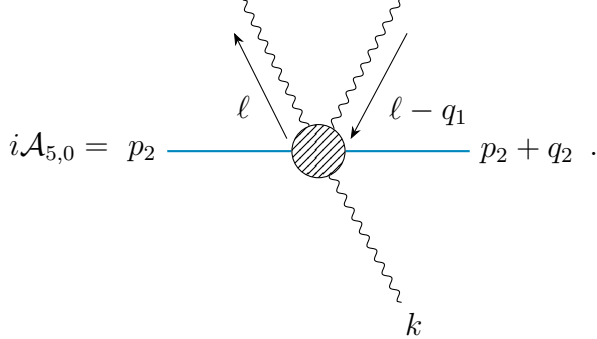


We will soon see that this diagram gives the dominant contribution to the wave-shape when the mass  $m_1$  of particle 1 is large. Its contribution to the amplitude can be computed in a manner which is almost identical to the impulse. The main novelty relative to our discussion of the impulse is the appearance of a five-point tree

---

<sup>6</sup>Terms in that equation 5.38 which involve derivatives of delta functions arise from the imaginary part of the amplitude when included correctly in the observable.

amplitude:



$$i\mathcal{A}_{5,0} = p_2 \text{ (horizontal line)} \quad p_2 + q_2 \text{ (horizontal line)} \quad (4.11)$$

If we choose the gauge of both polarisation vectors to be  $p_2$ , there are only three possible Feynman diagrams leading to a compact and (for our purposes) convenient expression for the amplitude:

$$\mathcal{A}_{5,0} = -4Q_2^3 \left[ \frac{\varepsilon^*(\ell) \cdot \varepsilon(\ell - q_1) \varepsilon^*(k) \cdot q_1}{2p_2 \cdot q_1} - \frac{\varepsilon^*(\ell) \cdot \varepsilon^*(k) \varepsilon(\ell - q_1) \cdot q_2}{2p_2 \cdot (\ell - q_1)} + \frac{\varepsilon(\ell - q_1) \cdot \varepsilon^*(k) \varepsilon^*(\ell) \cdot q_2}{2p_2 \cdot \ell} \right]. \quad (4.12)$$

Notice that the second and third terms are related by swapping the momenta  $\ell$  and  $q_1 - \ell$ . This is a symmetry of the rest of the diagram (4.10), so these last two terms in the five-point tree make an identical contribution in the cut. We do not indicate the helicity of the polarisation vectors: this information washes out in the completeness relation (since each polarisation vector in the product of amplitudes is multiplied by its conjugate polarisation).

To determine the contribution of the cut (4.10) to real part of the one-loop amplitude, we must sum the product of the five-point tree (4.12) and two three-point amplitudes over helicities. The helicity sum can be performed using the completeness relation of equation (4.7). Because the last two terms in the five-point tree (4.12) make an identical contribution to the cut, there are only two different polarisation sums to consider. The first term in equation (4.12) leads to the sum

$$\sum_{\text{helicities}} p_1 \cdot \varepsilon(\ell) p_1 \cdot \varepsilon^*(\ell - q_1) \frac{\varepsilon^*(\ell) \cdot \varepsilon(\ell - q_1) \varepsilon^*(k) \cdot q_1}{2p_2 \cdot q_1} = \left( m_1^2 + \frac{\ell \cdot (\ell - q_1) (p_1 \cdot p_2)^2}{p_2 \cdot \ell p_2 \cdot (\ell - q_1)} \right) \frac{\varepsilon^*(k) \cdot q_1}{2p_2 \cdot q_1}. \quad (4.13)$$

Notice that this term — specifically, the part appearing in brackets — bears a strong structural similarity with the numerator which appeared in the impulse, equation (4.8). The relationship between radiation and the impulse is an example of the “memory” effect, encountered here at the level of the one-loop integrand.

The second class of polarisation sum to be performed is

$$\begin{aligned} & \sum_{\text{helicities}} p_1 \cdot \varepsilon(\ell) p_1 \cdot \varepsilon^*(\ell - q_1) \frac{\varepsilon(\ell - q_1) \cdot \varepsilon^*(k) \varepsilon^*(\ell) \cdot q_2}{2p_2 \cdot \ell} \\ &= \left( p_1 \cdot q_2 + \frac{p_1 \cdot p_2 \ell \cdot q_2}{p_2 \cdot \ell} \right) \left( p_1 \cdot \varepsilon^*(k) - \frac{p_1 \cdot p_2}{p_2 \cdot (\ell - q_1)} (\ell - q_1) \cdot \varepsilon^*(k) \right) \frac{1}{2p_2 \cdot \ell}. \end{aligned} \quad (4.14)$$

Putting these together, diagram (4.10) leads to terms in the one-loop five-point amplitude given by

$$\begin{aligned} \mathcal{A}_{5,1} = & -4Q_1^2 Q_2^3 \int \frac{\hat{d}^D \ell}{\ell^2 (\ell - q_1)^2} \frac{1}{p_1 \cdot \ell + i\epsilon} \left[ \left( m_1^2 + \frac{\ell \cdot (\ell - q_1) (p_1 \cdot p_2)^2}{p_2 \cdot \ell p_2 \cdot (\ell - q_1)} \right) \frac{\varepsilon^*(k) \cdot q_1}{p_2 \cdot q_1} \right. \\ & + \left. \left( p_1 \cdot q_2 + \frac{p_1 \cdot p_2 \ell \cdot q_2}{p_2 \cdot \ell} \right) \left( p_1 \cdot \varepsilon^*(k) - \frac{p_1 \cdot p_2}{p_2 \cdot (\ell - q_1)} (\ell - q_1) \cdot \varepsilon^*(k) \right) \frac{2}{p_2 \cdot \ell} \right] + \dots, \end{aligned} \quad (4.15)$$

where the ellipsis indicates terms not captured by the cut.

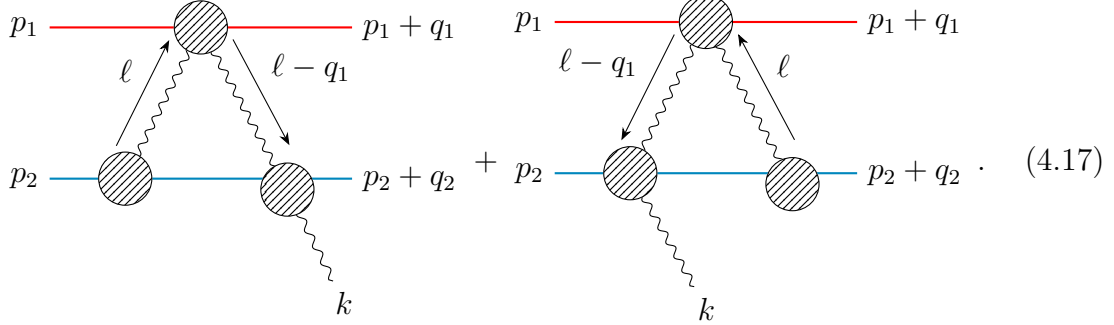
The contribution of this part of the amplitude to the waveshape involves taking the imaginary part of the explicit massive propagator. Including the rest of the structure of the waveshape, we find

$$\begin{aligned} \alpha_\eta(k)|_1 = & \frac{iQ_1^2 Q_2^3}{2m_1 m_2} \int \hat{d}^4 q_1 \hat{d}^4 q_2 \hat{\delta}(q_1 \cdot u_1) \hat{\delta}(q_2 \cdot u_2) \hat{\delta}^D(q_1 + q_2 + k) e^{-iq_1 \cdot b_1} e^{-iq_2 \cdot b_2} \\ & \times \int \frac{\hat{d}^4 \ell}{\ell^2 (\ell - q_1)^2} \hat{\delta}(p_1 \cdot \ell) \left[ \left( m_1^2 + \frac{\ell \cdot (\ell - q_1) (p_1 \cdot p_2)^2}{p_2 \cdot \ell p_2 \cdot (\ell - q_1)} \right) \frac{\varepsilon^*(k) \cdot q_1}{p_2 \cdot q_1} \right. \\ & + \left( p_1 \cdot \varepsilon^*(k) - \frac{p_1 \cdot p_2}{p_2 \cdot (\ell - q_1)} (\ell - q_1) \cdot \varepsilon^*(k) \right) \frac{2p_1 \cdot q_2}{p_2 \cdot \ell} \\ & \left. + \left( p_1 \cdot \varepsilon^*(k) - \frac{p_1 \cdot p_2}{p_2 \cdot (\ell - q_1)} (\ell - q_1) \cdot \varepsilon^*(k) \right) \frac{2p_1 \cdot p_2 \ell \cdot q_2}{(p_2 \cdot \ell)^2} \right]. \end{aligned} \quad (4.16)$$

To see how this term scales with the masses of the particles, scale the masses out from the momenta via  $p_i = m_i u_i$ . It is then clear that this part of the waveshape is proportional to  $m_1^0 m_2^{-2}$  so that, as we advertised above, this cut corresponds to the radiation emitted in the large  $m_1$  limit.

### Lorentz impulse: symmetric mass

The remaining single-particle cuts at order  $Q_1^2 Q_2^3$  are proportional to  $1/(m_1 m_2)$ . The cut diagrams are:



This topology can easily be determined using the methods discussed above; the only (slight) novelty is that the two Compton amplitudes which appear are most simply evaluated in terms of polarisation vectors in different gauges. Both diagrams make an equal contribution to the waveform so we may study only the first diagram.

The contribution of this diagram to the one-loop five-point amplitude can be written as

$$i\mathcal{A}_{5,1}^B = -i \int \frac{\hat{d}^D \ell}{\ell^2 (\ell - q_1)^2} \frac{1}{-2p_2 \cdot \ell + i\epsilon} K^B, \quad (4.18)$$

where  $K^B$  is the evaluation of the cut, namely

$$iK^B = -8iQ_1^2 Q_2^3 \sum_{\text{helicities}} p_2 \cdot \varepsilon^*(\ell) \varepsilon(\ell, p_1) \cdot \varepsilon^*(\ell - q_1, p_1) \varepsilon(\ell - q_1, p_2) \cdot \varepsilon^*(k, p_2). \quad (4.19)$$

We have introduced the notation  $\varepsilon(k, p)$  for the polarisation vectors corresponding to a photon with momentum  $k$  in gauge  $p$ . Note that we used different gauges for the polarisation vectors in different tree Compton amplitudes in the cut. However, it is an easy matter to change the gauge, and in particular we find it convenient to write

$$\varepsilon^\mu(\ell - q_1, p_1) = \varepsilon^\mu(\ell - q_1, p_2) - (\ell - q_1)^\mu \frac{p_1 \cdot \varepsilon(\ell - q_1, p_2)}{p_1 \cdot \ell}. \quad (4.20)$$

The helicity sum can then be performed in  $D$  dimensions straightforwardly. The contribution of the cut to the waveform is

$$\begin{aligned} \frac{iQ_1^2 Q_2^3}{m_1 m_2} & \int \hat{d}^D q_1 \hat{d}^D q_2 \hat{\delta}(q_1 \cdot u_1) \hat{\delta}(q_2 \cdot u_2) \hat{\delta}^D(q_1 + q_2 + k) e^{-iq_1 \cdot b_1} e^{-iq_2 \cdot b_2} \\ & \times \int \hat{d}^D \ell \frac{\hat{\delta}(u_2 \cdot \ell)}{\ell^2 (\ell - q_1)^2} K^B. \end{aligned} \quad (4.21)$$

where the quantity  $K^B$ , which is directly proportional to the polarisation sum, is

$$\begin{aligned}
K^B = & \frac{1}{(u_1 \cdot \ell)^2} \left[ u_1 \cdot \varepsilon^*(k, p_2) (u_1 \cdot \ell u_2 \cdot q_1 - u_1 \cdot u_2 \ell \cdot q_1) \right. \\
& + (\ell - q_1) \cdot \varepsilon^*(k, p_2) \left( u_1 \cdot u_2 u_1 \cdot \ell - \frac{(u_1 \cdot u_2)^2 \ell \cdot q_1}{u_2 \cdot q_1} + \frac{(u_1 \cdot \ell)^2}{u_2 \cdot q_1} \right) \\
& \left. - \ell \cdot \varepsilon^*(k, p_2) u_1 \cdot u_2 u_1 \cdot \ell \right]. \tag{4.22}
\end{aligned}$$

It is straightforward to recover  $Q_1^3 Q_2^2$  terms in the waveshape by swapping the particle labels 1 and 2. The  $Q_1^4 Q_2$  and  $Q_1 Q_2^4$  partial waveshapes are described below.

We have tested these results in a number of ways. Firstly, we have compared our expressions to the one-loop five-point Yang-Mills amplitudes presented in [29]. We also compared with the work of Shen [58], who iterated the classical equations to this order. Some care has to be taken to remove divergent terms in the results of reference [58] which result from Shen's merging procedure. Nevertheless we found agreement in this sector. Finally, as described below, we have performed our own computation in the classical theory and find full agreement.

## 4.2 QCD

Let us move to Yang-Mills at this point, and analyse some of the main features of the waveshape in QCD. For the purposes of our paper, the main difference between QED and Yang-Mills amplitudes is the handling of color degrees of freedom. In fact, now the waveshape will also include various color-dependent factors which enter diagram vertices. Here, we choose to represent the massive scalars and gluons in our problem in the fundamental  $T_{ij}^a$  and adjoint  $f^{abc}$  representation of the color group, respectively.

Our strategy is to proceed in the usual way, by exploiting the following gauge theory structure

$$\begin{aligned}
[T^a, T^b]_{ij} &= f^{abc} T_{ij}^c, \\
f^{dac} f^{cbe} - f^{dbc} f^{cae} &= f^{abc} f^{dce}, \tag{4.23}
\end{aligned}$$

to organise and expand our amplitudes (or cuts thereof) in a color basis, and focus on each gauge invariant sector independently.

Schematically, the one-loop amplitude can be expanded in a basis of color coefficients

$$\begin{aligned}
\mathcal{A}_{5,1}(p_1 \dots k) = & \mathcal{C} \left( \text{Diagram 1} \right) A_1 + \mathcal{C} \left( \text{Diagram 2} \right) A_2 \\
& + \mathcal{C} \left( \text{Diagram 3} \right) A_3 + \mathcal{C} \left( \text{Diagram 4} \right) A_4 + \mathcal{C} \left( \text{Diagram 5} \right) A_5 + \dots, \tag{4.24}
\end{aligned}$$

where  $A_i$  is the partial amplitude corresponding to the color factor  $C_i$ , and the expression in the ellipsis includes quantum corrections. Once the full amplitude is

Color type	$A_i$	Topologies
$\mathcal{C} \left( \text{Diagram} \right)$	$A_1, A_2$	
$\mathcal{C} \left( \text{Diagram} \right)$	$A_3$	
$\mathcal{C} \left( \text{Diagram} \right)$	$A_4, A_5$	

**Table 1:** Topologies contributing to the partial amplitudes of the color factors  $\mathcal{C}$ .

organised in terms of independent partial amplitudes, we can consider the classical limit of each one separately. However, now we have to restore factors of  $\hbar$  in both momenta and color coefficients, according to the prescription of [22].

We now take a moment to consider the partial amplitudes in (4.24). As we show in Table 1 – where we list the topologies appearing in the partial amplitudes –  $A_1$  and  $A_2$  involve only diagrams with no non-Abelian (pure-gluon) vertices. We recognise these as the QED amplitude sectors computed in the previous section. The contributions from these sectors can therefore be plugged into the QCD expression simply by dressing them with their given color factor. In this section we therefore focus on the terms which appear for the first time in the case of QCD – namely  $A_3$ ,  $A_4$  and  $A_5$ . As shown in Table 1 these partial amplitudes do involve non-Abelian topologies and must be calculated to find the full QCD result. We will refer to  $A_3$  and  $A_4$ ,  $A_5$  as the *pentagon-* and *maximally non-Abelian* partial amplitudes, respectively.

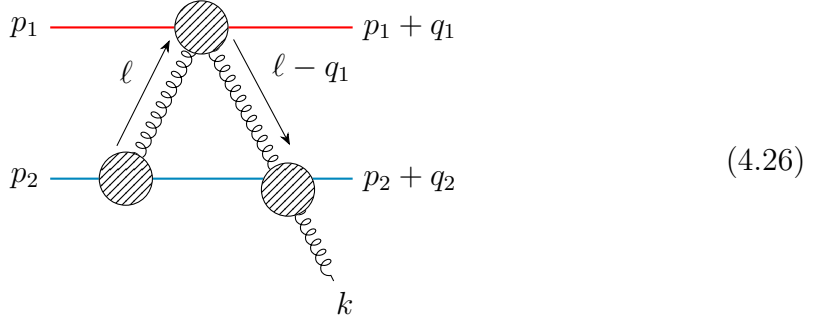
### Pentagon

We begin by looking at the partial amplitude  $A_3$ . The color factor of this amplitude is simply the color structure of the pentagon topology, given by

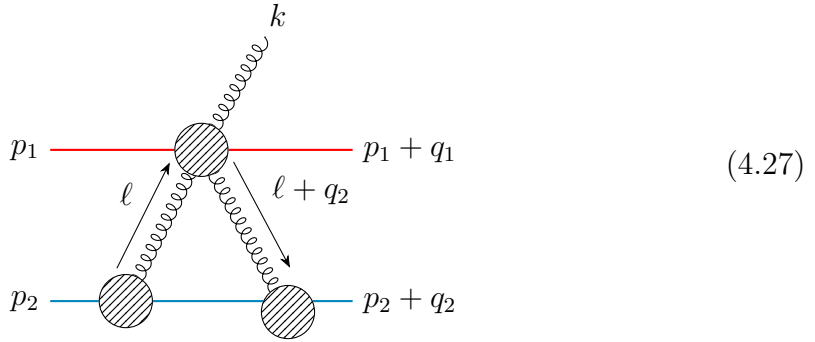
$$\mathcal{C} \left( \text{Diagram} \right) = f^{abc} C_1^b \cdot C_1^d C_2^c \cdot C_2^d, \quad (4.25)$$

where  $A$  is the adjoint index of the emitted gluon and  $C_i^a$  is the classical color charge of the massive body  $i$  [22]. In this section we will only discuss cutting the  $p_2$  propagator, as remaining cuts can be obtained by relabelling particles. There are

two cuts to consider:



and



We analyse the cuts along the same lines as in QED, extract the coefficient of the pentagon color factor, and merge the resulting expressions. For instance, the contribution of the first cut to the pentagon involves two Compton amplitudes. Here, the color structure (4.25) is obtained through the following observation. The YM-Compton can be essentially written only in terms of the QED one,<sup>7</sup> which is just  $\propto \varepsilon_1 \cdot \varepsilon_2$  in a convenient gauge. In fact, one finds

$$\mathcal{A}_{4,0} = 2ig^2 C_i^a C_i^b \varepsilon_1 \cdot \varepsilon_2 + 2g^2 f^{abc} C_i^c \frac{2p \cdot k_1}{q^2} \varepsilon_1 \cdot \varepsilon_2. \quad (4.28)$$

Then, in the cut 4.26 using the first term above for the upper sub-amplitude and the second for the lower one we reconstruct (4.25). Furthermore, since the polarisation vector structure is the same as in the symmetric-mass QED case, we can reuse our evaluation (4.22) of the quantity  $K^B$  in this cut.

The second cut requires parts of the QCD five-point amplitude. We may restrict to those parts of the amplitude which involve a single  $f^{abc}$  color structure to match to this pentagon. The relevant terms in the amplitude are

$$i\mathcal{A}_{5,0}^{(1f)} = \frac{4g^3 f^{abd} C_1^c C_1^d}{(k_1 + k_2)^2} \left[ \varepsilon_1 \cdot k_2 \varepsilon_2 \cdot \varepsilon_3 + \frac{\varepsilon_1 \cdot \varepsilon_2}{p \cdot (k_1 + k_2)} p \cdot k_2 \varepsilon_3 \cdot k_1 - (1 \leftrightarrow 2) \right] + \text{cycles}. \quad (4.29)$$

---

<sup>7</sup>The importance of this point was already stressed in [146]. One can verify this explicitly in  $D = 4$  or, perhaps even more clearly, by dimensionally reducing the  $D = 6$  amplitudes of [147].

We extract from this contribution terms which are missed by the previous cut. Here, it will be convenient to work in the gauge  $p_1 \cdot \varepsilon = 0$  for all external gluons, so we get to use the completeness relation (4.7) with  $q = p_1$ . At the end, we find the following expression for the real-part of the pentagon partial amplitude

$$\begin{aligned} \text{Re } A_3 = g^5 \int \hat{d}^D \ell \frac{\hat{\delta}(\ell \cdot p_2)}{\ell^2 (\ell + q_2)^2 (\ell - q_1)^2} & \left[ \left( \varepsilon^* \cdot p_2 \frac{p_1 \cdot p_2}{p_1 \cdot \ell} + \varepsilon^* \cdot q_2 \frac{(p_1 \cdot p_2)^2}{p_1 \cdot \ell p_1 \cdot k} \right) \frac{(\ell - q_1)^2}{2} \right. \\ & - \varepsilon^* \cdot p_2 \left( \frac{(k \cdot p_2)^2}{p_1 \cdot \ell} + \frac{p_1 \cdot \ell \ell \cdot k + p_1 \cdot k \ell \cdot q_1}{(p_1 \cdot \ell)^2} \right) + \varepsilon^* \cdot \ell \frac{p_1 \cdot p_2 p_2 \cdot k}{p_1 \cdot \ell} \\ & \left. + \varepsilon^* \cdot (\ell + q_2) \left( p_2^2 + \frac{p_1 \cdot p_2}{p_1 \cdot \ell} p_2 \cdot q_1 - \left( \frac{p_1 \cdot p_2}{p_1 \cdot \ell} \right)^2 \ell \cdot q_1 \right) \right]. \end{aligned} \quad (4.30)$$

### Maximally non-Abelian partial amplitude

Two of the most physically interesting gauge invariant sectors are  $A_4$  and  $A_5$ . We will refer to as “maximally non-Abelian” as their color factors involve two structure constants. Noting that these two sectors are related by particle relabelling, we will focus on  $A_4$  only. The color structure corresponding to this partial amplitude is now

$$C \left( \begin{array}{c} \textcolor{red}{\nearrow} \\ \textcolor{blue}{\square} \end{array} \right) = C_1^a f^{adb} f^{dAc} C_2^c \cdot C_2^b. \quad (4.31)$$

To compute the real part of  $A_4$  we work along the same lines of 4.1 and 4.2, so we skip some of the technical steps in this chapter. Furthermore, in order to avoid proliferation of long formulae, we only detail terms which involve a  $1/q_1^2$  denominator. In fact, this pole is important for radiation reaction purposes as we will explain later. We find that, for the aforementioned pole

$$\text{Re } A_4 \rightarrow \frac{16g^5 m_1 m_2}{q_1^2} \int \hat{d}^D \ell \hat{\delta}(u_2 \cdot \ell) \varepsilon_\eta^*(k) \cdot \sum_{i=1}^4 J_i, \quad (4.32)$$

from cutting line 2. Above, we have conveniently defined the vectors  $J_i^\mu$  as

$$J_1^\mu = -\frac{\ell^\mu}{(\ell + q_2)^2 (\ell - q_1)^2} \left( \frac{\gamma}{4 u_2 \cdot q_1} + \frac{\ell \cdot u_1}{\ell^2} \right), \quad (4.33)$$

$$J_2^\mu = \frac{q_1^\mu}{\ell^2 (\ell + q_2)^2 (\ell - q_1)^2} (\ell \cdot u_1 + \gamma u_2 \cdot q_1), \quad (4.34)$$

$$J_3^\mu = \frac{u_1^\mu}{\ell^2} \left( \frac{1}{4(\ell + q_2)^2} - \frac{(u_2 \cdot q_1)^2}{(\ell + q_2)^2 (\ell - q_1)^2} \right), \quad (4.35)$$

$$J_4^\mu = \frac{u_2^\mu}{\ell^2} \left( -\frac{\ell \cdot u_1}{4(\ell - q_1)^2 u_2 \cdot q_1} - \frac{\gamma}{4(u_2 \cdot q_1)^2} + \frac{(\gamma q_1 \cdot q_2 - q_1 \cdot u_2 q_2 \cdot u_1)}{(\ell + q_2)^2 (\ell - q_1)^2} \right). \quad (4.36)$$

This gauge invariant sector is actually simple enough that it can also be described through Feynman diagrams. Indeed, classically we find that only five diagrams contribute to  $A_4$ . These are

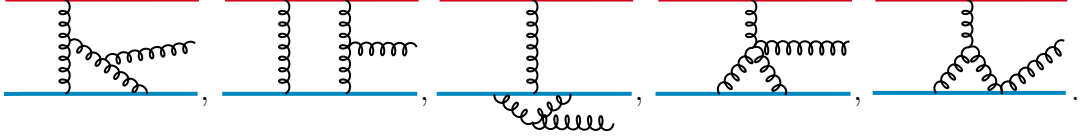
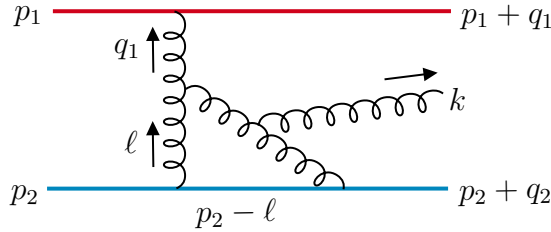


**Figure 1:** Feynman diagrams contributing classically to  $A_4$ .

Thus, we find it instructive to see how (4.32) can also be derived this way. To this end, and to further ease our narrative, we employ the gauge  $\varepsilon \cdot u_2 = 0$  and only look at the propagator structure

$$P^{-1} = \ell^2(\ell + q_2)^2(\ell - q_1)^2. \quad (4.37)$$

Then, it turns out that such pieces arise from the following diagram only



Using usual scalar QCD Feynman rules, this diagram is seen to correspond to

$$\text{Re } A_4 \rightarrow \frac{4g^5 m_1 m_2}{q_1^2} \int \hat{d}^D \ell \hat{\delta}(u_2 \cdot \ell) \frac{N}{\ell^2(\ell + q_2)^2(\ell - q_1)^2}. \quad (4.38)$$

Above, the numerator is found to have the following expression

$$N = u_1^\alpha \Pi_{\alpha\beta\gamma}(-q_1, q_1 - \ell, \ell) u_2^\gamma \Pi^{\beta\rho\sigma}(\ell - q_1, -k, -\ell - q_2) \varepsilon_{\eta, \rho}^*(k) u_2 \sigma, \quad (4.39)$$

where we conveniently defined the three gluon vertex with all incoming momenta as

$$\Pi_{\alpha\beta\gamma}(k, q, r) \equiv (k - q)_\gamma \eta_{\alpha\beta} + (q - r)_\alpha \eta_{\beta\gamma} + (r - k)_\beta \eta_{\alpha\gamma}. \quad (4.40)$$

Let us focus on this numerator then. A little algebra shows that this reduces to

$$N = -4\varepsilon_\eta^* \cdot \ell \ell \cdot u_1 + 4\varepsilon_\eta^* \cdot q_1 (\ell \cdot u_1 + \gamma q_1 \cdot u_2) - 4\varepsilon_\eta^* \cdot u_1 (q_1 \cdot u_2)^2, \quad (4.41)$$

which is valid on shell of the delta functions and classically. The remaining propagator structures can be confirmed in the same fashion. We omit their derivations since they are straightforward and do not present any new features. Furthermore we have checked (4.32) both against the results of [58] and with our automated code.

We will soon see how this kinematic sector is also responsible for non-Abelian radiation reaction.

## 5 Reaction

As we have seen in section 4.1 our amplitude expressions are well able to reproduce conservative classical data. In this part of the paper we show that the same happens for non conservative effects. For example, such contributions to observables can be explained in terms of the ALD force (after Abraham, Lorentz and Dirac) in classical electrodynamics, see for instance [59]. However, treatment of dissipative forces in both QCD and gravity is, at best, much more challenging. This is why our goal here is to show how these subtle classical effects can be treated in a concise and universal manner through amplitudes. As we will see, it is the imaginary part of amplitudes that has the effect of sourcing dissipation in this context. Not only that, in appendix A we show how cuts and imaginary parts are inherently related to classical electromagnetic forces.

Incidentally, as perhaps overlooked until now, we also demonstrate how radiation reaction enters the waveshape already at one loop. In fact, usually one has to deal with it at two loops of higher when computing momentum deflections [59, 110].

### 5.1 QED radiation reaction...

Let us begin with electrodynamics. As elucidated in section 2.2, to discuss non conservative dynamics we will only need the imaginary part of the amplitude. To be more precise, we will consider cuts in the channel involving Compton amplitudes. Indeed, we learnt in section 3.3 that these are the only ones that are not subtracted classically. Furthermore, as to the the real part of such diagrams, we expect this to be rendered quantum by an appropriate choice of renormalisation scheme. In fact, we will explicitly show how this happens in QED in the next chapter<sup>8</sup>. Conveniently for us,  $\text{Im } \mathcal{A}$  is simply obtained by appropriately cutting all relevant diagrams at this order. For simplicity we will be taking particle 1 to be static:  $m_2/m_1 \ll 1$ .

We start by considering cuts of diagrams of the following type

---

<sup>8</sup>Furthermore, see for instance [59].

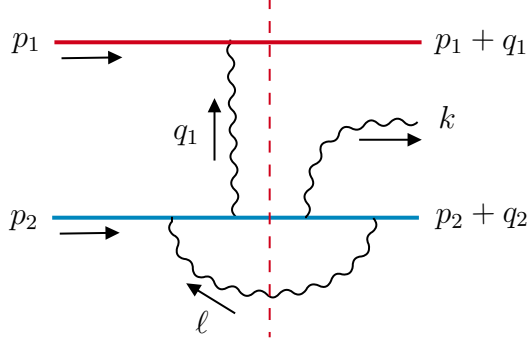


**Figure 2:** One of the Feynman diagram cuts needed for the radiated waveform calculation. The arrows indicate momentum flow.

To ease our calculation we will employ another useful trick. This consists of placing the  $q_1$  photon line on-shell too. Being rigorous, we shouldn't be allowed to do so: this cut isolates a tree point amplitude which vanishes on-shell in Minkowski. Nevertheless, it turns out that we can effectively cut this line as well. In fact, multiplying  $1/q_1^2$  by  $q_1^2$  does not strictly yield zero, but only gives a contact term which integrates to zero. Thus, for all our purposes  $1/q_1^2 \propto \delta(q_1^2)$ .

With these considerations in place, we can realise that we only need cuts of the following type

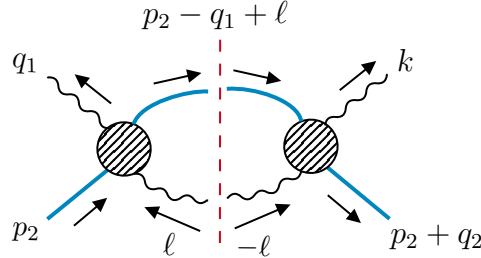


**Figure 3:** Unitarity cut isolating two tree level Compton amplitudes (5.1).

which are two particle cuts separating two tree level Compton amplitudes. We write such four point amplitude as

$$\mathcal{A}_{4,0}(p_1, k_1 \rightarrow p_2, k_2) = 2iQ^2 \varepsilon_\eta^\mu(k_1) \varepsilon_{\eta'}^{*\nu}(k_2) \mathcal{J}_{\mu\nu}(p_1, k_1 \rightarrow p_2, k_2), \quad (5.1)$$

where we are taking  $p_1, k_1$  incoming and  $p_2, k_2$  outgoing. Above, we have also defined

$$\mathcal{J}_{\mu\nu}(p_1, k_1 \rightarrow p_2, k_2) = \frac{p_{1\mu} p_{2\nu}}{p_1 \cdot k_1} + \frac{p_{2\mu} p_{1\nu}}{-p_1 \cdot k_2} - \eta_{\mu\nu}, \quad p_1 + k_1 = p_2 + k_2, \quad (5.2)$$

satisfying

$$\mathcal{J}_{\mu\nu} k_1^\mu \varepsilon^\nu(k_2) = \mathcal{J}_{\mu\nu} \varepsilon^\mu(k_1) k_2^\nu = 0. \quad (5.3)$$

Making use of these definitions, the cut is given explicitly by

$$\begin{aligned} \text{Cut}_2 = -4Q^4 \sum_{\eta''} \int \hat{d}^D \ell \hat{\delta}(2p_2 \cdot (\ell - q_1)) \hat{\delta}(\ell^2) \varepsilon_{\eta}^{*\mu}(q_1) \varepsilon_{\eta''}^{\nu}(\ell) \varepsilon_{\eta''}^{*\rho}(\ell) \varepsilon_{\eta'}^{*\sigma}(k) \\ \times \mathcal{J}_{\mu\nu}(p_2, -q_1 \rightarrow p_2 - q_1 + \ell, -\ell) \mathcal{J}_{\rho\sigma}(p_2 - q_1 + \ell, -\ell \rightarrow p_2 + q_2, k). \end{aligned} \quad (5.4)$$

We now proceed by using, just as in the previous sections, the gauge where  $\varepsilon \cdot p_2 = 0$ . This means performing the helicity sum through (4.7) with  $q = p_2$ . One soon obtains

$$\text{Cut}_2 = \frac{2Q^4}{m_2} \int \hat{d}^D \ell \hat{\delta}(u_2 \cdot (\ell - q_1)) \hat{\delta}(\ell^2) \left( \frac{\varepsilon_{\eta}^{*}(q_1) \cdot \ell \varepsilon_{\eta'}^{*}(k) \cdot \ell}{(u_2 \cdot q_1)^2} + \varepsilon_{\eta}^{*}(q_1) \cdot \varepsilon_{\eta'}^{*}(k) \right). \quad (5.5)$$

The loop integrals are easy to do here. The scalar one was first evaluated in [59]

$$\int \hat{d}^D \ell \hat{\delta}(u_2 \cdot (\ell - q_1)) \hat{\delta}(\ell^2) = \frac{u_2 \cdot k}{2\pi} \Theta(u_2 \cdot k), \quad (5.6)$$

and the tensor one follows by reduction. We obtain

$$\int \hat{d}^D \ell \hat{\delta}(u_2 \cdot (\ell - q_1)) \hat{\delta}(\ell^2) \ell^{\mu} \ell^{\nu} = -\frac{(u_2 \cdot k)^3}{2\pi(D-1)} (\eta^{\mu\nu} - D u_2^{\mu} u_2^{\nu}) \Theta(u_2 \cdot k), \quad (5.7)$$

finally leading to, taking  $D = 4$

$$\begin{aligned} \text{Cut}_2 &= \frac{2Q^4}{m_2} \int \hat{d}^4 \ell \hat{\delta}(u_2 \cdot (\ell - q_1)) \hat{\delta}(\ell^2) \left( \frac{\varepsilon_{\eta}^{*}(q_1) \cdot \ell \varepsilon_{\eta'}^{*}(k) \cdot \ell}{(u_2 \cdot q_1)^2} + \varepsilon_{\eta}^{*}(q_1) \cdot \varepsilon_{\eta'}^{*}(k) \right) \\ &= \frac{2Q^4}{m_2} u_2 \cdot k \Theta(u_2 \cdot k) \frac{1}{3\pi} \varepsilon_{\eta}^{*}(q_1) \cdot \varepsilon_{\eta'}^{*}(k). \end{aligned} \quad (5.8)$$

This result is quite simple and remarkable: the cut isolating two Compton amplitudes is proportional to a tree-level Compton amplitude itself (in the  $\varepsilon \cdot p_2$  gauge) times a geometric factor  $1/6\pi$ .

Having computed the two particle cut, we now have to fuse back the three point amplitude we had isolated at the start. To do so we reintroduce polarisation vectors in a generic gauge, getting

$$\varepsilon_{\eta}^{*}(q_1) \cdot \varepsilon_{\eta'}^{*}(k) = \varepsilon_{\eta}^{*\mu}(q_1) \varepsilon_{\eta'}^{*\nu}(k) \mathcal{J}_{\mu\nu}(p_2, -q_1 \rightarrow p_2 + q_2, k). \quad (5.9)$$

This allows us to obtain the total five point cut-amplitude  $\text{Cut}_3(q_1, k) \equiv \text{Cut}[\mathcal{A}_{5,1}(q_1, k)]$  from tree-level unitarity. At this point we also dress electric couplings with particle labels  $Q \rightarrow Q_i$

$$\begin{aligned} \text{Cut}_{3,\eta'} &= \frac{iQ_1}{q_1^2} \sum_{\eta} (2p_1 + q_1)_{\rho} \varepsilon_{\eta}^{\rho}(q_1) \text{Cut}_{2,\eta\eta'}(q_1, k) \\ &= \frac{4iQ_1 Q_2^4}{m_2^2} \frac{p_2 \cdot k}{3\pi} \frac{1}{q_1^2} \left( p_1 \cdot \varepsilon_{\eta'}^{*}(k) - \frac{\varepsilon_{\eta'}^{*}(k) \cdot p_2 p_1 \cdot k}{k \cdot p_2} \right. \\ &\quad \left. + \frac{p_1 \cdot p_2 \varepsilon_{\eta'}^{*}(k) \cdot q_1}{p_2 \cdot k} - \frac{p_1 \cdot p_2 \varepsilon_{\eta'}^{*}(k) \cdot p_2 k \cdot q_1}{(p_2 \cdot k)^2} \right). \end{aligned} \quad (5.10)$$

Above we have also set  $\Theta(u_2 \cdot k) = 1$ , which holds on the support of the  $d\Phi(k)$  integral of (2.10). Finally observe that  $2i \operatorname{Im} \mathcal{A} = \operatorname{Disc} \mathcal{A}$  where the cutting rules give the latter, thus the imaginary part of the amplitude is

$$\operatorname{Im} \mathcal{A}_{5,1} = \frac{4Q_1 Q_2^4}{m_2^2} \frac{p_2 \cdot k}{6\pi} \frac{1}{q_1^2} \left( p_1 \cdot \varepsilon_{\eta'}^*(k) - \frac{\varepsilon_{\eta'}^*(k) \cdot p_2 p_1 \cdot k}{k \cdot p_2} + \frac{p_1 \cdot p_2 \varepsilon_{\eta'}^*(k) \cdot q_1}{p_2 \cdot k} - \frac{p_1 \cdot p_2 \varepsilon_{\eta'}^*(k) \cdot p_2 k \cdot q_1}{(p_2 \cdot k)^2} \right). \quad (5.11)$$

We find the end result of our derivation to be evocative and simple: the classical one-loop five-point amplitude is, up to a factor, the tree level one times  $p_2 \cdot k$ . To complete the waveform calculation we substitute the amplitude into (2.10), giving

$$F^{\mu\nu}(x) = -i \frac{Q_1 Q_2^4}{6\pi m_2^2} \sum_{\eta} \int d\Phi(k) \int \hat{d}^4 q_1 \hat{d}^4 q_2 \hat{\delta}(q_1 \cdot u_1) \hat{\delta}(q_2 \cdot u_2) \hat{\delta}^4(k + q_1 + q_2) \times \frac{k \cdot u_2}{q_1^2} k^{[\mu} \varepsilon_{\eta}^{\nu]} \varepsilon_{\eta}^* \cdot \mathcal{J}(k, q_1) e^{-i(k \cdot x + q_1 \cdot b_1 + q_2 \cdot b_2)} + c.c. \quad (5.12)$$

Where we defined for convenience the classical current

$$\mathcal{J}^{\nu}(k, q_1) = \left( u_1^{\nu} + q_1^{\nu} \frac{u_1 \cdot u_2}{k \cdot u_2} - u_2^{\nu} \frac{k \cdot u_1}{k \cdot u_2} - u_2^{\nu} \frac{u_1 \cdot u_2 k \cdot q_1}{(k \cdot u_2)^2} \right) = \mathcal{J}^{\nu}(-k, -q_1). \quad (5.13)$$

In 7, we will explain how this contribution can be interpreted purely classically. This will be done through a derivation of the waveform that makes judicious use of the ALD force.

## 5.2 ...QCD radiation reaction...

We now analyse in some detail the non conservative dynamics of QCD. As it happens, the preparatory work of 4.2 will be very convenient for us.

In non-Abelian theories radiation reaction will be present as well, only under a more sophisticated disguise. In fact, from an amplitude standpoint, self force effects can be sourced by every diagram which has a cut isolating a Compton amplitude. As we explained, these cuts will yield an imaginary part of the waveshape that is not subtracted classically. What is more in Yang-Mills, is that we will have QED-like contributions as well as purely non-Abelian ones which involve three or four gluon vertices. We find that the non-Abelian radiation reaction channels are precisely those characterised by  $A_4$  (and  $A_5$ ) which we studied in section 4.2.

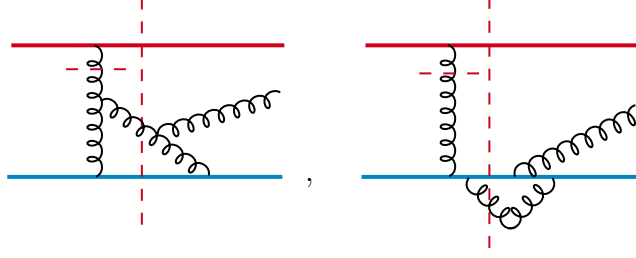


**Figure 4:** Two cuts contributing to non-Abelian radiation reaction. While the second cut appears in both kinematic sectors  $A_4$  (through a sub-sub-leading  $\hbar$  expansion of its color) and  $A_2$  (here with a leading color factor), the first topology belongs in  $A_4$  only. Here, we have also cut the single gluon line as explained in 5.1.

Let us then compute the radiation reaction diagrams of QCD. As before, we consider the following cut diagram

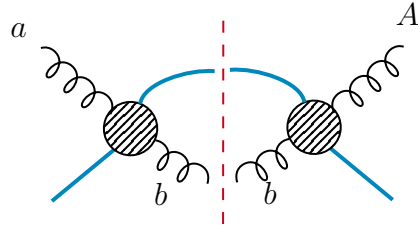


**Figure 5:** Cut relevant to radiation reaction in QCD. For clarity we have just indicated color indices, momentum routing is the same as in figure 3.

We keep in mind that the gluon  $a$  will have to be joined to particle 1. Indicating the full left/right YM Compton amplitudes with  $\mathcal{A}_{L,R}^{ab}$  the diagram reads

$$\text{Cut}_2 = \sum_{\text{helicities}} \int d\Phi(\ell) \hat{\delta}(2p_2 \cdot (\ell - q_1)) \mathcal{A}_L^{ab} \cdot \mathcal{A}_R^{bA}. \quad (5.14)$$

At this point it is useful to note again that the non-Abelian Compton amplitude  $\mathcal{A}^{ab} \equiv \mathcal{A}_{4,0}^{ab}$  can be written as (4.28)

$$\mathcal{A}^{ab} = C^a \cdot C^b A + f^{abc} C^c A', \quad (5.15)$$

where *both*  $A$  and  $A'$  are abelian Compton amplitudes, which differ only by a factor. Using this piece of knowledge we can expand the integrand in the following manner

$$\begin{aligned} \mathcal{A}_L^{ab} \cdot \mathcal{A}_R^{bA} &= (C_2^a \cdot C_2^b A_L + f^{abd} C_2^d A'_L) \cdot (C_2^b \cdot C_2^A A_R + f^{bAe} C_2^e A'_R) \\ &\approx C_2^a \cdot C_2^b \cdot C_2^b \cdot C_2^A A_L A_R + f^{abd} f^{bAe} C_2^d \cdot C_2^e A'_L A'_R, \end{aligned} \quad (5.16)$$

having ignored the cross terms since it's quantum.

Now, the simple relation above makes it very easy to interpret the structure of the cut in non-Abelian gauge theories. The first term in (5.16), the one proportional to  $C_2^a \cdot C_2^b \cdot C_2^b \cdot C_2^A$ , is exactly the one already encountered in QED in (5.8)! That is to say that

$$\sum_{\text{helicities}} \int d\Phi(\ell) \hat{\delta}(2p_2 \cdot (\ell - q_1)) A_L A_R = \frac{2g^4}{m_2} u_2 \cdot k \frac{1}{3\pi} \varepsilon_\eta^*(q_1) \cdot \varepsilon_{\eta'}^*(k). \quad (5.17)$$

In other words, what we had computed in QED was also part of the QCD story, only now multiplied by a constant color structure. It is immediate to see that the last, non-Abelian, term of (5.16) has (up to relabelling) the structure (4.31). This is precisely the color of the partial amplitude  $A_4$ . Then, for the computation of this channel we need precisely the  $1/q_1^2$  pole that we described in (4.32), entailing non-Abelian radiation reaction. From (4.32), the imaginary part of the five point amplitude is immediately obtained and it reads

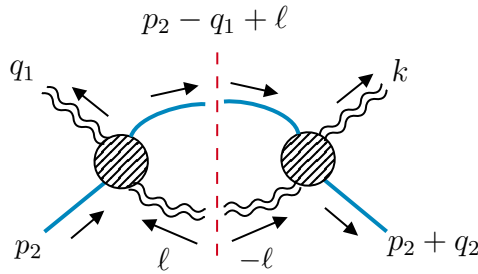
$$\text{Im } A_4 = \frac{8g^5 m_1 m_2}{q_1^2} \varepsilon_\mu^*(k) \int d\Phi(\ell) \hat{\delta}(u_2 \cdot (\ell - q_1)) \frac{(u_1 \cdot \ell + \gamma q_1 \cdot u_2) q_1^\mu - (u_2 \cdot q_1)^2 u_1^\mu}{(q_1 - \ell)^2 (\ell + k)^2}, \quad (5.18)$$

in a gauge where  $\varepsilon \cdot p_2 = 0$ .

### 5.3 ...GR radiation reaction

As a final application of this chapter, we will here tackle gravity self force radiation. This will indeed demonstrate how the dissipative effects are cleanly taken into account by our analytic framework.

Following the examples of QED and QCD we again focus on the 2-particle cut, just involving graviton lines now



having taken the leg with momentum  $q_1$  to be on-shell as well (as before, we keep in mind that this graviton will have to be reconnected with the worldline of particle 1).

The cut-amplitude is given by

$$\begin{aligned} \text{Cut}_2 = & \sum_{\text{helicities}} \int d\Phi(\ell) \hat{\delta}(2p_2 \cdot (\ell - q_1)) \\ & \times \mathcal{M}_{4,0}(p_2, -q_1 \rightarrow p_2 - q_1 + \ell, -\ell) \mathcal{M}_{4,0}(p_2 - q_1 + \ell, -\ell \rightarrow p_2 + q_2, k). \end{aligned} \quad (5.19)$$

This quantity can be greatly simplified by choosing, as we did before, a gauge in which graviton polarisations are orthogonal to  $p_2$ :  $\varepsilon_\mu \varepsilon_\nu p_2^\mu = \varepsilon_\mu \varepsilon_\nu p_2^\nu = 0$ . In this case the product of amplitudes becomes proportional to a single contraction [148]

$$\mathcal{M}_{4,0}(p_2, q_1, \ell) \mathcal{M}_{4,0}(p_2, k, \ell) = \frac{\kappa^4}{4} \frac{(p_2 \cdot k)^4}{(\ell + k)^2 (\ell - q_1)^2} (\varepsilon^*(q_1) \cdot \varepsilon(\ell) \varepsilon^*(\ell) \cdot \varepsilon^*(k))^2. \quad (5.20)$$

At this point we have to evaluate the sum over physical states. Note that we haven't been explicit about helicity assignments since these always come with opposite signs inside the loop. We have

$$\sum_{\text{helicities}} (\varepsilon^*(q_1) \cdot \varepsilon(\ell) \varepsilon^*(\ell) \cdot \varepsilon^*(k))^2 = \varepsilon^{*\mu}(q_1) \varepsilon^{*\nu}(k) \varepsilon^{*\rho}(q_1) \varepsilon^{*\sigma}(k) P_{\mu\nu\rho\sigma}(\ell), \quad (5.21)$$

where the projector over physical states reads, for the case of a massive gauge vector  $p_2$

$$P_{\mu\nu\rho\sigma}(\ell) = \sum_{\text{helicities}} \varepsilon_\mu(\ell) \varepsilon_\nu^*(\ell) \varepsilon_\rho(\ell) \varepsilon_\sigma^*(\ell) = \frac{1}{2} \left( P_{\mu\nu} P_{\rho\sigma} + P_{\mu\sigma} P_{\rho\nu} - \frac{2}{D-2} P_{\mu\rho} P_{\sigma\nu} \right). \quad (5.22)$$

Above we have defined

$$P^{\mu\nu}(\ell) = - \left( \eta^{\mu\nu} - \frac{\ell^{(\mu} u_2^{\nu)}}{\ell \cdot u_2} + \frac{\ell^\mu \ell^\nu}{(\ell \cdot u_2)^2} \right), \quad (5.23)$$

which is the projection over on shell states that we had used in the electromagnetic case. The contraction is then straightforward and yields<sup>9</sup>

$$\varepsilon^{*\mu} \varepsilon^{*\nu} \varepsilon^{*\rho} \varepsilon^{*\sigma} P_{\mu\nu\rho\sigma} = \left( \varepsilon^*(q_1) \cdot \varepsilon^*(k) + \frac{\varepsilon^*(q_1) \cdot \ell \varepsilon^*(k) \cdot \ell}{(u_2 \cdot \ell)^2} \right)^2 - \frac{1}{2} \left( \frac{\varepsilon^*(q_1) \cdot \ell \varepsilon^*(k) \cdot \ell}{(u_2 \cdot \ell)^2} \right)^2, \quad (5.24)$$

finally giving us a direct expression of the cut

$$\begin{aligned} \text{Cut}_2 = & \frac{\kappa^4}{8} (p_2 \cdot k)^4 \varepsilon_\mu^*(q_1) \varepsilon_\nu^*(q_1) \varepsilon_\rho^*(k) \varepsilon_\sigma^*(k) \int d\Phi(\ell) \hat{\delta}(p_2 \cdot (\ell - q_1)) \frac{1}{(\ell + k)^2 (\ell - q_1)^2} \\ & \times \left( \eta^{\mu\rho} \eta^{\nu\sigma} + \frac{1}{(u_2 \cdot \ell)^2} \eta^{\mu\rho} \ell^\nu \ell^\sigma + \frac{1}{2(u_2 \cdot \ell)^4} \ell^\mu \ell^\nu \ell^\rho \ell^\sigma \right). \end{aligned} \quad (5.25)$$

---

<sup>9</sup>At this point we have taken  $D = 4$ .

The integral is IR divergent; we discuss IR divergences further below.

It is then straightforward to reproduce a very compact expression of the five point amplitude's imaginary part from tree level unitarity

$$\begin{aligned} \text{Im } \mathcal{M}_{5,1} &= \frac{\kappa^5 (p_2 \cdot k)^4}{16 q_1^2} P_{\alpha\beta\mu\nu}(q_1) p_1^\alpha p_1^\beta \varepsilon_\rho^*(k) \varepsilon_\sigma^*(k) \int d\Phi(\ell) \frac{\hat{\delta}(p_2 \cdot (\ell - q_1))}{(\ell + k)^2 (\ell - q_1)^2} \\ &\quad \times \left( \eta^{\mu\rho} \eta^{\nu\sigma} + \frac{1}{(u_2 \cdot \ell)^2} \eta^{\mu\rho} \ell^\nu \ell^\sigma + \frac{1}{2(u_2 \cdot \ell)^4} \ell^\mu \ell^\nu \ell^\rho \ell^\sigma \right). \end{aligned} \quad (5.26)$$

We remind the reader that this result was achieved in a gauge where  $\varepsilon \cdot p_2 = 0$ , but one can still retrieve the explicitly gauge invariant expression substituting in

$$\varepsilon^\mu(k) \rightarrow \varepsilon^\mu(k) - \frac{\varepsilon(k) \cdot p_2}{k \cdot p_2} k^\mu. \quad (5.27)$$

It would be interesting to replicate (5.26) using purely classical methods, as we did for QED. One way to do this would be through the ‘‘MiSaTaQuWa’’ equations of [149, 150], which are known to describe linear self force in gravity. However, practical computations based on these (non-local) forces happen to be subtle. This is because they involve integrals of the (curved space) Green functions over the complete past history of the particle. We leave these exciting and challenging calculations to a future work.

As a final remark for this section, we would like to underline the universality of the two-particle cuts of Compton amplitudes (5.4), (5.14) and (5.19). As we hope it is clear by now, this object is crucial for the characterisation of the imaginary part of the full five point amplitude describing the waveform. However, the same object can be used, as was done for instance in [59], to describe  $\mathcal{O}(g^6)$  radiation reaction effects that alter the integrated momentum kick of the particle. Classically speaking, the physics of these two situations is different. The radiation reaction  $\mathcal{O}(g^5)$  contribution is a transient one<sup>10</sup> that doesn't affect the final trajectory. However, the emitted radiation and can still be observed in the waveform. Instead the  $\mathcal{O}(g^6)$  one is able to change the final net trajectory of the particle  $\Delta p^\mu$ . Nonetheless, this second (two loops) process is still entailed by Cut<sub>2</sub>: in this case one has to attach both mass less states of the cut into the second massive worldline.

## 6 Renormalisation

We now turn our attention to some subtleties associated with the divergences arising from loop diagrams of the type used in the waveshape calculations in the previous section. Specifically, we examine the structure of IR divergences and the renormalisation of UV divergences in QED. The former are dealt with by isolating the IR

---

<sup>10</sup>In QED this is described by a total derivative Schott term.

divergences in the manner indicated by Weinberg in [151], and performing an  $\hbar$  expansion of the IR divergent diagrams to find a complete cancellation of IR divergences in the classical waveshape.

We then proceed to address UV divergences by carrying out the one-loop renormalisation of the relevant vertices in the On-Shell renormalisation scheme. Doing this we find that the diagrams corresponding to vertex corrections do not contribute to the classical waveshape, thereby justifying the exclusion of such diagrams from the analysis of the previous sections.

### 6.1 Infrared divergences

We will now discuss the effect of infrared divergences arising from soft virtual photons in loop amplitudes. These virtual IR divergences arise from diagrams where soft photon loops are attached to on-shell external legs of a scattering amplitude in the manner illustrated below.

$$J_{nm} = \begin{array}{c} p_1 \\ \diagdown \\ \text{---} \\ \diagup \\ p_2' \end{array} + \begin{array}{c} p_1 \\ \diagdown \\ \text{---} \\ \diagup \\ p_2' \end{array} + \begin{array}{c} p_1 \\ \diagdown \\ \text{---} \\ \diagup \\ p_2' \end{array} + \dots$$

**Figure 6:** Infrared divergent diagrams in the 1-loop amplitude

IR divergences arise from the region where the virtual loop momentum  $|\ell|$  is much smaller than the momenta of external particles  $p_i$ . In this region, it is possible to show that the IR divergent amplitudes take the form [151]:

$$\mathcal{A}^{IR} = \left( \frac{1}{2} \frac{1}{(2\pi)^4} \sum_{nm} e^2 Q_n Q_m \eta_n \eta_m J_{nm} \right) \times \mathcal{A}^{\text{Hard}}, \quad (6.1)$$

where  $\mathcal{A}^{\text{Hard}}$  is what is left of the amplitude after removing the virtual photons lines, and the divergent factor  $J_{nm}$  is given by<sup>11</sup>

$$J_{nm} \equiv -i (p_n \cdot p_m) \int_{\mu \leq |\ell| \leq \Lambda} \frac{\hat{d}^4 \ell}{[\ell^2 + i\epsilon] [p_n \cdot \ell + i\eta_n \epsilon] [-p_m \cdot \ell + i\eta_m \epsilon]} \quad (6.2)$$

where  $\Lambda$  is a scale that defines the soft photons,  $\mu$  is an IR cutoff and  $\eta_n = \pm 1$  for outgoing and incoming particles respectively. In what follows, we will use primed indices to refer to outgoing particles so that  $\eta_1 = \eta_2 = -1$  and  $\eta'_1 = \eta'_3 = +1$ . Specifically, we will be interested in IR divergences of one-loop five-point amplitudes, so that  $\mathcal{A}^{IR} \equiv \mathcal{A}_{5,1}^{IR}$ ,  $\mathcal{A}^{\text{Hard}} \equiv \mathcal{A}_{5,0}^{\text{Hard}}$ .

Turning to the integral  $J_{nm}$ , we perform the integration over  $\ell^0$  by residues. In doing so, we will consider two distinct cases. First, we consider the case where one

---

<sup>11</sup> $D = 4$  here.

particle is incoming and the other outgoing. Then we consider the same integral when both particles are incoming/outgoing.

Let us start by taking particle  $n$  to be outgoing and  $m$  to be incoming. In this case the poles are  $\ell^0 = \pm|\boldsymbol{\ell}| \pm i\epsilon$ ,  $\ell^0 = \frac{\mathbf{p}_n \cdot \boldsymbol{\ell}}{p_n^0} - i\epsilon$  and  $\ell^0 = \frac{\mathbf{p}_m \cdot \boldsymbol{\ell}}{p_m^0} - i\epsilon$ . The important point in this case is that the poles associated with the massive propagators both lie on the same half of the complex  $\ell^0$  plane, so their contribution can be avoided entirely by closing the contour on the other side of the complex plane. In this case, we close the contour on the upper half plane, picking the pole  $\ell^0 = |\boldsymbol{\ell}| + i\epsilon$ . Evaluating the integral in this manner yields the result

$$\text{Re } J_{nm} = \frac{2\pi^2}{\beta_{nm}} \ln \left( \frac{1 + \beta_{nm}}{1 - \beta_{nm}} \right) \ln \left( \frac{\Lambda}{\mu} \right), \quad (6.3)$$

where  $\beta_{nm}$  is the relative velocity

$$\beta_{nm} \equiv \sqrt{1 - \frac{m_n^2 m_m^2}{(p_n \cdot p_m)^2}}. \quad (6.4)$$

We now consider the case where both particles are either incoming or outgoing. For definiteness, consider the case where both particles are outgoing so that  $\eta_n = \eta_m = 1$ . In which case the poles are located at

$$\begin{aligned} \ell^0 &= \pm|\boldsymbol{\ell}| \pm i\epsilon \\ \ell^0 &= \frac{\mathbf{p}_n \cdot \boldsymbol{\ell}}{p_n^0} - i\epsilon \\ \ell^0 &= \frac{\mathbf{p}_m \cdot \boldsymbol{\ell}}{p_m^0} + i\epsilon \end{aligned} \quad (6.5)$$

In this case, the poles of massive propagators lie on opposite sides of the complex plane, so that we would inevitably pick up one of these poles whichever way the contour is closed. Supposing we close the contour from above, we pick up a pole associated with the photon propagator and one from the massive propagators. The former contribution is identical to the integral above and gives the real part of the integral. The latter pole contributes another term which is [152]

$$\begin{aligned} \text{Im } J_{nm} &= -i (p_n \cdot p_m) \int_{\mu \leq |\boldsymbol{\ell}| \leq \Lambda} \frac{|\boldsymbol{\ell}|^2 \hat{d}|\boldsymbol{\ell}| \hat{d}\Omega(\mathbf{n})}{\left[ \left( \frac{\mathbf{p}_m \cdot \boldsymbol{\ell}}{p_m^0} \right)^2 - |\boldsymbol{\ell}|^2 + i\epsilon \right] [p_n^0 (\mathbf{p}_m \cdot \boldsymbol{\ell}) + p_m^0 (\mathbf{p}_n \cdot \boldsymbol{\ell}) + i\epsilon]} \\ &= 2\pi (p_n \cdot p_m) \ln \left( \frac{\Lambda}{\mu} \right) \int \frac{\hat{d}\Omega(\mathbf{n})}{\left[ \left( \frac{\mathbf{p}_m \cdot \mathbf{n}}{p_m^0} \right)^2 - 1 + i\epsilon \right] [p_n^0 (\mathbf{p}_m \cdot \mathbf{n}) + p_m^0 (\mathbf{p}_n \cdot \mathbf{n}) + i\epsilon]} \end{aligned} \quad (6.6)$$

The last integral is most easily evaluated by going to the rest frame of particle  $m$  such that  $\mathbf{p}_m \cdot \mathbf{n} = 0$  and  $p_m^0 (\mathbf{p}_n \cdot \mathbf{n}) = m_m m_n \gamma_{nm} \beta_{nm} (\hat{\beta} \cdot \mathbf{n})$  where  $\gamma_{nm} = p_n \cdot p_m / m_n m_m$  is the Lorentz factor and  $\beta_{nm}$  the relative velocity. In this frame the integral becomes

$$4\pi^2 (p_n \cdot p_m) \ln \left( \frac{\Lambda}{\mu} \right) \int_{-1}^1 \frac{\hat{d}x}{m_n m_m \gamma_{nm} \beta_{nm} [x + i\epsilon]} \quad (6.7)$$

where we have oriented such that  $\hat{\beta} \cdot \mathbf{n} = \cos \theta \equiv x$ . Finally, we make use of the identity

$$\frac{1}{x + i\epsilon} = \text{PV} \left( \frac{1}{x} \right) - \frac{i}{2} \hat{\delta}(x) \quad (6.8)$$

and, noting that only the second term contributes to the integral by parity, we arrive at the result

$$\text{Im } J_{nm} = -\frac{4i\pi^3}{\beta_{nm}} \ln \left( \frac{\Lambda}{\mu} \right). \quad (6.9)$$

Note that is also possible to recover this imaginary divergence in the spirit of section 2.2. It is straightforward to check that cutting the massive propagators attaching to the virtual photon lines recovers the result above. To summarise, we find that the infrared divergences contain both real and imaginary parts. The diagrams where the virtual photons attach to one incoming and one outgoing leg yield purely real IR divergences, while the diagrams in which the virtual photon attaches to two incoming/outgoing legs give both real and imaginary divergences.

We are now ready to address the issue of whether these IR divergences contribute to the classical waveshape. We do so by examining the  $\hbar$  expansion of the sum:

$$\frac{1}{2(2\pi)^4} \sum_{nm} Q_n Q_m \eta_n \eta_m J_{nm}. \quad (6.10)$$

Noting that the one-loop amplitude is suppressed by a factor  $Q^2/\hbar$  relative to the tree amplitude, we identify the quantum parts of  $J_{nm}$  as those of order  $\hbar^2$ . We denote the incoming and outgoing massive momenta by  $p_1, p_2$  and  $p'_1, p'_2$  respectively such that  $\eta_1 = \eta_2 = -1$  and  $\eta'_1 = \eta'_2 = +1$  and  $Q_1 = Q'_1, Q_2 = Q'_2$ . Using momentum conservation, we write

$$\begin{aligned} p'_1 &= p_1 + q \\ p'_2 &= p_2 - q - k. \end{aligned} \quad (6.11)$$

Furthermore, from the on-shell conditions we have

$$\begin{aligned} p_1 \cdot q &= \mathcal{O}(\hbar^2) \\ p_2 \cdot q &= -p_2 \cdot k + \mathcal{O}(\hbar^2) \end{aligned} \quad (6.12)$$

Using this it is straightforward to expand  $J_{nm}$  in powers of  $\hbar$  noting that the  $\hbar$  dependence of follows from expanding the dot products  $p_n \cdot p_m$  using the on-shell conditions. We will find it convenient to express our results in terms of the in terms of the the Lorentz factor and relative velocity

$$\gamma \equiv \frac{p_1 \cdot p_2}{m_1 m_2} \quad v \equiv \sqrt{1 - \frac{1}{\gamma^2}}. \quad (6.13)$$

## 6.2 Real divergence

We now examine the  $\hbar$  expansion of the real divergences in (6.3). To ensure that these divergences are quantum, we must show that the  $\mathcal{O}(\hbar^0)$  and  $\mathcal{O}(\hbar)$  terms vanish in the sum over  $(n, m)$ . Since we are considering real divergences, all values of  $(n, m)$  contribute to the sum. Considering the  $\mathcal{O}(\hbar^0)$  terms first, it is easy to check the sum of terms cancels exactly. Consider for example the part of the sum proportional to  $Q_1^2$ , we have

$$\frac{1}{2(2\pi)^4} e^2 Q_1^2 \operatorname{Re} (\eta_1 \eta_1 J_{11} + 2\eta_1 \eta'_1 J_{11'} + \eta'_1 \eta'_1 J_{1'1'}) \quad (6.14)$$

To this order, we have that  $p_1 \cdot p_1 = p_1 \cdot p'_1 = p'_1 \cdot p'_1 = m_1^2$  and since  $J_{nm}$  is a function of  $p_n \cdot p_m$  we conclude that  $J_{11} = J_{11'} = J_{1'1'}$  but due to the sign differences arising from the  $\eta$  factors, we find that this sum vanishes. It is easy to verify that a similar cancellation occurs for the terms proportional to  $Q_1^2$  and  $Q_1 Q_2$ . We conclude that the  $\mathcal{O}(\hbar^0)$  terms do not contribute to the real IR divergences.

Turning to the  $\mathcal{O}(\hbar)$  terms, we start by noting that the terms in the sum proportional to  $Q_i^2$  for  $i = 1, 2$  still cancel in the same manner as before. This is because the equality  $p_i \cdot p_i = p_i \cdot p'_i = p'_i \cdot p'_i$  still holds to this order (they only differ by terms of  $\mathcal{O}(\hbar^2)$ ). We therefore only need to look at the terms proportional to  $Q_1 Q_2$ . Noting that the terms  $J_{12} = J_{21}$  do not contribute powers of  $\hbar$ , we are left with:

$$\frac{1}{(2\pi)^4} e^2 Q_1 Q_2 \operatorname{Re} (\eta_1 \eta'_2 J_{12'} + 2\eta'_1 \eta_2 J_{1'2} + \eta'_1 \eta'_2 J_{1'2'}). \quad (6.15)$$

Expanding each term to linear order in  $\hbar$  using (6.3) and the kinematics (6.12) we find that

$$\operatorname{Re} \eta_1 \eta'_2 J_{12'} = \frac{2\pi^2 m_1 m_2 k \cdot p_1 (2\gamma^2 m_1^2 m_2^2 + m_1^2 m_2^2 (v \log(\frac{1-v}{1+v}) - 2))}{\gamma^3 v^4} \quad (6.16)$$

$$\operatorname{Re} \eta'_1 \eta_2 J_{1'2} = -\frac{2\pi^2 m_1 m_2 k \cdot p_2 (2\gamma^2 m_1^2 m_2^2 + m_1^2 m_2^2 (v \log(\frac{1-v}{1+v}) - 2))}{\gamma^3 v^4} \quad (6.17)$$

$$\operatorname{Re} \eta'_1 \eta'_2 J_{1'2'} = -\frac{2\pi^2 m_1 m_2 (k \cdot p_1 - k \cdot p_2) (2\gamma^2 m_1^2 m_2^2 + m_1^2 m_2^2 (v \log(\frac{1-v}{1+v}) - 2))}{\gamma^3 v^4} \quad (6.18)$$

These terms once again cancel in the sum. Having established that the terms of  $\hbar$  cancel, we conclude that the real infrared divergences do not contribute classically.

### 6.3 Imaginary part

The  $\hbar$  expansion of the imaginary IR divergences proceeds in the manner as in the previous sections, where we now expand:

$$\text{Im } J_{nm} = -\frac{4i\pi^3}{\beta_{nm}} \ln\left(\frac{\Lambda}{\mu}\right). \quad (6.19)$$

This time however, the sum does not run over all pairs  $(n, m)$  but only those for which  $\eta_n = \eta_m$ . It is precisely this restriction of the sum which prevents the classical contributions from cancelling. We find that the term  $(n, m) = (1', 2')$  in the sum yields a classical contribution which survives the sum due to the absence of the terms  $(1, 2')$  and  $(1', 2)$  in the imaginary part, so that the imaginary part of the amplitude contains a classical IR divergence. Nevertheless, this divergence drops out of the waveform due to the simplification discussed in section 3.3.

### 6.4 QCD and gravity

The analysis of IR divergences in QCD and gravity proceeds broadly in the same manner. Soft divergences arising from graphs where a soft messenger connects two massive lines have the same fate as in QED, and do not contribute to the waveshape.

There are two major differences in QCD and gravity, however. First, in both theories, soft divergences also arise in diagrams where a soft messenger connects a massive to a *massless* line. Imaginary IR divergences in such diagrams do indeed have classical implications, and are discussed in references [94, 130, 131, 153]. Second, in QCD, collinear divergences arise at the level of the amplitude. It would be interesting to explore the classical implications of these collinear divergences in future.

### 6.5 Renormalisation

We now turn to the UV divergences arising from vertex corrections, with the aim of justifying the exclusion of such diagrams from the calculation of the QED waveshape in the preceding sections. It suffices for this purpose to consider the renormalisation of the one-loop Compton amplitude. We start by subtracting the one-loop divergences in the self energy, three-point vertex, and four-point vertex diagrams using the on-shell renormalisation scheme. The remaining finite results are then expanded in powers of  $\hbar$  revealing a cancellation of the classical terms at one-loop.

To start, we rewrite the bare Lagrangian for scalar QED in terms of the renormalised fields by defining<sup>12</sup>

$$\begin{aligned} \phi &= \sqrt{Z_2} \phi_0 \\ A^\mu &= \sqrt{Z_3} A_0^\mu \\ e &= \sqrt{Z_e} e_0 \end{aligned} \quad (6.20)$$

---

<sup>12</sup>In this section, we use the symbol  $e$  to represent a generic charge.

so that

$$\begin{aligned}\mathcal{L}_{\text{bare}} = & -\frac{1}{4}Z_3 F_{\mu\nu} F^{\mu\nu} + Z_2 \partial^\mu \phi^* \partial_\mu \phi - Z_2 m_0^2 \phi^* \phi \\ & + ie Z_1 A^\mu (\phi^* \partial_\mu \phi - \phi \partial_\mu \phi^*) + e^2 Z_4 A^\mu A_\mu \phi^* \phi,\end{aligned}\quad (6.21)$$

where we have further defined  $Z_1 = \sqrt{Z_3} Z_2 Z_e$  and  $Z_4 = Z_3 Z_2 Z_e$ . We then expand the bare Lagrangian using  $Z_i = 1 + \delta_i$  and  $Z_2(m_0^2 - m^2) = \delta_m$  to obtain the counterterm Lagrangian

$$\begin{aligned}\mathcal{L}_{\text{ct}} = & -\frac{1}{4}\delta_3 F_{\mu\nu} F^{\mu\nu} + \delta_2 (\partial^\mu \phi^* \partial_\mu \phi - m^2 \phi^* \phi) - \delta_m \phi^* \phi \\ & + ie \delta_1 A^\mu (\phi^* \partial_\mu \phi - \phi \partial_\mu \phi^*) + e^2 \delta_4 A^\mu A_\mu \phi^* \phi,\end{aligned}\quad (6.22)$$

from which we read off the Feynman rules for the counterterm vertices:

$$\begin{aligned}\Sigma_{\text{ct}}(p^2) &= i(\delta_2(p^2 - m^2) - \delta_m) \\ \Gamma_{\text{ct}}^\mu(p, q) &= -ie \delta_1 (2p^\mu - q^\mu) \\ \Gamma_{\text{ct}}^{\mu\nu}(p, q, k) &= 2ie^2 \delta_4 g^{\mu\nu}\end{aligned}\quad (6.23)$$

In what follows, we will consider three types of vertex corrections. First, we have the self energy correction

$$\Sigma(p^2) = \Sigma_{\text{loop}}(p^2) + \Sigma_{\text{ct}}(p^2), \quad (6.24)$$

where the first and second terms refer to the one-loop diagram and the counterterm diagram respectively. The 1PI cubic and quartic vertices are defined in a similar manner

$$\begin{aligned}\Gamma^\mu(p, q) &= \Gamma_{\text{loop}}^\mu(p, q) + \Gamma_{\text{ct}}^\mu(p, q) \\ \Gamma^{\mu\nu}(p, q, k) &= \Gamma_{\text{loop}}^{\mu\nu}(p, q, k) + \Gamma_{\text{ct}}^{\mu\nu}(p, q, k)\end{aligned}\quad (6.25)$$

where  $\Gamma^\mu(p, q)$  refers to a cubic vertex with incoming momentum  $p$  and outgoing photon momentum  $q$ . Likewise  $\Gamma^{\mu\nu}(p, q, k)$  refers to a four-point vertex with photon momenta  $q$  and  $k$  emitted. Note that here, we do not include the tree-level vertices in our definition of  $\Gamma^\mu$  and  $\Gamma^{\mu\nu}$ .

We renormalise our diagrams in the on-shell scheme. In this scheme, we impose the following renormalisation conditions for the self energy diagrams:

$$\begin{aligned}\Sigma(p^2 \rightarrow m^2) &= 0 \\ \frac{d}{dp^2} \Sigma(p^2 \rightarrow m^2) &= 0\end{aligned}\quad (6.26)$$

where it is understood that the on-shell condition is applied after taking the required derivative. These conditions ensure that the renormalised propagator coincides with the free propagator near the pole  $p^2 = m^2$ . This allows us to neglect self energy corrections in external lines since the on-shell renormalised propagator is still truncated by inverse (free) propagator factors in the LSZ formula .

The renormalisation conditions for the three-point and four-point vertices are defined in the limit of zero photon momenta, in this limit the vertices are generically of the form:

$$\begin{aligned} -ie\Gamma^\mu(p, q \rightarrow 0) &= -ieF(p^2)p^\mu \\ ie^2\Gamma^{\mu\nu}(p, q \rightarrow 0, k \rightarrow 0) &= ie^2F_1(p^2)g^{\mu\nu} + ie^2F_2(p^2)p^\mu p^\nu. \end{aligned} \quad (6.27)$$

The renormalisation conditions then are

$$F(p^2) = 0 \quad F_1(p^2) = 0, \quad (6.28)$$

for the cubic and quartic vertices respectively. The above conditions are sufficient to fix the counterterms to be

$$\begin{aligned} \delta_m &= \Sigma_{\text{loop}}(p^2 \rightarrow m^2) = 0 \\ \delta_2 &= -\frac{d}{dp^2}\Sigma_{\text{loop}}(p^2 \rightarrow m^2) \\ \delta_1 &= -F_{\text{loop}}(p^2) \\ \delta_4 &= -\frac{1}{2}F_{1,\text{loop}}(p^2). \end{aligned} \quad (6.29)$$

It is straightforward to check through explicit calculations that the counterterms above are sufficient to subtract all divergences arising from loop corrections. In the limit of zero photon momenta, the form factors of the three-point and four-point vertices are fixed by the Ward identities:

$$\begin{aligned} F_{\text{loop}}(p^2) &= \frac{d\Sigma_{\text{loop}}(p^2)}{dp^2} \\ F_{1,\text{loop}}(p^2) &= 2\frac{d\Sigma_{\text{loop}}(p^2)}{dp^2} \\ F_{2,\text{loop}}(p^2) &= -4\frac{d^2\Sigma_{\text{loop}}(p^2)}{(dp^2)^2} \end{aligned} \quad (6.30)$$

Comparing this with (6.29), we see that the Ward identity implies the following equality for the counterterms

$$\delta_1 = \delta_2 = \delta_4. \quad (6.31)$$

The Ward identity makes the task of determining the counterterms significantly easier. Conversely, it serves as a nontrivial check if the counterterms for each vertex are calculated independently.

We can now proceed to consider the overall contribution of these vertices. We will consider three classes of diagrams separately. First, we have the diagrams resulting from the self energy corrections:

$$\begin{aligned} \mathcal{D}_{\text{self}}(p, k, q) &= (-ie)^2(2p - q)^\mu G(p - q)(2p - q - k)^\nu \\ &\quad + (-ie)^2(2p - k)^\mu G(p - k)(2p - q - k)^\nu \end{aligned} \quad (6.32)$$

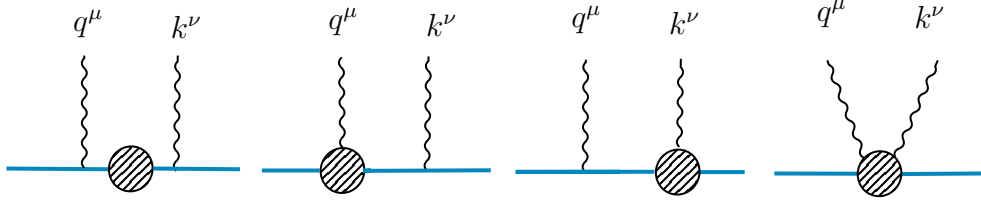


**Figure 7:** Diagrams arising from corrections to the propagator, cubic, and quartic vertices, where the blobs represent 1PI vertex corrections. We have suppressed the crossed diagrams.

where  $G(p - q)$  is the renormalised propagator given by

$$G(p - q) = \frac{i}{(p - q)^2 - m^2 + i\epsilon} [i\Sigma((p - q)^2)] \frac{i}{(p - q)^2 - m^2 + i\epsilon}. \quad (6.33)$$

We also have the diagrams containing corrections to the three point vertex:

$$\begin{aligned} \mathcal{D}_{\text{Cubic}}^{\mu\nu}(p, k, q) = & (-ie)^2 \frac{i\Gamma^\mu(p, q)(2p - q - k)^\nu}{(p - q)^2 - m^2 + i\epsilon} + (-ie)^2 \frac{(2p - q)^\mu i\Gamma^\nu(p - q, k)}{(p - q)^2 - m^2 + i\epsilon} \\ & + (\mu \leftrightarrow \nu), \end{aligned} \quad (6.34)$$

and finally, we have the four-point vertex correction

$$\mathcal{D}_{\text{Quartic}}^{\mu\nu}(p, k, q) = ie^2\Gamma^{\mu\nu}(p, q, k). \quad (6.35)$$

We can now examine the  $\hbar$  expansions of each of the terms above. To ensure that the vertex corrections are quantum, we want the diagrams containing vertex corrections to be suppressed by one power of  $\hbar$  relative to the tree-level diagrams. Since the loop corrections are suppressed by a factor of  $e^2/\hbar$ , this amounts to ensuring that the rest of the diagram is  $\mathcal{O}(\hbar^2)$ .

Starting with the self energy diagram, let us focus on the first term in (6.32). Expanding  $\Sigma((p - q)^2)$  in small  $q$  yields the series

$$\Sigma((p - q)^2) = \Sigma(p^2) + (-2p \cdot q + q^2)\Sigma'(p^2) + \frac{1}{2}(-2p \cdot q + q^2)^2\Sigma''(p^2), \quad (6.36)$$

where the primes denote derivatives with respect to the argument  $p^2$ . Inserting this into the propagator  $G(p - q)$  and putting  $p$  on-shell gives

$$\begin{aligned} G(p - q) = & \left[ \frac{i}{-2p \cdot q + q^2 - i\epsilon} \right]^2 i\Sigma(p^2 \rightarrow m^2) + \left[ \frac{i^2}{-2p \cdot q + q^2 - i\epsilon} \right] i\Sigma'(p^2 \rightarrow m^2) \\ & + \frac{i^3}{2} \Sigma''(p^2 \rightarrow m^2) \end{aligned} \quad (6.37)$$

The first two terms vanish identically by virtue of the renormalisation conditions (6.26). We thus find that the only parts of  $\mathcal{D}_{\text{self}}$  that could yield a classical contribution are

$$\frac{ie^2}{2}(2p-q)^\mu\Sigma''(p^2 \rightarrow m^2)(2p-q-k)^\nu + \frac{ie^2}{2}(2p-k)^\mu\Sigma''(p^2 \rightarrow m^2)(2p-q-k)^\nu. \quad (6.38)$$

As we will see below, these terms will ultimately cancel against a similar contribution originating from  $\mathcal{D}_{\text{Quartic}}$ . To this end, consider the form of  $\mathcal{D}_{\text{Quartic}}$  in an  $\hbar$  expansion. The leading order piece follows from taking  $q = k = 0$ , in which case it takes the form given in (6.27):

$$\mathcal{D}_{\text{Quartic}}^{\mu\nu}(p, 0, 0) = ie^2 F_1(p^2) g^{\mu\nu} + ie^2 F_2(p^2) p^\mu p^\nu \quad (6.39)$$

The first term vanishes by the renormalisation conditions while the second is rewritten using the Ward identity (6.30) so that

$$\mathcal{D}_{\text{Quartic}}^{\mu\nu}(p, 0, 0) = -4ie^2 \Sigma''(p^2) p^\mu p^\nu. \quad (6.40)$$

It is easy to see that this exactly compensates the terms proportional to  $p^\mu p^\nu$  in (6.38). We conclude that the terms of order  $\hbar^0$  vanish in the sum  $\mathcal{D}_{\text{self}} + \mathcal{D}_{\text{Quartic}}$ .

Turning to the terms linear in  $\hbar$ , we see that powers of  $\hbar$  can arise in two ways in  $\mathcal{D}_{\text{Quartic}}$ : terms which arise from introducing photon momenta in the scalar coefficients ( $F_1(p^2)$  and  $F_2(p^2)$ ) and terms arising from introducing photon momenta in the tensor structure  $p^\mu p^\nu$ . The latter terms are still cancelled by the contributions in (6.38) for the simple reason that they end up having the same tensor structure. As for the variation of scalar coefficients, the fact that the form factors are functions of  $p^2$  implies that switching on the photon momenta  $q$  and  $k$  leads to the following order  $\hbar$  corrections :

$$\begin{aligned} F_1((p-q-k)^2) &= F_1(p^2) - 2p \cdot (q+k) F'_1(p^2) + \mathcal{O}(\hbar^2) \\ F_2((p-q-k)^2) &= F_2(p^2) - 2p \cdot (q+k) F'_2(p^2) + \mathcal{O}(\hbar^2). \end{aligned} \quad (6.41)$$

We see that the leading correction is proportional  $2p \cdot (q+k)$  which, due to the on-shell condition for the outgoing momentum  $(p-k-q)^2 = m^2$ , is in fact  $\mathcal{O}(\hbar^2)$ . We conclude that the sum of  $\mathcal{D}_{\text{Quartic}}$  and  $\mathcal{D}_{\text{self}}$  contains no classical terms.

Turning to the cubic vertices, we again find that terms which are proportional to  $F(p^2)$  vanish by the renormalisation conditions, while the leading variation of the scalar form factors are proportional to  $p \cdot (k+q)$  which are  $\mathcal{O}(\hbar^2)$  on-shell. This ensures that the diagrams containing the corrected three-point vertices are suppressed by a power of  $\hbar$  relative to the tree-level diagrams. With this we arrive at the anticipated result that the vertex corrections do not contribute to the classical waveshape in QED.

## 7 Classical confirmation

This part of the paper is devoted to confirming our waveshape expressions integrating the classical equations of motion. We begin by focusing on the conservative part. Since the methods are standard, we will be brief.

Our first order of business is to decide what classical object should be compared to the waveshape. One place to start is with the classical field strength in Fourier space, namely

$$F_{\mu\nu}(x) = i \int \hat{d}^4 k \frac{e^{-ik \cdot x}}{k^2} k_{[\mu} \tilde{A}_{\nu]}(k) k^2 . \quad (7.1)$$

We have written  $\tilde{A}(k)$  for the Fourier components of the gauge field  $A_\mu(x)$ , and we have extracted a factor of  $k^2$  from  $\tilde{A}(k)$ ; this factor is always present on account of the Maxwell equations. The integral over  $k$  is defined with retarded boundary conditions. Standard manipulation of the  $k$  integral at large distances  $x$  from the scattering event leads to the field strength in the form

$$F_{\mu\nu}(x) = -\frac{1}{4\pi|\mathbf{x}|} 2 \operatorname{Re} \int_0^\infty \hat{d}\omega e^{-i\omega u} \sum_\eta k_{[\mu} \varepsilon_{\nu]}^\eta(k) \left( i\varepsilon^{\eta*}(k) \cdot \tilde{A}(k) k^2 \right) , \quad (7.2)$$

evaluated in the on-shell limit  $k^2 \rightarrow 0$  with  $k = (\omega, \omega\mathbf{x}/|\mathbf{x}|)$ . The retarded time appearing here is  $u = x^0 - |\mathbf{x}|$ . Comparing with equation (2.13), we identify the classical counterpart of the waveshape as

$$\begin{aligned} \alpha_\eta(k) &= \langle \psi | S^\dagger a_\eta(k) S | \psi \rangle \\ &= i\varepsilon^{\eta*}(k) \cdot \tilde{A}(k) k^2 . \end{aligned} \quad (7.3)$$

The problem then is to compute the gauge field in momentum space at the relevant perturbative order. Here we focus on the waveshape in the large  $m_1$  limit, which simplifies the problem since we can presume that particle 1 is stationary and therefore does not radiate. Leaving aside the self-field of particle 2 for now (we will include it below using the ALD force) we need only consider the motion of particle 2 in the Coulomb field of particle 1. The radiation field is entirely due to this accelerated motion, so the problem is to determine the field of particle 2 in perturbation theory. Working in Fourier space, the Maxwell equation to be solved (in Lorenz gauge) is

$$-k^2 \tilde{A}^\mu(k) = Q_2 \int d\tau v_2^\mu(\tau) e^{ik \cdot x_2(\tau)} , \quad (7.4)$$

where  $x_2(\tau)$  is the position of particle 2 and  $v_2(\tau)$  is its proper velocity. The position and velocity can be written as a perturbative series

$$x_2(\tau) = b_2 + u_2 \tau + \Delta^{(1)} x_2(\tau) + \Delta^{(2)} x_2(\tau) + \dots , \quad (7.5)$$

around the straight-line trajectory  $b_2 + u_2\tau$ . The objects  $\Delta^{(n)}x_2(\tau)$  are corrections to the trajectory at a given perturbative order; inspection of the Lorentz force law shows that  $\Delta^{(n)}x_2(\tau)$  is of order  $Q_1^n Q_2^n$ . Similarly, the velocity can be written as

$$v_2(\tau) = u_2 + \Delta^{(1)}v_2(\tau) + \Delta^{(2)}v_2(\tau) + \dots . \quad (7.6)$$

In this notation, the order  $Q_1^2 Q_2^3$  part of the acceleration field is

$$\begin{aligned} -k^2 \Delta^{(2)} \tilde{A}^\mu(k) = Q_2 \int d\tau e^{ik \cdot (b_2 + u_2\tau)} & \left[ \Delta^{(2)}v_2^\mu(\tau) + ik \cdot \Delta^{(1)}x_2(\tau) \Delta^{(1)}v_2^\mu(\tau) \right. \\ & \left. + u_2^\mu \left( ik \cdot \Delta^{(2)}x_2(\tau) - \frac{1}{2}(k \cdot \Delta^{(1)}x_2(\tau))^2 \right) \right]. \end{aligned} \quad (7.7)$$

However, in view of equation (7.3) we are only interested in projection of this radiation field onto a polarisation vector in the on-shell limit  $k^2 \rightarrow 0$ . We are then free to choose the gauge of the polarisation vector to suit us. It is clear that the choice  $\varepsilon^{\eta*}(k) \cdot u_2 = 0$  simplifies the calculation (and indeed this is the choice we made in section 4.1).

It remains to compute the quantities  $\Delta^{(2)}v_2(\tau)$ ,  $\Delta^{(1)}v_2(\tau)$  and  $\Delta^{(1)}x_2(\tau)$ . Of these, the first order perturbations  $\Delta^{(1)}v_2(\tau)$  and  $\Delta^{(1)}x_2(\tau)$  can be found in section 6 of reference [59]. The second-order term  $\Delta^{(2)}v_2(\tau)$  can be computed by iterating the Lorentz force at one further order than performed in that reference, using precisely the same method. The result is

$$\begin{aligned} \Delta^{(2)}v_2^\mu(\tau) = \frac{iQ_1^2 Q_2^2}{m_2^2} \int \hat{d}^D \ell_1 \hat{d}^D \ell_2 & \frac{\hat{\delta}(\ell_1 \cdot u_1) \hat{\delta}(\ell_2 \cdot u_2)}{\ell_1^2 \ell_2^2} \frac{e^{-i(\ell_1 + \ell_2) \cdot (b_2 + u_2\tau)}}{(\ell_1 \cdot u_2)^2 ((\ell_1 + \ell_2) \cdot u_2)^2} \\ & \times \ell_2^{[\mu} u_1^{\nu]} \left( \ell_1 \cdot u_2 \ell_{1[\nu} u_{1\rho]} u_2^\rho + u_{2\nu} \ell_{2\rho} \ell_1^{[\rho} u_1^{\sigma]} u_{2\sigma} \right). \end{aligned} \quad (7.8)$$

We must now combine the results and compare to the waveshape in eq. (4.16). To do so, we find it convenient to define

$$\begin{aligned} R_1 &= -iQ_2 \int d\tau e^{ik \cdot (b_2 + u_2\tau)} \Delta^{(2)}v_2(\tau) \cdot \varepsilon^*(k), \\ R_2 &= -iQ_2 \int d\tau e^{ik \cdot (b_2 + u_2\tau)} ik \cdot \Delta^{(1)}x_2(\tau) \Delta^{(1)}v_2(\tau) \cdot \varepsilon^*(k). \end{aligned} \quad (7.9)$$

in the on-shell limit, so that the waveshape is  $R_1 + R_2$ . It is then necessary to relabel the variables of integration before comparing to the waveshape. In  $R_1$ , for instance, this can be achieved by setting  $\ell_1 = \ell$ ,  $\ell_2 = q_1 - \ell$ . Combining everything, we found

$$R_1 + R_2 = \frac{iQ_1^2 Q_2^3}{m_2^2} \int \hat{d}^4 q_1 \hat{d}^4 q_2 \hat{\delta}(q_1 \cdot u_1) \hat{\delta}(q_2 \cdot u_2) \hat{\delta}^D(q_1 + q_2 + k) e^{-iq_1 \cdot b_1} e^{-iq_2 \cdot b_2} \mathcal{R} \quad (7.10)$$

where the kernel  $\mathcal{R}$  is

$$\begin{aligned} \mathcal{R} = \int \hat{d}^D \ell \frac{\hat{\delta}(\ell \cdot u_1)}{\ell^2(\ell - q_1)^2} & \left[ \varepsilon^* \cdot u_1 \frac{u_1 \cdot u_2 k \cdot \ell - k \cdot u_1 \ell \cdot u_2 - \ell \cdot (\ell - q_1) u_1 \cdot u_2}{(\ell \cdot u_2)^2} \right. \\ & + \varepsilon^* \cdot (\ell - q_1) \left( \frac{1}{k \cdot u_2} + \frac{1}{k \cdot u_2} \frac{(u_1 \cdot u_2)^2 \ell \cdot (\ell - q_1)}{(\ell \cdot u_2)^2} \right. \\ & \left. \left. + u_1 \cdot u_2 \frac{k \cdot u_1 \ell \cdot u_2 - k \cdot \ell u_1 \cdot u_2}{(\ell \cdot u_2)^2 (\ell - q_1) \cdot u_2} \right) \right]. \end{aligned} \quad (7.11)$$

This quantity should be directly comparable to our previous expression for the waveshape in equation (4.16). To see that the expressions do indeed match, it is necessary to take advantage of properties of the integrals involved. For example we may neglect  $\ell^2$  in the numerator of the kernel  $\mathcal{R}$ : as this cancels one of the photon propagators the result will be a contact term. It is also useful to note, for example, that

$$\begin{aligned} \int \hat{d}^D \ell \frac{\hat{\delta}(\ell \cdot u_1)}{\ell^2(\ell - q_1)^2} \varepsilon^* \cdot (\ell - q_1) \frac{\ell \cdot (\ell - q_1)}{\ell \cdot u_2 (\ell - q_1) \cdot u_2} \\ = -\frac{1}{2} \int \hat{d}^D \ell \frac{\hat{\delta}(\ell \cdot u_1)}{\ell^2(\ell - q_1)^2} \varepsilon^* \cdot q_1 \frac{\ell \cdot (\ell - q_1)}{\ell \cdot u_2 (\ell - q_1) \cdot u_2}. \end{aligned} \quad (7.12)$$

When the dust settles, we do indeed find a complete match with the waveshape in equation (4.16). Even in electrodynamics, it is significantly easier to determine the waveshape using amplitudes once the relevant cuts are known: the QFT-based approach separates structural aspects of the waveshape (for example the delta functions and  $q$  integrals) from the dynamics from the start. The dynamics is elegantly captured in the cuts, avoiding rather lengthy algebra.

Let us now move onto dissipative terms. As we stressed before, in electrodynamics, we are lucky enough that radiation reaction can be systematically computed through the ALD force [154–156]. This non-conservative force prescribes the following momentum kick

$$\frac{dp_2^\mu}{d\tau} = \frac{Q_2^2}{6\pi m_2} \left( \frac{d^2 p_2^\mu}{d\tau^2} + \frac{p_2^\mu}{m_2^2} \frac{dp_2}{d\tau} \cdot \frac{dp_2}{d\tau} \right), \quad (7.13)$$

which is supplementing the lower order deflection due to the Lorentz force.

To see how (7.13) feeds in  $F^{\mu\nu}(x)$  at order  $Q_1 Q_2^4$  we start from the LO velocity correction updated through the Lorentz force only. If we expand perturbatively the four velocity of particle 2

$$u_2^\mu(\tau) = u_2^\mu + u_{2,\text{LO}}^\mu(\tau) + \dots \quad (7.14)$$

then the first correction to the constant term is [59]

$$u_{2,\text{LO}}^\mu(\tau) = -\frac{Q_1 Q_2}{m_2} \int \hat{d}^4 q \hat{\delta}(q \cdot u_1) e^{iq \cdot (b_{12} - u_2 \tau)} \frac{u_{2\nu} q^{[\mu} u_1^{\nu]}}{q^2 q \cdot u_2}, \quad (7.15)$$

with  $b_{12} = b_1 - b_2$ . Now we feed this into (7.13) noting that, at the lowest order, we only need to consider the first term  $\propto d^2 p^\mu / d\tau^2$ . In this way we obtain updated velocity and particle trajectory (integrating once more) caused by radiation reaction

$$\begin{aligned} u_{2,\text{ALD}}^\mu(\tau) &= \frac{Q_2^2}{6\pi m_2} \int_{-\infty}^\tau d\tau \frac{d^2 u_{2,\text{LO}}^\mu}{d\tau^2} = i \frac{Q_1 Q_2^3}{6\pi m_2^2} \int \hat{d}^4 q \hat{\delta}(q \cdot u_1) e^{iq \cdot (b_{12} - u_2 \tau)} \frac{u_{2\nu} q^{[\mu} u_1^{\nu]}}{q^2}, \\ x_{2,\text{ALD}}^\mu(\tau) &= \int_{-\infty}^\tau d\tau u_{2,\text{ALD}}^\mu = - \frac{Q_1 Q_2^3}{6\pi m_2^2} \int \hat{d}^4 q \hat{\delta}(q \cdot u_1) e^{iq \cdot (b_{12} - u_2 \tau)} \frac{u_{2\nu} q^{[\mu} u_1^{\nu]}}{q^2 q \cdot u_2}. \end{aligned} \quad (7.16)$$

The crucial step is to now use the ALD data (7.16) to solve the field equations with retarded boundary conditions

$$\partial^2 A^\mu(x) = Q_2 \int d\tau u_{2,\text{ALD}}^\mu(\tau) \delta^4(x - x(\tau)). \quad (7.17)$$

After going to momentum space, a short calculation leads to

$$\begin{aligned} -k^2 \tilde{A}^\mu(k) &= \dots + Q_2 \int d\tau e^{ik \cdot (b + u_2 \tau)} (u_{2,\text{ALD}}^\mu(\tau) + ik \cdot x_{\text{ALD}}(\tau) u_2^\mu) \\ &= \dots + i \frac{Q_1 Q_2^4}{6\pi m_2^2} \int \hat{d}^4 q_1 \hat{d}^4 q_2 e^{iq_1 \cdot b_1} e^{iq_2 \cdot b_2} \hat{\delta}(q_1 \cdot u_1) \hat{\delta}(q_2 \cdot u_2) \hat{\delta}^4(k + q_1 + q_2) \\ &\quad \times \frac{k \cdot u_2}{q_1^2} \left( u_1^\mu + q_1^\mu \frac{u_1 \cdot u_2}{k \cdot u_2} - u_2^\mu \frac{k \cdot u_1}{k \cdot u_2} - u_2^\mu \frac{u_1 \cdot u_2 k \cdot q_1}{(k \cdot u_2)^2} \right), \end{aligned} \quad (7.18)$$

at the relevant  $Q_1 Q_2^4$  order. One can already see that things start to look familiar: the quantity inside the brackets is exactly the source we defined earlier in (5.13). To complete the calculation we simply have to contract with a polarisation vector according to (7.3) to get

$$\begin{aligned} i\varepsilon^*(k) \cdot \tilde{A}(k) k^2 &= \frac{Q_1 Q_2^4}{6\pi m_2^2} \int \hat{d}^4 q_1 \hat{d}^4 q_2 e^{iq_1 \cdot b_1} e^{iq_2 \cdot b_2} \hat{\delta}(q_1 \cdot u_1) \hat{\delta}(q_2 \cdot u_2) \hat{\delta}^4(k + q_1 + q_2) \\ &\quad \times \frac{k \cdot u_2}{q_1^2} \varepsilon^*(k) \cdot \mathcal{J}(k, q_1), \end{aligned} \quad (7.19)$$

clearly matching  $\alpha_\eta(k)$  derived with amplitudes (5.12).

Let us remark that the term in the ALD acceleration  $\propto d^2 p^\mu / d\tau^2$  which gave rise to the relevant correction (7.16) is known in the literature as a “Schott term” [157]. This contribution is leading in the coupling with respect to  $\propto p^\mu (dp/d\tau)^2$  but, importantly, is a total time derivative. This means that it does not contribute to the total emitted radiation, albeit being necessary to maintain the system’s energy-momentum balance. Remarkably, our derivation shows that this transient correction is the only one which secretly sources dissipated radiation, at one loop.

## 8 Conclusions

In this paper we investigated how next-to-leading-order radiation fields can be elegantly computed using the techniques of modern scattering amplitudes.

Building upon the KMOC formalism of [59], we characterised NLO radiation fields in terms of the real and imaginary parts of a waveshape. The real part is extracted by cutting one massive line of a five-point one-loop amplitude, whereas the imaginary part is obtained by a double cut of this amplitude. With this arrangement, all remaining propagators are defined through a principal-value prescription. This propagator structure emerges directly from the Feynman  $i\epsilon$  prescription together with the split into real and imaginary parts, with no further intervention by hand.

Our organisation of the observable provides two key benefits. First, it improves computational efficiency: the cancellation of apparently singular inverse powers of  $\hbar$  (the “superclassical” terms) can be trivialised. Second, this organisation clarifies the underlying physics. Both real and imaginary parts have separate, gauge invariant, physical meaning.

The real part describes the radiation emitted by a body moving under the influence of essentially conservative forces: for example, a charge accelerated by the Lorentz force in the field of a different charge. In contrast, the imaginary part captures intrinsically dissipative effects: radiation generated under the influence of the particle’s self field. In electrodynamics, this can be understood as the portion of radiation generated by the action of the Abraham-Lorentz-Dirac force on the charge. Indeed the factor  $i$  between the real and imaginary part of the waveshape points to the breaking of time-reversal symmetry. It is worth noting that the acceleration of the charge at this order originates in a Schott term; the total impulse on the charge vanishes, but the time-dependent acceleration nevertheless leaves an imprint on the radiation field of the particle. In our description, this aspect of radiation reaction at one loop order is directly related to a simple unitarity cut involving a product of two Compton amplitudes in electrodynamics, Yang-Mills theory and gravity.

Radiation reaction is a consequence of self-force. For point-like objects, this inevitably entails some kind of regulation and renormalisation of singularities. Our approach is directly rooted in traditional quantum field theory, so we took advantage of the opportunity to explain how the usual procedure of renormalisation in quantum field theory removes the real part of certain diagrams. The terms in question are intuitively quantum mechanical, for example, the renormalisation of the QED vertex which has the (quantum-mechanical) consequence of the running coupling. Using the on-shell renormalisation scheme, we showed that this class of diagram indeed cancels from classical computations. As the counterterms are real, they do not affect the imaginary parts of these graphs — which capture the effects of radiation reaction, and are perfectly classical. It may be worth remarking that our result is scheme-independent as it is an observable quantity. However in other schemes (for example

$\overline{\text{MS}}$ ) apparently relevant terms from these diagrams would only cancel at the level of the observable itself.

An interesting aspect of renormalisation of the waveform is that various quantum-mechanical diagrams are infrared divergent. A subset of these divergences are an obstacle to the on-shell scheme; we showed that these divergences are all quantum in nature so that the on-shell scheme is valid in the classical limit. In electrodynamics, all infrared divergences cancel in the waveshape. However theories with self-interacting massless messengers (Yang-Mills theory and gravity) retain a residual IR divergence [94, 130, 131, 153].

We tested our QFT-based computations in electrodynamics by comparing to a fully classical computation of the complete radiation field at order  $Q^5$ , finding detailed agreement. The classical computation, although not especially arduous, is nevertheless more involved than the elegant approach based on generalised unitarity, once the relevant cuts are understood. Although electrodynamics is a comparatively simple theory, nevertheless it is rich enough to provide a very stimulating laboratory to understand many aspects of the dialogue between amplitudes and classical physics, especially since it is often rather straightforward to pass from electrodynamics to Yang-Mills theory [22, 158, 159].

Turning to future directions, it would be very interesting to understand the physical meaning of the real and imaginary parts of the waveshape beyond one loop. Our initial motivation to study these real and imaginary parts arose from studying references [36, 39], where the authors simplified other observables (the impulse and radiated momentum) after splitting into real and imaginary parts. The authors of references [36, 39] found this approach useful at both one and two loops. A first topic, then, would be to study the waveshape at two loops. Is it possible to link a well-defined part of the observable to radiation reaction at this order? What pole prescription emerges for the various propagators?

A related motivation for studying real and imaginary parts of the waveshape emerges from eikonal and related approaches to amplitudes in the classical limit, especially [38, 40, 42, 136, 137]. The essence of these approaches is that classical physics arises from a stationary-phase approximation at the level of the path integral. Amplitudes in the classical limit are essentially perturbative expansions of this phase. Because the phase has the structure  $\exp(iS/\hbar)$ , the expansion introduces inverse powers of  $\hbar$ ; these cancel in observables. The relevant product in the expansion of the phase has the momentum-space interpretation of a convolution, emerging from a cut (see, for example [19] for more on this link). Thus we should expect an interplay between real and imaginary parts and the cancellation of “superclassical” terms in amplitudes at *all* orders. Indeed, in our work, we found that superclassical terms cancelled completely at the level of cuts after splitting into real and imaginary parts. This greatly simplifies the computation of the relevant cuts. Consequently we think it is very likely that this kind of organisation will be particularly useful at higher

orders.

There is also still a great deal of interesting physics to be understood without facing the extremely challenging situation at two loops. Capturing the physics of black hole spin in the tree-level waveform already requires an understanding of the Compton amplitude with spin, including relevant contact terms. These have been recently studied by different groups, for example [160–164]. At one loop, we also need the five-point analogue of the tree Compton amplitude which appears in the relevant one-loop cuts.

Throughout this article, our focus was on the waveshape generated during a scattering experiment. It would obviously be very exciting if our computations could be analytically continued using some appropriate algorithm to the bound state case, perhaps along the lines of references [63, 64, 165].

We believe that our work shows once again that the perturbative structure of classical interactions is clarified when generalised unitarity and the double copy are exploited. Methods based on scattering amplitudes successfully factorise observables into a general kinematic structure (eg an integral over a waveshape) and a dynamical object (the waveshape) which must be determined. Generalised unitarity determines the dynamical content (the waveshape) from foreknowledge of its general analytic structure. The double copy allows us to bypass much of the complexity of gravity. Although our methods at first sight seem foreign to classical physics, obviously they successfully capture classical physics. We believe that a deeper understanding of these ideas should be available from a classical perspective. For instance, in section 5.3 we found an expression for the waveshape originating from the acceleration of a body under its own gravitational self-field. Our method makes it obvious that this phenomenon is the double-copy of the radiation emitted a charge accelerated by its ALD force. Can we then understand self-forces in gravity (for example the MiSaTaQuWa equations [149, 150]) more generally as a double copy? We leave all these questions for future work.

## Acknowledgments

We particularly thank John Joseph Carrasco for collaborating with us in the early stages of this work, when he contributed significant ideas which enhanced our understanding of the physics. We also thank Andreas Brandhuber, Graham Brown, Gang Chen, Stefano De Angelis, Joshua Gowdy, Aidan Herderschee, Radu Roiban, Fei Teng, and Gabriele Travaglini for cooperating with us with the submission of this manuscript. Our work has also benefited from useful discussions with Andrea Cristofoli, Kays Haddad, Franz Herzog, Anton Ilderton, Alasdair Ross, Justin Vines, Pablo Vives Matasan and Mao Zeng.

This research was supported in part by the National Science Foundation under Grant No. NSF PHY-1748958. AE is sponsored by a Higgs Fellowship. DOC

is supported by the U.K. Science and Technology Facility Council (STFC) grant ST/P000630/1. MS is supported by a Principal’s Career Development Scholarship from the University of Edinburgh and the School of Physics and Astronomy. IVH is supported by the Knut and Alice Wallenberg Foundation under grants KAW 2018.0116 (From Scattering Amplitudes to Gravitational Waves) and KAW 2018.0162. For the purpose of open access, the author has applied a Creative Commons Attribution (CC BY) licence to any Author Accepted Manuscript version arising from this submission.

## A A derivation of the ALD force with cuts

In this appendix we propose a classical derivation of radiation reaction which further supports the theory developed in 2.2. There, we related non conservative effects to the imaginary part of (cuts of) the five-point one-loop amplitude. Specifically, here we will demonstrate how the Schott term in (7.13) arises from a double cut integral which highly resembles the ones in section 5. We are inspired by Coleman’s lectures on relativistic radiation [166].

Let us start by considering the electromagnetic field strength tensor  $F^{\mu\nu}$  and compute it in a close neighborhood of the particle. We will work in an arbitrary number of dimensions  $D$  to consistently drop scaleless contributions, and only at the end take  $D = 4$ . The field’s Fourier transform with retarded boundary conditions reads

$$F_{\mu\nu}(0) = iQ \int \hat{d}^D k \int_{-\infty}^0 d\tau e^{ik \cdot r(\tau)} \frac{k_{[\mu} u_{\nu]}(\tau)}{k^2}, \quad (\text{A.1})$$

with  $k^2 \equiv (k^0 + i\epsilon)^2 - \mathbf{k}^2$ . Note that we set for simplicity  $x = 0$  in the field’s argument. We now sit on top of the particle and expand all space-time dependent quantities in a series of small proper time such that  $\tau \sim k^{-1} \ll 1$ . Guided by the fact that 7.13 involves quantities with three  $\tau$ -derivatives, we expand the position  $r^\mu(\tau)$  up to terms which involve the particle’s acceleration change  $\dot{a}^\mu$ . Thus we have

$$r^\mu(\tau) \approx u^\mu \tau + \frac{1}{2} a^\mu \tau^2 + \frac{1}{6} \tau^3 \dot{a}^\mu, \quad u^\mu(\tau) \approx u^\mu + a^\mu \tau + \frac{1}{2} \tau^2 \dot{a}^\mu, \quad (\text{A.2})$$

which we can substitute inside (A.1) to obtain

$$\begin{aligned} F_{\mu\nu}(0) = iQ \int \hat{d}^D k \int_{-\infty}^0 d\tau e^{ik \cdot u \tau} \frac{k_{[\mu}}{k^2} & \left( u_{\nu]} + \tau a_{\nu]} + \frac{1}{2} i\tau^2 k \cdot a u_{\nu]} \right. \\ & \left. + \frac{1}{2} i\tau^3 k \cdot a a_{\nu]} + \frac{1}{2} \tau^2 \dot{a}_{\nu]} - \frac{1}{8} \tau^4 (k \cdot a)^2 u_{\nu]} + \frac{1}{6} i\tau^3 k \cdot \dot{a} u_{\nu]} \right) + \dots \end{aligned} \quad (\text{A.3})$$

Note again that in this expansion  $\tau k \sim 1$  so above we have kept terms up to order  $\tau^3/k \sim \tau^2/k^2 \sim \tau^4$  in the second line.

Next, we begin to simplify our expression using standard symmetry arguments and dimensional analysis. In fact, we will exploit the result that scaleless integrals vanish in `dimreg`:  $\int d^D k k^{-p} = 0$ . Let us look at the zero-th order term. Here, we will often find it useful to use the decomposition  $k^\mu = k \cdot u u^\mu + k_\perp^\mu$ . Then, the first piece of A.3 is

$$\int \hat{d}^D k \int_{-\infty}^0 d\tau e^{ik \cdot u \tau} \frac{k^{[\mu} u^{\nu]}}{k^2} = \int \hat{d}^D k \frac{i}{k \cdot u - i\epsilon} \frac{k_\perp^{[\mu} u^{\nu]}}{k^2} = 0, \quad (\text{A.4})$$

because of the anti-symmetric  $k_\perp^\mu$  integrand<sup>13</sup>. Regarding to the second term in (A.3), we find it to be zero since it is scaleless. Indeed, using similar steps, one brings this integral to the form

$$\int \hat{d}^D k \int_{-\infty}^0 d\tau e^{ik \cdot u \tau} \frac{k_{[\mu} a_{\nu]}}{k^2} \tau = i u_{[\mu} a_{\nu]} \int \hat{d}^{D-1} |\mathbf{k}| \frac{1}{|\mathbf{k}|^2} = 0, \quad (\text{A.5})$$

in dimensional regularization. We won't discuss each term singularly, but similar arguments can be applied to the other pieces in (A.3). Some of them involve a tensor numerator that yields a vanishing result once the integral is reduced, and on the support of  $k^2 = 0$  and  $a \cdot u = 0$ .

In the end, we find that only two terms survive, after integrating out  $\tau$  the field strength looks like

$$F_{\mu\nu}(0) = Q \int \hat{d}^D k \frac{k_{[\mu}}{k^2} \left( \frac{\dot{a}_{\nu]}}{(k \cdot u - i\epsilon)^3} - \frac{k \cdot \dot{a} u_{\nu]}}{(k \cdot u - i\epsilon)^4} \right), \quad (\text{A.6})$$

For the first term we exploit symmetry along the  $k_\perp$  integral to write  $k_{[\mu} \dot{a}_{\nu]} = k \cdot u u_{[\mu} \dot{a}_{\nu]}$ . Then, a simple tensor reduction of the  $k$  integral of the second one yields

$$\int \hat{d}^D k \frac{k_{[\mu} u_{\nu]}}{k^2} \frac{k \cdot \dot{a}}{(k \cdot u - i\epsilon)^4} = \frac{\dot{a}_{[\mu} u_{\nu]}}{D-1} \int \hat{d}^D k \frac{1}{k^2} \frac{1}{(k \cdot u - i\epsilon)^2}, \quad (\text{A.7})$$

in the end we obtain the following

$$F_{\mu\nu}(0) = -Q \frac{D}{D-1} \dot{a}_{[\mu} u_{\nu]} \int \hat{d}^D k \frac{1}{k^2} \frac{1}{(k \cdot u - i\epsilon)^2}. \quad (\text{A.8})$$

Our final task is to perform the  $k$  integration. Therefore, we first write

$$\frac{1}{(k \cdot u - i\epsilon)^2} = - \frac{d}{d(k \cdot u)} \frac{1}{k \cdot u - i\epsilon} \quad (\text{A.9})$$

and then use the Sokhotski–Plemelj formula (3.32) for both denominators. At this point, `dimreg` instructs once more to drop all principal value parts of the propagators.

---

<sup>13</sup>In a frame where  $u^\mu = (1, \mathbf{0})$ , the  $k_\perp^\mu$  directions are simply the spatial ones.

Essentially, we are taking the imaginary part of the integral now. We finally remain with

$$F_{\mu\nu}(0) = \frac{Q}{3} \dot{a}_{[\mu} u_{\nu]} \int \hat{d}^4 k \hat{\delta}(k^2) \hat{\delta}'(k \cdot u) = \frac{Q}{6\pi} \dot{a}_{[\mu} u_{\nu]}, \quad (\text{A.10})$$

having taken  $D = 4$ .

Nicely, this last expression (A.10) matches the Schott term in (7.13). What is interesting here is to see how the double cut of 2.2 reverberates in our final steps of the proof. To this end one can interpret the fact the differentiated delta function  $\hat{\delta}'(k \cdot u)$  in (A.10) as a small  $q$ -expansion of  $\hat{\delta}(u \cdot (\ell - q))$  in 5.

## References

- [1] A. Antonelli, A. Buonanno, J. Steinhoff, M. van de Meent and J. Vines, *Energetics of two-body Hamiltonians in post-Minkowskian gravity*, *Phys. Rev. D* **99** (2019) 104004, [[1901.07102](#)].
- [2] V. Kalogera et al., *The Next Generation Global Gravitational Wave Observatory: The Science Book*, [2111.06990](#).
- [3] M. Khalil, A. Buonanno, J. Steinhoff and J. Vines, *Energetics and scattering of gravitational two-body systems at fourth post-Minkowskian order*, *Phys. Rev. D* **106** (2022) 024042, [[2204.05047](#)].
- [4] A. Buonanno, M. Khalil, D. O'Connell, R. Roiban, M. P. Solon and M. Zeng, *Snowmass White Paper: Gravitational Waves and Scattering Amplitudes*, in *2022 Snowmass Summer Study*, 4, 2022, [2204.05194](#).
- [5] H. Kawai, D. C. Lewellen and S. H. H. Tye, *A Relation Between Tree Amplitudes of Closed and Open Strings*, *Nucl. Phys. B* **269** (1986) 1–23.
- [6] Z. Bern, J. J. M. Carrasco and H. Johansson, *New Relations for Gauge-Theory Amplitudes*, *Phys. Rev. D* **78** (2008) 085011, [[0805.3993](#)].
- [7] Z. Bern, J. J. M. Carrasco and H. Johansson, *Perturbative Quantum Gravity as a Double Copy of Gauge Theory*, *Phys. Rev. Lett.* **105** (2010) 061602, [[1004.0476](#)].
- [8] Z. Bern, T. Dennen, Y.-t. Huang and M. Kiermaier, *Gravity as the Square of Gauge Theory*, *Phys. Rev. D* **82** (2010) 065003, [[1004.0693](#)].
- [9] Z. Bern, L. J. Dixon, D. C. Dunbar and D. A. Kosower, *One loop n point gauge theory amplitudes, unitarity and collinear limits*, *Nucl. Phys. B* **425** (1994) 217–260, [[hep-ph/9403226](#)].
- [10] Z. Bern, L. J. Dixon, D. C. Dunbar and D. A. Kosower, *Fusing gauge theory tree amplitudes into loop amplitudes*, *Nucl. Phys. B* **435** (1995) 59–101, [[hep-ph/9409265](#)].
- [11] N. E. J. Bjerrum-Bohr, J. F. Donoghue and P. Vanhove, *On-shell Techniques and Universal Results in Quantum Gravity*, *JHEP* **02** (2014) 111, [[1309.0804](#)].

- [12] N. E. J. Bjerrum-Bohr, J. F. Donoghue, B. R. Holstein, L. Plante and P. Vanhove, *Light-like Scattering in Quantum Gravity*, *JHEP* **11** (2016) 117, [[1609.07477](#)].
- [13] N. E. J. Bjerrum-Bohr, P. H. Damgaard, G. Festuccia, L. Planté and P. Vanhove, *General Relativity from Scattering Amplitudes*, *Phys. Rev. Lett.* **121** (2018) 171601, [[1806.04920](#)].
- [14] A. Guevara, A. Ochiroya and J. Vines, *Scattering of Spinning Black Holes from Exponentiated Soft Factors*, *JHEP* **09** (2019) 056, [[1812.06895](#)].
- [15] N. Moynihan and J. Murugan, *On-Shell Electric-Magnetic Duality and the Dual Graviton*, [2002.11085](#).
- [16] Z. Bern, H. Ita, J. Parra-Martinez and M. S. Ruf, *Universality in the classical limit of massless gravitational scattering*, *Phys. Rev. Lett.* **125** (2020) 031601, [[2002.02459](#)].
- [17] A. Cristofoli, P. H. Damgaard, P. Di Vecchia and C. Heissenberg, *Second-order Post-Minkowskian scattering in arbitrary dimensions*, *JHEP* **07** (2020) 122, [[2003.10274](#)].
- [18] N. Moynihan, *Scattering Amplitudes and the Double Copy in Topologically Massive Theories*, *JHEP* **12** (2020) 163, [[2006.15957](#)].
- [19] J. Parra-Martinez, M. S. Ruf and M. Zeng, *Extremal black hole scattering at  $\mathcal{O}(G^3)$ : graviton dominance, eikonal exponentiation, and differential equations*, *JHEP* **11** (2020) 023, [[2005.04236](#)].
- [20] K. Haddad and A. Helset, *The double copy for heavy particles*, [2005.13897](#).
- [21] B. Sahoo, *Classical Sub-subleading Soft Photon and Soft Graviton Theorems in Four Spacetime Dimensions*, *JHEP* **12** (2020) 070, [[2008.04376](#)].
- [22] L. de la Cruz, B. Maybee, D. O'Connell and A. Ross, *Classical Yang-Mills observables from amplitudes*, *JHEP* **12** (2020) 076, [[2009.03842](#)].
- [23] M. Accettulli Huber, A. Brandhuber, S. De Angelis and G. Travaglini, *Eikonal phase matrix, deflection angle and time delay in effective field theories of gravity*, *Phys. Rev. D* **102** (2020) 046014, [[2006.02375](#)].
- [24] D. Bonocore, *Asymptotic dynamics on the worldline for spinning particles*, *JHEP* **02** (2021) 007, [[2009.07863](#)].
- [25] G. Mogull, J. Plefka and J. Steinhoff, *Classical black hole scattering from a worldline quantum field theory*, *JHEP* **02** (2021) 048, [[2010.02865](#)].
- [26] W. T. Emond, Y.-T. Huang, U. Kol, N. Moynihan and D. O'Connell, *Amplitudes from Coulomb to Kerr-Taub-NUT*, [2010.07861](#).
- [27] C. Cheung, N. Shah and M. P. Solon, *Mining the Geodesic Equation for Scattering Data*, *Phys. Rev. D* **103** (2021) 024030, [[2010.08568](#)].
- [28] S. Mougiakakos and P. Vanhove, *Schwarzschild-Tangherlini metric from scattering amplitudes in various dimensions*, *Phys. Rev. D* **103** (2021) 026001, [[2010.08882](#)].

[29] J. J. M. Carrasco and I. A. Vazquez-Holm, *Loop-Level Double-Copy for Massive Quantum Particles*, [2010.13435](#).

[30] J.-W. Kim and M. Shim, *Gravitational Dyonic Amplitude at One-Loop and its Inconsistency with the Classical Impulse*, *JHEP* **02** (2021) 217, [\[2010.14347\]](#).

[31] N. E. J. Bjerrum-Bohr, T. V. Brown and H. Gomez, *Scattering of Gravitons and Spinning Massive States from Compact Numerators*, *JHEP* **04** (2021) 234, [\[2011.10556\]](#).

[32] R. Gonzo and A. Pokraka, *Light-ray operators, detectors and gravitational event shapes*, *JHEP* **05** (2021) 015, [\[2012.01406\]](#).

[33] L. de la Cruz, *Scattering amplitudes approach to hard thermal loops*, *Phys. Rev. D* **104** (2021) 014013, [\[2012.07714\]](#).

[34] N. E. J. Bjerrum-Bohr, P. H. Damgaard, L. Planté and P. Vanhove, *Classical gravity from loop amplitudes*, *Phys. Rev. D* **104** (2021) 026009, [\[2104.04510\]](#).

[35] N. E. J. Bjerrum-Bohr, P. H. Damgaard, L. Planté and P. Vanhove, *The Amplitude for Classical Gravitational Scattering at Third Post-Minkowskian Order*, [2105.05218](#).

[36] E. Herrmann, J. Parra-Martinez, M. S. Ruf and M. Zeng, *Radiative classical gravitational observables at  $\mathcal{O}(G^3)$  from scattering amplitudes*, *JHEP* **10** (2021) 148, [\[2104.03957\]](#).

[37] A. Cristofoli, R. Gonzo, D. A. Kosower and D. O’Connell, *Waveforms from Amplitudes*, [2107.10193](#).

[38] Z. Bern, J. Parra-Martinez, R. Roiban, M. S. Ruf, C.-H. Shen, M. P. Solon et al., *Scattering Amplitudes and Conservative Binary Dynamics at  $\mathcal{O}(G^4)$* , *Phys. Rev. Lett.* **126** (2021) 171601, [\[2101.07254\]](#).

[39] E. Herrmann, J. Parra-Martinez, M. S. Ruf and M. Zeng, *Gravitational Bremsstrahlung from Reverse Unitarity*, *Phys. Rev. Lett.* **126** (2021) 201602, [\[2101.07255\]](#).

[40] P. Di Vecchia, C. Heissenberg, R. Russo and G. Veneziano, *The eikonal approach to gravitational scattering and radiation at  $\mathcal{O}(G^3)$* , *JHEP* **07** (2021) 169, [\[2104.03256\]](#).

[41] Y. F. Bautista, A. Guevara, C. Kavanagh and J. Vines, *From Scattering in Black Hole Backgrounds to Higher-Spin Amplitudes: Part I*, [2107.10179](#).

[42] A. Cristofoli, R. Gonzo, N. Moynihan, D. O’Connell, A. Ross, M. Sergola et al., *The Uncertainty Principle and Classical Amplitudes*, [2112.07556](#).

[43] A. Manu, D. Ghosh, A. Laddha and P. V. Athira, *Soft radiation from scattering amplitudes revisited*, *JHEP* **05** (2021) 056, [\[2007.02077\]](#).

[44] Z. Bern, A. Luna, R. Roiban, C.-H. Shen and M. Zeng, *Spinning black hole binary*

*dynamics, scattering amplitudes, and effective field theory,*  
*Phys. Rev. D* **104** (2021) 065014, [[2005.03071](#)].

- [45] Y. F. Bautista and A. Laddha, *Soft Constraints on KMOC Formalism*, [2111.11642](#).
- [46] R. Aoude and A. Ochirov, *Classical observables from coherent-spin amplitudes*, *JHEP* **10** (2021) 008, [[2108.01649](#)].
- [47] A. Brandhuber, G. Chen, G. Travaglini and C. Wen, *Classical gravitational scattering from a gauge-invariant double copy*, *JHEP* **10** (2021) 118, [[2108.04216](#)].
- [48] A. Brandhuber, G. Chen, G. Travaglini and C. Wen, *A new gauge-invariant double copy for heavy-mass effective theory*, *JHEP* **07** (2021) 047, [[2104.11206](#)].
- [49] A. Brandhuber, G. Chen, H. Johansson, G. Travaglini and C. Wen, *Kinematic Hopf Algebra for Bern-Carrasco-Johansson Numerators in Heavy-Mass Effective Field Theory and Yang-Mills Theory*, *Phys. Rev. Lett.* **128** (2022) 121601, [[2111.15649](#)].
- [50] G. Cho, R. A. Porto and Z. Yang, *Gravitational radiation from inspiralling compact objects: Spin effects to fourth Post-Newtonian order*, [2201.05138](#).
- [51] Z. Bern, D. Kosmopoulos, A. Luna, R. Roiban and F. Teng, *Binary Dynamics Through the Fifth Power of Spin at  $\mathcal{O}(G^2)$* , [2203.06202](#).
- [52] W.-M. Chen, M.-Z. Chung, Y.-t. Huang and J.-W. Kim, *The 2PM Hamiltonian for binary Kerr to quartic in spin*, [2111.13639](#).
- [53] F. Alessio and P. Di Vecchia, *Radiation reaction for spinning black-hole scattering*, [2203.13272](#).
- [54] F. Febres Cordero, M. Kraus, G. Lin, M. S. Ruf and M. Zeng, *Conservative Binary Dynamics with a Spinning Black Hole at  $\mathcal{O}(G^3)$  from Scattering Amplitudes*, [2205.07357](#).
- [55] G. Menezes and M. Sergola, *NLO deflections for spinning particles and Kerr black holes*, *JHEP* **10** (2022) 105, [[2205.11701](#)].
- [56] W. D. Goldberger and A. K. Ridgway, *Radiation and the classical double copy for color charges*, *Phys. Rev. D* **95** (2017) 125010, [[1611.03493](#)].
- [57] A. Luna, R. Monteiro, I. Nicholson, D. O’Connell and C. D. White, *The double copy: Bremsstrahlung and accelerating black holes*, *JHEP* **06** (2016) 023, [[1603.05737](#)].
- [58] C.-H. Shen, *Gravitational Radiation from Color-Kinematics Duality*, *JHEP* **11** (2018) 162, [[1806.07388](#)].
- [59] D. A. Kosower, B. Maybee and D. O’Connell, *Amplitudes, Observables, and Classical Scattering*, *JHEP* **02** (2019) 137, [[1811.10950](#)].
- [60] G. U. Jakobsen, G. Mogull, J. Plefka and J. Steinhoff, *Classical Gravitational Bremsstrahlung from a Worldline Quantum Field Theory*, *Phys. Rev. Lett.* **126** (2021) 201103, [[2101.12688](#)].

[61] T. Adamo, A. Cristofoli, A. Ilderton and S. Klisch, *All-order waveforms from amplitudes*, [2210.04696](#).

[62] G. Cho, A. Gopakumar, M. Haney and H. M. Lee, *Gravitational waves from compact binaries in post-Newtonian accurate hyperbolic orbits*, *Phys. Rev. D* **98** (2018) 024039, [[1807.02380](#)].

[63] G. Kälin and R. A. Porto, *From Boundary Data to Bound States*, *JHEP* **01** (2020) 072, [[1910.03008](#)].

[64] G. Kälin and R. A. Porto, *From boundary data to bound states. Part II. Scattering angle to dynamical invariants (with twist)*, *JHEP* **02** (2020) 120, [[1911.09130](#)].

[65] G. Cho, G. Kälin and R. A. Porto, *From Boundary Data to Bound States III: Radiative Effects*, [2112.03976](#).

[66] C. Cheung, I. Z. Rothstein and M. P. Solon, *From Scattering Amplitudes to Classical Potentials in the Post-Minkowskian Expansion*, *Phys. Rev. Lett.* **121** (2018) 251101, [[1808.02489](#)].

[67] S. Foffa, P. Mastrolia, R. Sturani, C. Sturm and W. J. Torres Bobadilla, *Static two-body potential at fifth post-Newtonian order*, *Phys. Rev. Lett.* **122** (2019) 241605, [[1902.10571](#)].

[68] S. Foffa, R. A. Porto, I. Rothstein and R. Sturani, *Conservative dynamics of binary systems to fourth Post-Newtonian order in the EFT approach II: Renormalized Lagrangian*, *Phys. Rev. D* **100** (2019) 024048, [[1903.05118](#)].

[69] S. Foffa and R. Sturani, *Conservative dynamics of binary systems to fourth Post-Newtonian order in the EFT approach I: Regularized Lagrangian*, *Phys. Rev. D* **100** (2019) 024047, [[1903.05113](#)].

[70] S. Foffa and R. Sturani, *Heredity terms at next-to-leading order in two-body gravitational dynamics*, *Phys. Rev. D* **101** (2020) 064033, [[1907.02869](#)].

[71] M. Levi, S. Mousiakakos and M. Vieira, *Gravitational cubic-in-spin interaction at the next-to-leading post-Newtonian order*, *JHEP* **01** (2021) 036, [[1912.06276](#)].

[72] L. Blanchet, S. Foffa, F. Larroutuou and R. Sturani, *Logarithmic tail contributions to the energy function of circular compact binaries*, *Phys. Rev. D* **101** (2020) 084045, [[1912.12359](#)].

[73] W. D. Goldberger and I. Z. Rothstein, *An Effective Field Theory of Quantum Mechanical Black Hole Horizons*, *JHEP* **04** (2020) 056, [[1912.13435](#)].

[74] R. Aoude, K. Haddad and A. Helset, *On-shell heavy particle effective theories*, *JHEP* **05** (2020) 051, [[2001.09164](#)].

[75] M. Levi, A. J. Mcleod and M. Von Hippel,  *$N^3LO$  gravitational spin-orbit coupling at order  $G^4$* , *JHEP* **07** (2021) 115, [[2003.02827](#)].

[76] J. Blümlein, A. Maier, P. Marquard and G. Schäfer, *Testing binary dynamics in*

gravity at the sixth post-Newtonian level, *Phys. Lett. B* **807** (2020) 135496, [[2003.07145](#)].

[77] M. Levi, A. J. Mcleod and M. Von Hippel, *NNNLO gravitational quadratic-in-spin interactions at the quartic order in G*, [2003.07890](#).

[78] M. Levi and F. Teng, *NLO gravitational quartic-in-spin interaction*, *JHEP* **01** (2021) 066, [[2008.12280](#)].

[79] J. Blümlein, A. Maier, P. Marquard and G. Schäfer, *The fifth-order post-Newtonian Hamiltonian dynamics of two-body systems from an effective field theory approach: potential contributions*, *Nucl. Phys. B* **965** (2021) 115352, [[2010.13672](#)].

[80] S. Foffa, R. Sturani and W. J. Torres Bobadilla, *Efficient resummation of high post-Newtonian contributions to the binding energy*, *JHEP* **02** (2021) 165, [[2010.13730](#)].

[81] W. D. Goldberger, J. Li and I. Z. Rothstein, *Non-conservative effects on spinning black holes from world-line effective field theory*, *JHEP* **06** (2021) 053, [[2012.14869](#)].

[82] J. Blümlein, A. Maier, P. Marquard and G. Schäfer, *The 6th post-Newtonian potential terms at  $O(G_N^4)$* , *Phys. Lett. B* **816** (2021) 136260, [[2101.08630](#)].

[83] S. Foffa and R. Sturani, *Near and far zones in two-body dynamics: An effective field theory perspective*, *Phys. Rev. D* **104** (2021) 024069, [[2103.03190](#)].

[84] G. L. Almeida, S. Foffa and R. Sturani, *Tail contributions to gravitational conservative dynamics*, *Phys. Rev. D* **104** (2021) 124075, [[2110.14146](#)].

[85] J.-W. Kim, M. Levi and Z. Yin, *Quadratic-in-spin interactions at fifth post-Newtonian order probe new physics*, *Phys. Lett. B* **834** (2022) 137410, [[2112.01509](#)].

[86] A. Edison and M. Levi, *A tale of tails through generalized unitarity*, [2202.04674](#).

[87] J.-W. Kim, M. Levi and Z. Yin,  *$N^3LO$  Spin-Orbit Interaction via the EFT of Spinning Gravitating Objects*, [2208.14949](#).

[88] M. K. Mandal, P. Mastrolia, R. Patil and J. Steinhoff, *Gravitational Spin-Orbit Hamiltonian at NNNLO in the post-Newtonian framework*, [2209.00611](#).

[89] J.-W. Kim, M. Levi and Z. Yin,  *$N^3LO$  Quadratic-in-Spin Interactions for Generic Compact Binaries*, [2209.09235](#).

[90] G. L. Almeida, S. Foffa and R. Sturani, *Gravitational radiation contributions to the two-body scattering angle*, [2209.11594](#).

[91] M. K. Mandal, P. Mastrolia, R. Patil and J. Steinhoff, *Gravitational Quadratic-in-Spin Hamiltonian at NNNLO in the post-Newtonian framework*, [2210.09176](#).

[92] W. D. Goldberger and I. Z. Rothstein, *An Effective field theory of gravity for extended objects*, *Phys. Rev. D* **73** (2006) 104029, [[hep-th/0409156](#)].

[93] W. D. Goldberger and I. Z. Rothstein, *Dissipative effects in the worldline approach to black hole dynamics*, *Phys. Rev. D* **73** (2006) 104030, [[hep-th/0511133](#)].

[94] W. D. Goldberger and A. Ross, *Gravitational radiative corrections from effective field theory*, *Phys. Rev. D* **81** (2010) 124015, [[0912.4254](#)].

[95] M. Levi and J. Steinhoff, *Spinning gravitating objects in the effective field theory in the post-Newtonian scheme*, *JHEP* **09** (2015) 219, [[1501.04956](#)].

[96] M. Levi and J. Steinhoff, *Next-to-next-to-leading order gravitational spin-orbit coupling via the effective field theory for spinning objects in the post-Newtonian scheme*, *JCAP* **01** (2016) 011, [[1506.05056](#)].

[97] M. Levi and J. Steinhoff, *Next-to-next-to-leading order gravitational spin-squared potential via the effective field theory for spinning objects in the post-Newtonian scheme*, *JCAP* **01** (2016) 008, [[1506.05794](#)].

[98] M. Levi and J. Steinhoff, *Complete conservative dynamics for inspiralling compact binaries with spins at the fourth post-Newtonian order*, *JCAP* **09** (2021) 029, [[1607.04252](#)].

[99] S. Foffa, P. Mastrolia, R. Sturani and C. Sturm, *Effective field theory approach to the gravitational two-body dynamics, at fourth post-Newtonian order and quintic in the Newton constant*, *Phys. Rev. D* **95** (2017) 104009, [[1612.00482](#)].

[100] W. D. Goldberger, S. G. Prabhu and J. O. Thompson, *Classical gluon and graviton radiation from the bi-adjoint scalar double copy*, *Phys. Rev. D* **96** (2017) 065009, [[1705.09263](#)].

[101] W. D. Goldberger and A. K. Ridgway, *Bound states and the classical double copy*, *Phys. Rev. D* **97** (2018) 085019, [[1711.09493](#)].

[102] R. A. Porto, *The effective field theorist's approach to gravitational dynamics*, *Phys. Rept.* **633** (2016) 1–104, [[1601.04914](#)].

[103] M. Levi, *Effective Field Theories of Post-Newtonian Gravity: A comprehensive review*, *Rept. Prog. Phys.* **83** (2020) 075901, [[1807.01699](#)].

[104] G. Kälin and R. A. Porto, *Post-Minkowskian Effective Field Theory for Conservative Binary Dynamics*, *JHEP* **11** (2020) 106, [[2006.01184](#)].

[105] G. Kälin, Z. Liu and R. A. Porto, *Conservative Dynamics of Binary Systems to Third Post-Minkowskian Order from the Effective Field Theory Approach*, *Phys. Rev. Lett.* **125** (2020) 261103, [[2007.04977](#)].

[106] G. Kälin, Z. Liu and R. A. Porto, *Conservative Tidal Effects in Compact Binary Systems to Next-to-Leading Post-Minkowskian Order*, *Phys. Rev. D* **102** (2020) 124025, [[2008.06047](#)].

[107] C. Dlapa, G. Kälin, Z. Liu and R. A. Porto, *Dynamics of binary systems to fourth Post-Minkowskian order from the effective field theory approach*, *Phys. Lett. B* **831** (2022) 137203, [[2106.08276](#)].

[108] C. Dlapa, G. Kälin, Z. Liu and R. A. Porto, *Conservative Dynamics of Binary Systems at Fourth Post-Minkowskian Order in the Large-Eccentricity Expansion*, *Phys. Rev. Lett.* **128** (2022) 161104, [[2112.11296](#)].

[109] G. Kälin, J. Neef and R. A. Porto, *Radiation-Reaction in the Effective Field Theory Approach to Post-Minkowskian Dynamics*, [2207.00580](#).

[110] C. Dlapa, G. Kälin, Z. Liu, J. Neef and R. A. Porto, *Radiation Reaction and Gravitational Waves at Fourth Post-Minkowskian Order*, [2210.05541](#).

[111] C. Schubert, *An Introduction to the worldline technique for quantum field theory calculations*, *Acta Phys. Polon. B* **27** (1996) 3965–4001, [[hep-th/9610108](#)].

[112] N. Ahmadianiaz, O. Corradini, J. M. Dávila and C. Schubert, *Gravitational Compton Scattering from the Worldline Formalism*, *Int. J. Mod. Phys. Conf. Ser.* **43** (2016) 1660201.

[113] G. U. Jakobsen, G. Mogull, J. Plefka and J. Steinhoff, *Gravitational Bremsstrahlung and Hidden Supersymmetry of Spinning Bodies*, [2106.10256](#).

[114] J. P. Edwards, C. M. Mata, U. Müller and C. Schubert, *New Techniques for Worldline Integration*, *SIGMA* **17** (2021) 065, [[2106.12071](#)].

[115] G. U. Jakobsen, G. Mogull, J. Plefka and J. Steinhoff, *SUSY in the Sky with Gravitons*, [2109.04465](#).

[116] G. U. Jakobsen and G. Mogull, *Conservative and Radiative Dynamics of Spinning Bodies at Third Post-Minkowskian Order Using Worldline Quantum Field Theory*, *Phys. Rev. Lett.* **128** (2022) 141102, [[2201.07778](#)].

[117] G. U. Jakobsen, G. Mogull, J. Plefka and B. Sauer, *All things retarded: radiation-reaction in worldline quantum field theory*, *JHEP* **10** (2022) 128, [[2207.00569](#)].

[118] G. U. Jakobsen and G. Mogull, *Linear Response, Hamiltonian and Radiative Spinning Two-Body Dynamics*, [2210.06451](#).

[119] F. Comberiati and L. de la Cruz, *Classical off-shell currents*, [2212.09259](#).

[120] Z. Bern, C. Cheung, R. Roiban, C.-H. Shen, M. P. Solon and M. Zeng, *Scattering Amplitudes and the Conservative Hamiltonian for Binary Systems at Third Post-Minkowskian Order*, *Phys. Rev. Lett.* **122** (2019) 201603, [[1901.04424](#)].

[121] Z. Bern, C. Cheung, R. Roiban, C.-H. Shen, M. P. Solon and M. Zeng, *Black Hole Binary Dynamics from the Double Copy and Effective Theory*, *JHEP* **10** (2019) 206, [[1908.01493](#)].

[122] Z. Bern, J. Parra-Martinez, R. Roiban, M. S. Ruf, C.-H. Shen, M. P. Solon et al., *Scattering Amplitudes, the Tail Effect, and Conservative Binary Dynamics at  $O(G4)$* , *Phys. Rev. Lett.* **128** (2022) 161103, [[2112.10750](#)].

[123] N. Isgur and M. B. Wise, *Weak Decays of Heavy Mesons in the Static Quark Approximation*, *Phys. Lett. B* **232** (1989) 113–117.

[124] H. Georgi, *An Effective Field Theory for Heavy Quarks at Low-energies*, *Phys. Lett. B* **240** (1990) 447–450.

[125] M. E. Luke and A. V. Manohar, *Reparametrization invariance constraints on heavy particle effective field theories*, *Phys. Lett. B* **286** (1992) 348–354, [[hep-ph/9205228](#)].

[126] M. Neubert, *Heavy quark symmetry*, *Phys. Rept.* **245** (1994) 259–396, [[hep-ph/9306320](#)].

[127] A. V. Manohar and M. B. Wise, *Heavy quark physics*, vol. 10. 2000.

[128] P. H. Damgaard, K. Haddad and A. Helset, *Heavy Black Hole Effective Theory*, *JHEP* **11** (2019) 070, [[1908.10308](#)].

[129] A. Luna, I. Nicholson, D. O’Connell and C. D. White, *Inelastic Black Hole Scattering from Charged Scalar Amplitudes*, *JHEP* **03** (2018) 044, [[1711.03901](#)].

[130] A. Herderschee, R. Roiban and F. Teng, *The sub-leading scattering waveform from amplitudes*, *To appear* (2023) .

[131] A. Brandhuber, G. Brown, G. Chen, S. De Angelis, J. K. Gowdy and G. Travaglini, *One-loop gravitational bremsstrahlung and waveforms from a heavy-mass effective field theory*, *To appear* (2023) .

[132] A. Georgoudis, C. Heissenberg and I. Vazquez-Holm, *One-loop five-point amplitude for classical scattering*, *To appear* (2023) .

[133] R. Monteiro, D. O’Connell, D. Peinador Veiga and M. Sergola, *Classical solutions and their double copy in split signature*, *JHEP* **05** (2021) 268, [[2012.11190](#)].

[134] G. Travaglini et al., *The SAGEX Review on Scattering Amplitudes*, [2203.13011](#).

[135] D. A. Kosower, R. Monteiro and D. O’Connell, *The SAGEX Review on Scattering Amplitudes, Chapter 14: Classical Gravity from Scattering Amplitudes*, [2203.13025](#).

[136] P. Di Vecchia, C. Heissenberg, R. Russo and G. Veneziano, *The eikonal operator at arbitrary velocities I: the soft-radiation limit*, *JHEP* **07** (2022) 039, [[2204.02378](#)].

[137] P. Di Vecchia, C. Heissenberg, R. Russo and G. Veneziano, *Classical Gravitational Observables from the Eikonal Operator*, [2210.12118](#).

[138] P. H. Damgaard, L. Plante and P. Vanhove, *On an exponential representation of the gravitational S-matrix*, *JHEP* **11** (2021) 213, [[2107.12891](#)].

[139] D. Neill and I. Z. Rothstein, *Classical Space-Times from the S Matrix*, *Nucl. Phys. B* **877** (2013) 177–189, [[1304.7263](#)].

[140] J. J. M. Carrasco and I. A. Vazquez-Holm, *Extracting Einstein from the loop-level double-copy*, *JHEP* **11** (2021) 088, [[2108.06798](#)].

[141] R. Britto, R. Gonzo and G. R. Jehu, *Graviton particle statistics and coherent states from classical scattering amplitudes*, *JHEP* **03** (2022) 214, [[2112.07036](#)].

[142] G. 't Hooft and M. J. G. Veltman, *DIAGRAMMAR*, *NATO Sci. Ser. B* **4** (1974) 177–322.

[143] G. F. Sterman, *An Introduction to quantum field theory*. Cambridge University Press, 8, 1993.

[144] M. Srednicki, *Quantum field theory*. Cambridge University Press, 1, 2007.

[145] M. D. Schwartz, *Quantum Field Theory and the Standard Model*. Cambridge University Press, 3, 2014.

[146] N. E. J. Bjerrum-Bohr, J. F. Donoghue and P. Vanhove, *On-shell Techniques and Universal Results in Quantum Gravity*, *JHEP* **02** (2014) 111, [[1309.0804](#)].

[147] C. Cheung and D. O'Connell, *Amplitudes and Spinor-Helicity in Six Dimensions*, *JHEP* **07** (2009) 075, [[0902.0981](#)].

[148] Z. Bern, *Perturbative quantum gravity and its relation to gauge theory*, *Living Rev. Rel.* **5** (2002) 5, [[gr-qc/0206071](#)].

[149] Y. Mino, M. Sasaki and T. Tanaka, *Gravitational radiation reaction to a particle motion*, *Phys. Rev. D* **55** (1997) 3457–3476, [[gr-qc/9606018](#)].

[150] T. C. Quinn and R. M. Wald, *An Axiomatic approach to electromagnetic and gravitational radiation reaction of particles in curved space-time*, *Phys. Rev. D* **56** (1997) 3381–3394, [[gr-qc/9610053](#)].

[151] S. Weinberg, *Infrared photons and gravitons*, *Phys. Rev.* **140** (1965) B516–B524.

[152] C. Heissenberg, *Infrared divergences and the eikonal exponentiation*, *Phys. Rev. D* **104** (2021) 046016, [[2105.04594](#)].

[153] R. A. Porto, A. Ross and I. Z. Rothstein, *Spin induced multipole moments for the gravitational wave amplitude from binary inspirals to 2.5 Post-Newtonian order*, *JCAP* **09** (2012) 028, [[1203.2962](#)].

[154] H. A. Lorentz, *La théorie électromagnétique de Maxwell et son application aux corps mouvants*, vol. 25. EJ Brill, 1892.

[155] M. Abraham, *Prinzipien der dynamik des elektrons*, *Annalen der Physik* **315** (1902) 105–179, [<https://onlinelibrary.wiley.com/doi/10.1002/andp.19023150105>].

[156] P. A. M. Dirac, *Classical theory of radiating electrons*, *Proc. Roy. Soc. Lond. A* **167** (1938) 148–169.

[157] G. A. Schott, *Electromagnetic radiation and the mechanical reactions arising from it: being an Adams Prize Essay in the University of Cambridge*. University Press, 1912.

[158] L. de la Cruz, A. Luna and T. Schepner, *Yang-Mills observables: from KMOC to eikonal through EFT*, *JHEP* **01** (2022) 045, [[2108.02178](#)].

[159] Z. Bern, J. P. Gatica, E. Herrmann, A. Luna and M. Zeng, *Scalar QED as a toy*

*model for higher-order effects in classical gravitational scattering,*  
*JHEP* **08** (2022) 131, [[2112.12243](#)].

- [160] R. Aoude, K. Haddad and A. Helset, *Searching for Kerr in the 2PM amplitude*,  
*JHEP* **07** (2022) 072, [[2203.06197](#)].
- [161] N. E. J. Bjerrum-Bohr, G. Chen and M. Skowronek, *Classical Spin Gravitational Compton Scattering*, [2302.00498](#).
- [162] L. Cangemi, M. Chiodaroli, H. Johansson, A. Ochirov, P. Pichini and E. Skvortsov, *Kerr Black Holes Enjoy Massive Higher-Spin Gauge Symmetry*, [2212.06120](#).
- [163] Z. Bern, D. Kosmopoulos, A. Luna, R. Roiban and F. Teng, *Binary Dynamics Through the Fifth Power of Spin at  $\mathcal{O}(G^2)$* , [2203.06202](#).
- [164] Y. F. Bautista, A. Guevara, C. Kavanagh and J. Vines, *Scattering in Black Hole Backgrounds and Higher-Spin Amplitudes: Part II*, [2212.07965](#).
- [165] T. Adamo and R. Gonzo, *Bethe-Salpeter equation for classical gravitational bound states*, [2212.13269](#).
- [166] S. Coleman, *Classical Electron Theory from a Modern Standpoint*. RAND Corporation, Santa Monica, CA, 1961.